

Uncovering hidden species diversity of alopoglossid lizards in Amazonia, with the description of three new species of *Alopoglossus* (Squamata: Gymnophthalmoidae)

Marco Antônio Ribeiro-Júnior¹  | Paola María Sánchez-Martínez² | Leandro João Carneiro de Lima Moraes³ | Uécson Suendel Costa de Oliveira⁴ | Vinícius Tadeu de Carvalho^{5,6} | Dante Pavan⁷ | Erik Henrique de Lacerda Choueri³ | Fernanda P. Werneck⁸ | Shai Meiri⁹

¹School of Zoology, Tel Aviv University, Tel Aviv, Israel

²Grupo de Morfología y Ecología Evolutiva, Instituto de Ciencias Naturales, Universidad Nacional de Colombia, Bogotá, D.C, Colombia

³Instituto Nacional de Pesquisas da Amazônia, Manaus, Brazil

⁴Programa de Pós-graduação em Biotecnologia e Biodiversidade/PPG Bionorte, Universidade Federal do Acre, Rio Branco, Brazil

⁵Programa de Pós-graduação em Diversidade Biológica e Recursos Naturais, Universidade Regional do Cariri, Crato, Brazil

⁶Laboratório de Evolução e Genética Animal, Universidade Federal do Amazonas, Manaus, Brazil

⁷Ecosfera Consultoria e Pesquisa em Meio Ambiente, Itapina, Brazil

⁸Coordenação de Biodiversidade, Programa de Coleções Científicas Biológicas, Instituto Nacional de Pesquisas da Amazônia, Manaus, Brazil

⁹Steinhardt Museum of Natural History, Tel Aviv University, Tel Aviv, Israel

Correspondence

Marco Antônio Ribeiro-Júnior, School of Zoology, Tel Aviv University, Tel Aviv 6997801, Israel.
Email: majunior@gmail.com

Funding information

Partnerships for Enhanced Engagement in Research from the U.S. National Academy of Sciences and U.S. Agency of International Development; Gans Collections and Charitable Fund Inc.; L'Oréal-Unesco For Women in Science Program; CNEC WorleyParsons Engenharia S.A.; Instituto de Desenvolvimento Sustentável Mamirauá, Instituto Chico Mendes de Conservação da Biodiversidade; Fundação de Amparo à Pesquisa do Estado do Amazonas; Gordon and Betty Moore Foundation; Conselho Nacional de Desenvolvimento Científico e Tecnológico; Rector scholarship; Alexander and Eva Lester Fund

Abstract

Alopoglossus is a Neotropical lizard genus the taxonomy of which has extensively evolved over the past decade. Previous works suggest that many species still remain unnamed in this genus. Here, we expand the knowledge of *Alopoglossus* diversity in Amazonian lowlands. Molecular phylogenetic relationships, and species boundaries, were inferred based on the variation of mitochondrial (*Cytb* and *ND4*) and nuclear (*SNCAIP* and *PRLR*) loci. Morphological variation was assessed through analyses of external morphology of 401 specimens, covering the entire distribution range of *Alopoglossus angulatus* and its closely related taxa, and hemipenes of five specimens were examined. Combined, our evidence supports the recognition of three new species. We describe these species and redefine *A. amazonius* sensu stricto, increasing the number of known *Alopoglossus* species to 18. Our study also presents the first detailed descriptions of hemipenes for the genus.

KEYWORDS

cryptic species, hemipenial description, molecular phylogeny, reptiles, South America

Contributing authors: Paola María Sánchez-Martínez (paola.sanmart@gmail.com); Leandro João Carneiro de Lima Moraes (leandro.jclm@gmail.com); Uécson Suendel Costa de Oliveira (uecson@gmail.com); Vinícius Tadeu de Carvalho (anfibus.repteis@gmail.com); Dante Pavan (dtpavan@yahoo.com.br); Erik Henrique de Lacerda Choueri (chouerik@gmail.com); Fernanda P. Werneck (fewerneck@gmail.com); Shai Meiri (uncshai@gmail.com)

Zoobank Link: LSID: <http://zoobank.org/urn:lsid:zoobank.org:pub:0D363005-0660-45E0-9CBB-1F918005DC7E>

Online ISSN: 1439-0469

Resumo

Alopoglossus é um gênero de lagarto neotropical que a taxonomia tem evoluído substancialmente na última década. Trabalhos prévios sugerem que muitas espécies ainda não foram descritas neste gênero. Neste trabalho nós ampliamos o conhecimento da diversidade de *Alopoglossus* na Amazônia. Relações filogenéticas e delimitação de espécies foram inferidas baseadas na variação de loci mitocondriais (*Cytb* and *ND4*) e nucleares (*SNCAIP* and *PRLR*). Variações morfológicas foram acessadas através da análise da morfologia externa de 401 espécimes cobrindo toda a distribuição de *Alopoglossus angulatus* e espécies próximas, e a morfologia hemipeniana através da análise de órgãos de cinco espécimes. Combinadas as nossas evidências suportam o reconhecimento de três novas espécies. Nós descrevemos essas espécies e redefinimos *A. amazonius* sensu stricto, aumentando o número de espécies de *Alopoglossus* para 18. Nosso estudo também apresenta a primeira descrição detalhada de hemipênis para o gênero.

1 | INTRODUCTION

Amazonia is the largest tropical forest in the world (Primack & Corlett, 2005). At the same time, this is the region where substantial knowledge gaps hamper our perception on taxonomy, distribution and evolutionary patterns of the native biota (Linnean, Wallacean, and Darwinian shortfalls, respectively; Hortal et al., 2015). These shortfalls are maintained by several factors, among which the significant amount of cryptic species diversity plays a fundamental role (Fouquet et al., 2007; Funk et al., 2012; Vacher et al., 2020). Recent studies have demonstrated that many taxa thought to be widely distributed within Amazonia are, in fact, complexes of narrowly distributed species. The evolutionary history of the region has thus emerged as far more complex than previously thought (Fouquet et al., 2014; Geurgas & Rodrigues, 2010; Marques-Souza et al., 2019; Nunes et al., 2012; Oliveira et al., 2016; Ortiz et al., 2018; Silva et al., 2018; Vacher et al., 2020).

One of these Amazonian taxa containing cryptic species are the lizards of the family Alopoglossidae. Although targeted by some phylogenetic studies in the last decades (Castoe et al., 2004; Goicoechea et al., 2016; Morales et al., 2020; Pellegrino et al., 2001; Ribeiro-Júnior, Choueri, et al., 2020; Ribeiro-Júnior et al., 2020), taxonomic status of species and genera in this family is still controversial. For example, based on genetic and morphological data, Morales et al. (2020) recently suggested *Ptychoglossus* Boulenger, 1890 as synonym of *Alopoglossus* Boulenger, 1885. Concurrently, and based on same type of data, Ribeiro-Júnior, Meiri, et al. (2020), Ribeiro-Júnior, Choueri, et al. (2020) showed that *Alopoglossus angulatus* sensu lato comprises at least nine cryptic species. The ambiguous definition for some of the traditionally used characters to diagnose *Alopoglossus* species (mostly based on the general shape of scales on the neck sides) resulted in groupings of several species under single nominal forms and the misidentification of several species in the genus (see

Ribeiro-Júnior, 2018). Ribeiro-Júnior, Meiri, et al. (2020) suggested that the informative morphological characters of the alopoglossid species need to be comprehensively redefined before any changes at the genus level can be made. Here we follow the taxonomy suggested in the most comprehensive phylogenetic study of alopoglossid diversification (Goicoechea et al., 2016).

Alopoglossidae comprises two genera (*Alopoglossus* and *Ptychoglossus*; Goicoechea et al., 2016; but see Morales et al., 2020). *Alopoglossus* species are characterized by having keeled scales on the forelimbs, and rhomboid, laterally imbricating dorsal scales (Harris, 1994), and includes 15 species: *Alopoglossus amazonius* Ruthven (1924), *A. andeanus* Ruibal (1952), *A. angulatus* (Linnaeus, 1758), *A. atriventris* Duellman (1973), *A. avilapiresae* Ribeiro-Júnior, Choueri, et al. (2020), *A. buckleyi* (O'Shaughnessy, 1881), *A. carinicaudatus* (Cope, 1876), *A. collii* Ribeiro-Júnior, Choueri, et al. (2020), *A. copii* Boulenger (1885), *A. embera* Peloso and Morales (2017), *A. festae* Peracca (1904), *A. lehmanni* Ayala and Harris (1984), *A. meloi* Ribeiro-Júnior (2018), *A. theodorusi* Ribeiro-Júnior, Meiri, et al. (2020), and *A. viridiceps* Torres-Carvajal and Lobos (2014). The genus is widely distributed in northern South America, and inhabits leaf litter of forests, plantations, and savanna-forest transitions, at elevations of 30–2500 m above sea level (Köhler et al., 2012; Ribeiro-Júnior, 2018; Ribeiro-Júnior & Amaral, 2017; Ribeiro-Júnior, Choueri, et al., 2020; Ribeiro-Júnior et al., 2008; Ribeiro-Júnior, Meiri, et al., 2020; Torres-Carvajal & Lobos, 2014). Three species of *Alopoglossus* occur in eastern Amazonia (*A. angulatus*, *A. meloi*, and *A. theodorusi*), while the remaining 12 species have a western distribution (Ribeiro-Júnior, Choueri, et al., 2020).

Morphologically, a monophyletic group composed by *A. angulatus*, *A. andeanus*, *A. avilapiresae*, *A. meloi*, *A. theodorusi*, *A. amazonius*, *A. collii*, and *A. carinicaudatus* share non-granular, keeled and imbricate scales on neck as an apomorphic diagnostic character (Ribeiro-Júnior, Choueri, et al., 2020). This character was traditionally used to

group all of them under the name *A. angulatus* (Köhler et al., 2012). Among species of this group, *A. amazonius* and *A. meloi* were the only ones sharing four pairs of chin shields (three pairs in all other species; Ribeiro-Júnior, Choueri, et al., 2020). However, after morphological evaluations of museum specimens, we noticed that a genetically divergent population from southwestern Amazonia (*A. "Southwest"* sensu Ribeiro-Júnior, Choueri, et al., 2020) also possess such a combination of neck scale condition and four pairs of chin shields. This finding indicates that, despite recent elucidation, the real diversity of this genus is still underestimated.

Here we delimit species boundaries and redefine phylogenetic relationships within *Alopoglossus*. To reach this goal, we obtained morphological and genetic data from new specimens and tissue samples from the Amazonas and Pará states (Brazil) and, through an integrative analytical approach, revealed the existence of three undescribed species. Some of the specimens representing these species were previously identified as *A. amazonius*, and they were used to define the diagnosis of it in Ribeiro-Júnior, Choueri, et al. (2020). Therefore, we describe those three new species and redefine *A. amazonius* sensu stricto. Moreover, we present the first detailed hemipenial description for *Alopoglossus*, and discuss on remaining taxonomy issues associated with this genus.

2 | MATERIAL AND METHODS

Based on 66 genetic samples (65 sequences from GenBank—Ribeiro-Júnior, Choueri, et al., 2020, and one newly generated in the course of this study; Table S1), and 401 specimens for morphological analyses (including five specimens for hemipenial morphology; List S1), we assessed the existence of separately evolving lineages and potential taxonomic impacts by comparing the congruence of molecular- and morphological-based analyses of species boundaries (Miralles & Vences, 2013; Padial et al., 2010). The molecular-based analyses included: (1) phylogenetic inferences considering variation of a concatenated dataset of four loci, two mitochondrial (mtDNA) and two nuclear (nuDNA); (2) distance-based and tree-based species delimitation analyses, supported by the variation of the best sampled and most variable mtDNA locus in our dataset; and (3) gene trees and haplotype networks considering the variation for each of the fragments of nuDNA loci. Morphology-based analyses included: (1) univariate and multivariate statistics and qualitative comparisons for differences in external morphology; and (2) qualitative comparisons for differences in hemipenial morphology. In each of these approaches, we search for differences among

samples that could indicate speciation of independently evolving lineages through reduction or absence of gene flow (Miralles & Vences, 2013). In molecular analyses, this can be inferred through reduction or absence of allele sharing (especially in syntopic specimens), and congruent divergences considering mtDNA and nuDNA diversification (Miralles & Vences, 2013). In morphological analyses, speciation can be inferred through fixed and unambiguous meristic characters, measurement variation and/or color patterns (Wiens & Servedio, 2000). In some cases, data were unavailable for a given lineage for some of the delimitation inferences. Thus, we used a conservative hypothesis of species boundaries for evidenced distinct groups recovered by a majority consensus of more than 50% of applied inferences (Padial et al., 2010). We followed the scheme proposed by Vieites et al. (2009) to designate the delimited groups as candidate species. Therefore, we considered taxonomic units that are molecularly distinct monophyletic groups and supported by unambiguous diagnostic morphological characters as new species (sp. nov.). We formally describe the three lineages meeting these criteria as new species. We consider lineages that were distinct based on molecular data sets and analyses, but presented morphological homogeneity, as deep conspecific lineages (DCLs), but do not describe them as new species.

2.1 | Molecular data sampling and analyses

To infer phylogenetic relationships, we compiled a molecular dataset focused on sequences of *A. angulatus* group downloaded from the GenBank online repository (Clark et al., 2016). Most of the downloaded sequences were generated by a recent taxonomic revision of this group (Ribeiro-Júnior, Choueri, et al., 2020). Gene sampling included four protein-coding loci, two from the mtDNA (cytochrome B, *Cytb*; NADH dehydrogenase subunit 4, *ND4*), and two from the nuDNA (synuclein alpha interacting protein gene, *SNCAIP*; prolactin receptor gene, *PRLR*). Taxon sampling included the nominal *A. angulatus* and closely related species *A. carinicaudatus*, *A. collii*, *A. avilapiresae* and *A. amazonius* (Ribeiro-Júnior, Choueri, et al., 2020). We also included in the dataset some hypothesized candidate species recently suggested in the literature (Moraes et al., 2020; Ribeiro-Júnior, Choueri, et al., 2020). Molecular data were generated for a newly collected specimen from the Lower Juruá River basin, state of Amazonas, Brazil. Sequences from the closely related species *Alopoglossus atriventris*, and the genus *Arthrosaura* Boulenger, 1885 were selected as outgroups for phylogenetic analyses. The final dataset comprised 61 individuals of the *A. angulatus* group and five

TABLE 1 Best-fit partition schemes and models of nucleotide substitution used for Bayesian phylogenetic analysis

Partition	Model	Gene - codon
1	GTR+ Γ	<i>Cytb</i> - 1; <i>ND4</i> - 3
2	K80+ Γ	<i>Cytb</i> - 2; <i>ND4</i> - 1; <i>SNCAIP</i> - 2
3	K80+ Γ +I	<i>PRLR</i> - 2; <i>PRLR</i> - 3
4	HKY+I	<i>Cytb</i> - 3; <i>ND4</i> - 2; <i>SNCAIP</i> - 1; <i>SNCAIP</i> - 3; <i>PRLR</i> - 1

outgroups. Loci coverage by terminals of the *A. angulatus* group was 52/61 (*ND4*), 47/61 (*Cytb*), 37/61 (*PRLR*) and 36/61 (*SNCAIP*). We did not include one *ND4* GenBank (accession number MN813037), generated by Morales et al. (2020), due to incongruences in sample locality and voucher.

For the newly generated molecular data, we extracted genomic DNA from tissue samples stored in 100% ethanol following the protocols of the Wizard® Genomic DNA Purification Kit (Promega, Madison, WI, USA). We amplified the *ND4* gene using primers *ND4L/ND4H* (Arévalo et al., 1994), following methods of Moraes et al. (2020). PCR products were purified with PEG (polyethyleneglycol) 8000 and sequenced using the Big Dye Terminator sequencing kit (Applied Biosystems, Waltham, MA, USA) in the automated sequencer ABI 3130 XL (Applied Biosystems, Waltham, MA, USA) of the Laboratório Temático de Biologia Molecular (LTBM), at the Instituto Nacional de Pesquisas da Amazônia (INPA). Consensus sequence was obtained using Geneious 8 (Kearse et al., 2012). Accession numbers and complete information related to sequences included in the final dataset can be found in Table S1.

Each gene was independently aligned using the MAFFT 7 online (Katoh & Standley, 2013) under default parameters, except that we used the G-INS-i strategy, which is best suited for global homologous sequences (Katoh & Standley, 2013), and realigned considering reading frame. For the complete phylogenetic inferences, we concatenated the loci, leading to a final alignment with 1790 base pairs (bp). Using this alignment, we assessed the phylogenetic relationships among individuals using both Bayesian inference (BI) and maximum likelihood (ML) optimality criteria in MrBayes 3.2.6 (Ronquist et al., 2012) and RaxML 8.2.10 (Stamatakis, 2014), respectively. These inferences were conducted on the CIPRES Science Gateway online server (Miller et al., 2010). For the BI, we divided the dataset considering first, second, and third positions of the codon of each gene and conducted the search for the best-fitting substitution models and partition schemes with PartitionFinder 2.1.1 (Lanfear et al., 2017), under the Bayesian information criterion (BIC). Best scheme indicated four partitions, and the best-fitting nucleotide substitution models are presented at Table 1. We conducted the analysis under two independent runs of 10^7 generations, starting with random trees and four MCMC chains (one cold), sampled every 10,000 generations. We assessed convergence of parameters (standard deviation of split frequencies <0.01 and estimated sample size >200) using Tracer 1.7 (Rambaut et al., 2018) and discarded a 10% burn-in of samples and trees. The ML analysis was conducted applying the GTR+ Γ model and 1000 replicates to estimate non-parametric bootstrapping values.

Species delimitation analyses applied to the mtDNA variation were conducted considering the best sampled locus in our dataset (*ND4*, 52/61 individuals, 638 bp). We applied a distance-based method Approximate Barcode Gap Discovery (ABGD; Puillandre et al., 2012), using an online server (<https://bioinfo.mnhn.fr/abi/public/abgd/abgdweb.html>), and a tree-based method Generalized Mixed Yule Coalescent with multiple threshold (GMYC; Fujisawa & Barraclough, 2013). For the ABGD delimitation, we used the Jukes-Cantor (JC) genetic distance correction, a prior of intraspecific

divergence (P) between 0.001 and 0.1, a proxy for minimum relative gap width (X) of 0.5, and 30 steps ($n = 30$). Based on an intraspecific divergence of 1% (arbitrary threshold recognized in vertebrate delimitation) and the end of a plateau for group number (Puillandre et al., 2012), we kept the 17th partition ($p = 0.0127$) to delimit the species. For the GMYC delimitation, we firstly reconstructed a time-calibrated ultrametric tree using the software BEAST 2.6 (Bouckaert et al., 2014), using the same nucleotide substitution models detailed for the complete phylogenetic inferences, an uncorrelated relaxed clock lognormal and a Yule speciation process prior. Time calibration was performed using a nucleotide substitution rate recognized to lizard mtDNA: mean of 0.0065 substitutions/my (standard deviation = 0.0025) (Macey et al., 1998). Despite having been estimated for a subset of loci, this rate has been applied as an overall representative of protein-coding loci of squamate mtDNA (e.g. Guo et al., 2019; Werneck et al., 2012). We performed two parallel runs of 50^7 iterations and 10% of initial burn-in, and assessed the convergence of parameters under the same criteria of the complete phylogenetic inferences. We extracted the maximum clade credibility tree with a burn-in of 25%, and performed the multiple threshold delimitation using only the *A. angulatus* group through the GMYC function of the “splits” package (Ezard et al., 2009) in R (R Core Team, 2013).

To further explore for evidence of allele sharing among lineages, we inferred gene trees and haplotype networks for each of the nuDNA loci. Gene trees were inferred under BI and ML optimality criteria, using the same softwares and methods described above. Using the ML gene trees, we built the haplotype networks with HaploView (Barrett et al., 2005). Moreover, with Mega 7 (Kumar et al., 2016), we computed the mean uncorrected pairwise genetic distances for the *ND4* between and within delimited species with 1000 bootstrap replicates to assess standard errors, and missing data removed after pairwise deletion. Values of genetic distance are presented as mean \pm standard error (%).

2.2 | Morphological data collection and analyses

We examined the external morphology of 401 *Alopoglossus* specimens (33 *A. amazonius*, six *A. andeanus*, 221 *A. angulatus*, 64 *A. avilapiresae*, seven *A. carinicaudatus*, nine *A. collii*, 23 *A. meloi*, seven *A. theodorusi*, and 29 morphologically distinct specimens). Specimens originate from Brazil, French Guiana, Suriname, Guyana, Colombia, Ecuador and Peru (see type series in the main text and Supporting Information), deposited in the following herpetological collections: Museu Paraense Emílio Goeldi, Belém, Brazil (MPEG); Museu de Zoologia da Universidade de São Paulo, São Paulo, Brazil (MZUSP); Museu de História Natural Capão da Imbuia, Curitiba, Brazil (MHNCL); Instituto de Pesquisas Científicas e Tecnológicas do Estado do Amapá, Macapá, Brazil (IEPA); Coleção de Anfíbios e Répteis, Instituto Nacional de Pesquisas da Amazônia, Manaus, Brazil (INPA-H); Departamento de Ecologia, Instituto Nacional de Pesquisas da Amazônia, Manaus, Brazil (APL); Universidade de Brasília, Brasília, Brazil (CHUNB); Laboratório de Anfíbios e Répteis, Universidade Federal do Rio Grande do Norte,

Natal, Brazil (AAGARDA), Coleção de Zoologia Paulo Bührnheim, Universidade Federal do Amazonas, Manaus, Brazil (CZPB-RP); Museo de Zoología de la Pontificia Universidad Católica del Ecuador, Quito, Ecuador (QCAZ); Centro de Ornitología y Biodiversidad, Lima, Peru (CORDIBI); the Academy of Natural Sciences of Drexel University, Philadelphia, USA (ANSP); the American Museum of Natural History, New York, USA (AMNH); the Museum of Comparative Zoology, Cambridge, USA (MCZ); the National Museum of Natural History, Washington, DC, USA (USNM); the University of Michigan Museum of Zoology, Ann Arbor, USA (UMMZ); and the Naturalis Biodiversity Center, Leiden, The Netherlands (RMNH); and the Muséum National d'Histoire Naturelle de Paris, France (MNHN-RA). Museum acronyms follow Sabaj-Perez (2016), with the addition of Laboratório da Albertina Lima, Instituto Nacional de Pesquisas da Amazônia, Manaus, Brazil (APL), Laboratório de Anfíbios e Répteis, Universidade Federal do Rio Grande do Norte, Natal, Brazil (AAGARDA), and Coleção de Zoologia Paulo Bührnheim, Universidade Federal do Amazonas, Manaus, Brazil (CZPB-RP). Comparisons with other species are based on literature data (see Ribeiro-Júnior, Choueri, et al., 2020).

Measurements were taken with digital calipers (± 0.1 mm). Scales were counted and other morphological characters were observed using a stereomicroscope. We measured (abbreviations in parentheses): snout-vent length (SVL), from the border of cloaca to the tip of snout; axilla-groin length (AGL), from the anterior margin of the hind limb to the posterior margin of the forelimb; head depth (HD) at the highest point dorsoventrally; head width (HW) at the widest point; head length (HL) from the anterior margin of tympanic aperture to the tip of snout; neck length (NL), from the posterior margin of the tympanic aperture to the anterior margin of the forelimb; forelimb length (FL); hindlimb length (HLL); shank length (ShL); tail length (TL). The meristic characters are (abbreviations in parentheses): dorsal scales (D), counted from the parietals posteriorly to the insertion of hindlimbs; ventrals (V), counted between the interbrachial and preanal shields; scale rows around the midbody (Mb); scale rows around the tail, immediately posterior to the cloaca; supraoculars (So); suboculars (Sbo); postoculars (Po); superciliaries (Sc); loreal (L); frenocular (Fr); supralabials (Sl); infralabials (Il); scales on sides of neck (Neck), in transverse rows; pairs of chin shields (Pairs); granular scales between the pairs of chin shields (BtwP); gulars (G), counted between the interbrachial and mental plates; femoral pores (Pores); lamellae under fourth finger (F); lamellae under fourth toe (T). The nomenclature of scale characters follows Ribeiro-Júnior (2018) and Ribeiro-Júnior, Meiri, et al. (2020), Ribeiro-Júnior, Choueri, et al. (2020).

We used univariate and multivariate statistics to test quantitative morphological distinctness between the groups of specimens delimited by molecular analyses. Specimens unsampled on the molecular datasets were included in a given group according to morphological congruences. Ribeiro-Júnior, Choueri, et al. (2020) provided detailed comparisons of species of the *A. angulatus* group, thus we focus on comparing species morphologically and molecularly related to the new species. This includes specimens with four pairs of chin shields (*A. amazonius*, *A. meloi*, and two

candidate species), and species of the *A. avilapiresae* group (one candidate species from the Tapajós River region and its closest related species [*A. avilapiresae* and *A. theodorusi*]). We investigated the degree of species overlap in the morphospace through principal component analyses (PCA), under six distinct partitions: 1) meristic characters (except femoral pores) of specimens with four pairs of chin shields; 2) meristic characters of only male specimens with four pairs of chin shields (including then femoral pores; found only in males); 3) meristic characters (except femoral pores) of specimens of a candidate species from Tapajós River region and its closest related species; 4) meristic characters of only male specimens of a candidate species from Tapajós River region and its closest relatives (including femoral pores); 5) measurements (except tail length) of specimens with four pairs of chin shields; and 6) measurements (except tail length) of specimens of a candidate species from Tapajós River region and its closest related species. We assessed for statistical significance in morphological differences among species using one-way ANOVA (with species as main factor), with post hoc Tukey HSD test for pairwise species comparisons. These statistical analyses were calculated using PAST v.3.26 (Hammer et al., 2001).

We examined coloration in life based on photographs of living specimens, and coloration in preservative based on holotypes. Variation in coloration in preservative was assessed in museum specimens. We created a distribution map using QGIS Las Palmas (v.2.18.3; <http://www.qgis.org/es/site/>), considering both molecular- and morphological designations (datum =WGS 1984).

The format of new species descriptions follows Ribeiro-Júnior et al. (2016), Ribeiro-Júnior, Meiri, et al. (2020), Ribeiro-Júnior, Choueri, et al. (2020), using the standardization of the nomenclature of alopoglossid and gymnophthalmid morphological characters suggested by Ribeiro-Júnior (2018).

Qualitative comparisons of hemipenial morphology were based on partially everted organs from five of the analyzed specimens. We prepared three hemipenes following the protocol described by Manzani and Abe (1988), with modifications proposed by Pesantes (1994) and Zaher and Prudente (2003). We examined two others deposited in the INPA for comparisons (*A. angulatus* [INPA-H 26240], and *A. avilapiresae* [INPA-H 9515]). Hemipenial descriptions follow the terminology in Dowling and Savage (1960), Uzzell (1973), Zaher (1999), Myers et al. (2009), and Nunes (2011). Comparisons with others species are based on literature data (Harris, 1994; Nunes, 2011; Peloso & Ávila-Pires, 2010).

3 | RESULTS

3.1 | Molecular analyses

Both BI and ML complete phylogenetic inferences recovered two deeply diverging and strongly supported clades within the *A. angulatus* group (Figure 1). One of these major clades is represented by samples of the nominal *A. angulatus*, which is broadly distributed in

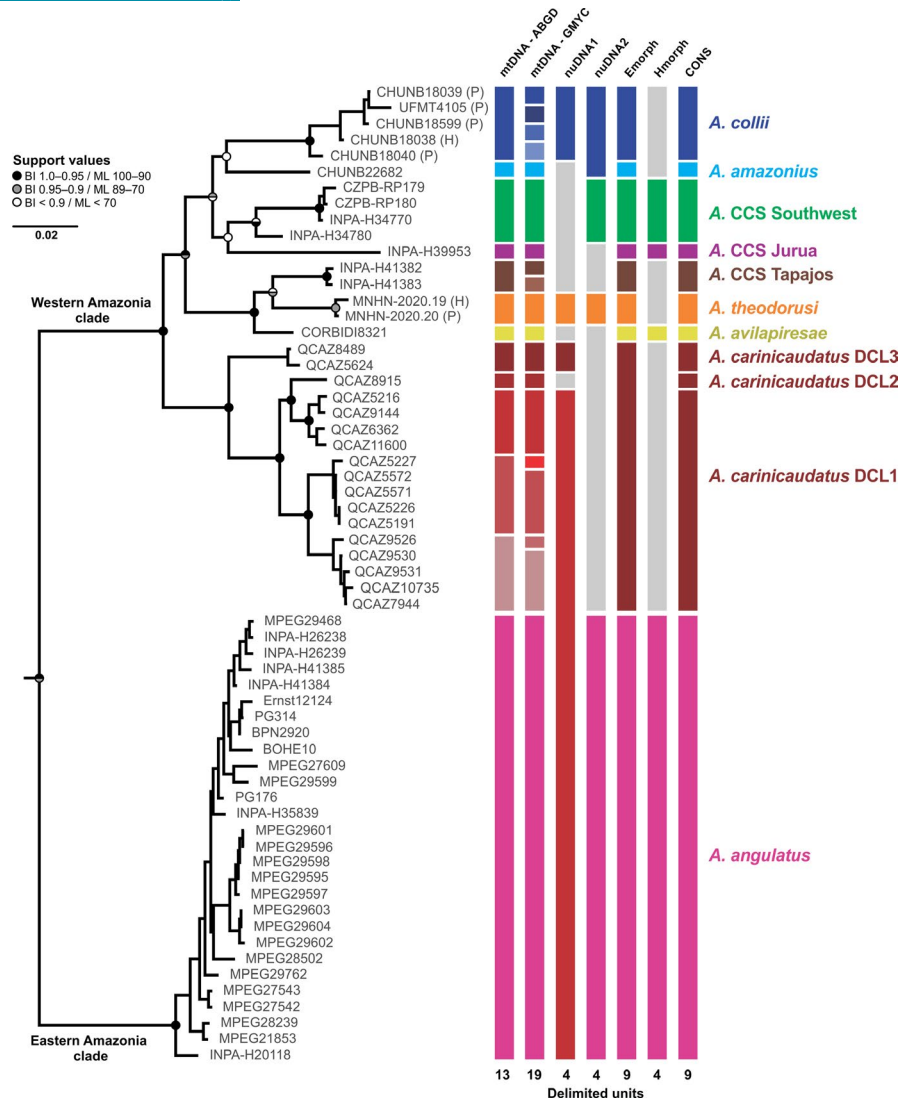


FIGURE 1 Phylogenetic relationships and integrative species delimitation within the *Alopoglossus angulatus* group. Phylogenetic tree inferred from the concatenated dataset of four loci (two mitochondrial, mtDNA +two nuclear, nuDNA) under Bayesian inference (BI). Nodal support values are shown inside divided circles (upper portion indicate posterior probabilities of BI and lower portion bootstraps of the Maximum Likelihood inference). Support values closer to terminal nodes and outgroups were omitted to improve visualization. Branch scale is indicated in number of substitutions per site. Results of delimitation analyses are summarized in colored panels at right of the tree. These analyses are based on molecular (mtDNA ABGD, mtDNA GMYC, nuDNA1, nuDNA2) and morphological variation (Emorph and Hmorph), leading to a majority rule conservative consensus of delimited species (CONS). mtDNA ABGD and mtDNA GMYC represent evidence from respective distance-based and tree-based species delimitation analyses, applied to the mitochondrial DNA; nuDNA1 and nuDNA2 represent evidence for nuclear DNA gene tree topologies and haplotype networks; Emorph and Hmorph represent evidence for external and hemipenial morphology. Light gray bars indicate unavailable evidence for that specific sample/clade. The three new species described in this study are highlighted as Confirmed Candidate Species (CCS) and DCL stands for the Deep Conspecific Lineages. H = holotype; P = paratype

eastern Amazonia and with relatively shallow and poorly supported internal divergences. In contrast, the second major clade present deeper internal divergences, and is mostly distributed in western Amazonia (exceptions are four samples from eastern Amazonia). This Western Amazonia clade contains lineages historically subsumed under *A. angulatus*, some of which were recently erected as new species (*A. carinicaudatus*, *A. amazonius*, *A. avilapiresae* and *A. collii*) (Ribeiro-Júnior, Choueri, et al., 2020). When represented by more than one sample, monophyly of species in this Western Amazonia

clade (*A. carinicaudatus*, *A. collii* and *A. theodorusi*) were corroborated with a high nodal support (Figure 1).

Some of the samples within the Western Amazonia clade did not cluster with nominal species and were not nested within them. Instead, they are highly divergent and most likely correspond to candidate species according to the new evidence presented below. Initial divergence within the Western Amazonia clade segregated *Alopoglossus carinicaudatus* from the other lineages. However, a considerable degree of divergence was also evident for samples

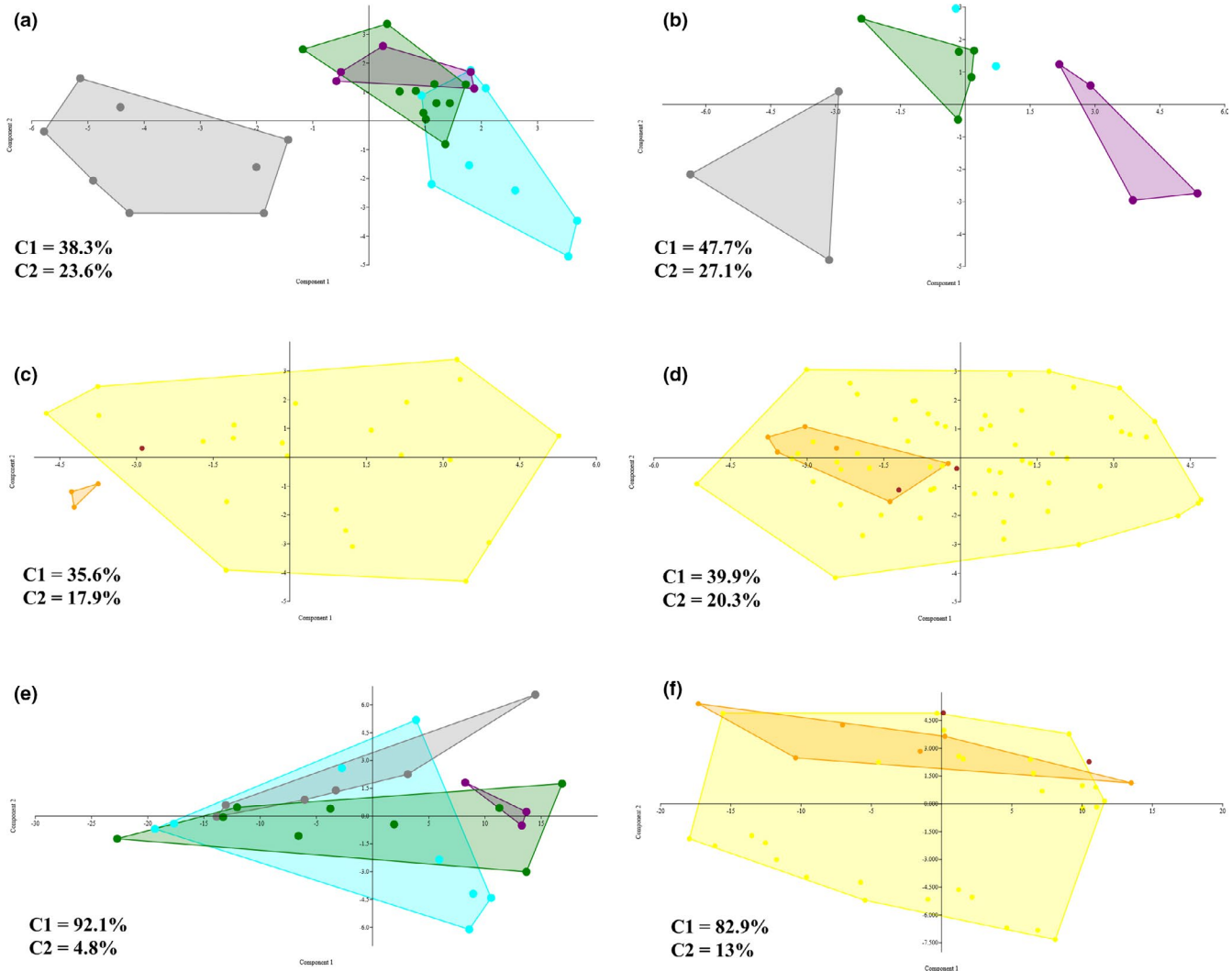


FIGURE 2 Principal component analysis comparing the overlapping degree of target species groups of *Alopoglossus* considering external morphology (meristic characters and measurements). The characters recovered as most important for the first and second axis are, respectively, shown in parentheses. (a) Meristic characters, except femoral pores, of specimens with four pairs of chin shields (scales on sides of neck; lamellae under the fourth toes). (b) Meristic characters of only male specimens with four pairs of chin shields (femoral pores; scales on sides of neck). (c) Meristic characters, except femoral pores, of specimens of the *A. avilapiresae* species group (scales between the third pair of chin shields; lamellae under fourth toes). (d) Meristic characters of only male specimens of the *A. avilapiresae* species group (femoral pores; dorsal scales). (e) Measurements, except tail length, of specimens with four pairs of chin shields (snout-vent length; axilla-groin length). (f) Measurements, except tail length, of specimens of the *A. avilapiresae* species group (snout-vent length; hind limb length). Distinct colors correspond to that presented in Figure 1: *A. amazonius* (light blue); *A. meloi* (gray); *A. "Jurua"* (purple); *A. "Southwest"* (green); *A. avilapiresae* (yellow); *A. theodorusi* (orange); *A. "Tapajos"* (brown)

attributed to *A. carinicaudatus* (Figure 1). A secondary split in this clade occurred between strongly supported subclade containing samples from Peru and eastern Amazonia (representing *A. avilapiresae*, *A. theodorusi* and one candidate species from the Tapajós river region: *A. "Tapajos"*), and a moderately well-supported subclade with samples from western Amazonia (representing *A. collii*, *A. amazonius* and two candidate species: *A. "Jurua"* and *A. "Southwest"*). Branch lengths indicate that Western Amazonia clade lineages are highly divergent from each other, but their interrelationships are poorly supported in both Bayesian inference and maximum likelihood analyses (Figure 1).

The ABGD species delimitation analysis delimited 13 evolutionary units (Figure 1): five of them correspond to nominal species

(*A. angulatus*, *A. collii*, *A. amazonius*, *A. avilapiresae* and *A. theodorusi*), another five distinct evolutionary units were recovered within a clade containing samples attributed to *A. carinicaudatus*, and the remaining three evolutionary units could not be attributed to any of the described species and correspond to the aforementioned candidate species. Results of the GMYC method mostly mirrored the ABGD, but recovered more (19) delimited evolutionary units. In this analysis, *A. carinicaudatus* was split into seven evolutionary units, *A. collii* into four and the candidate species from the Tapajós River region in two (Figure 1).

The variation of the nuclear DNA helped to consolidate some of the boundaries among samples, reinforcing the distinctiveness of a

candidate species from southwestern Amazonia and of *Alopoglossus theodorusi* (Figure 1, Figures S1 and S2). However, evidence of allele sharing, and absence of reciprocal monophyly, is notable among the nominal species pairs *A. carinicaudatus* versus *A. angulatus*, and *A. amazonius* versus *A. collii*. Despite this, these species pairs are allopatrically distributed, and are divergent in mtDNA and morphology (Figure 1).

3.2 | Morphological analyses

The PCA exploring the variation of 16 meristic characters (all characters, except femoral pores) of both males and females with four pairs of chin shields showed a complete segregation only between samples of *Alopoglossus meloi* and the remaining ones. In this analysis, *A. amazonius* marginally overlaps with the two candidate species identified based on molecular evidence from southwestern Amazonia (Figure 2a). However, considering only meristic characters of male specimens with four pairs of chin shields ($n = 17$, including femoral pores), we found almost no overlap among clusters representing nominal species and candidate species (Figure 2b). Similarly, the PCA summarizing meristic variation showed complete overlap between specimens of the candidate species from Tapajós River region and its closest relatives (Figure 2c). But, considering only males and including femoral pores ($n = 17$), a complete segregation is evident for clusters representing *A. theodorusi* and the candidate species, while the last one overlapped with *A. avilapiresae* (Figure 2d). The PCA of the measurements of specimens with four pairs of chin shields ($n = 9$, except tail length) showed complete segregation only between *A. amazonius* and one candidate species (Figure 2e), while the PCA comparing specimens of a candidate species from Tapajós River region and its closest relatives presented a complete segregation only between *A. theodorusi* and the candidate species (Figure 2f).

Univariate statistical analyses (ANOVA) revealed variable degrees of morphological divergence in meristic characters and measurements among examined groups. Nine meristic characters and two measurements present significant differences considering specimens with four pairs of chin shields (Table 3). There were significant differences in Tukey HSD in most meristic characters (Table 3), except for Po, G, and T. However, we could not test the differences in

the meristic characters So, Sc, Sbo, Pairs, Sl, and Il due to absence of variance in two or more groups of specimens. Considering measurements, significant differences were found with the Tukey HSD only in HD and SL. The candidate species from the Tapajós River region is represented by only two specimens, and because no variance was detected in its meristic characters, only tests considering measurements were applied comparing this taxon with its closest related species. According to the Tukey HSD test, most of the measurements do not differ significantly among these taxa, except for the HL of *Alopoglossus avilapiresae* and *A. theodorusi* (longer head in *A. avilapiresae*). A summary of the variation in meristic characters and measurements among specimens are presented in Tables 4 and 5, and a summary of the overall support of external morphology (Emorph) for species limits is presented in Figure 1.

3.3 | Integration of evidence lines and the consensus of taxonomic status

We applied a conservative consensus on species boundaries using a majority rule approach to integrate the limits inferred from different data sources. Notably, besides recovering the molecular and morphological distinctiveness of the included nominal species, three specimen groups were recovered under this approach as quite distinct from each other and in relation to the nominal species. We therefore consider these specimen groups as representative of new species, two of which composed by samples from southwestern Amazonia (*Alopoglossus* sp. nov. "Southwest" and *A. sp. nov.* "Jurua"), and one composed by samples from the Tapajós River region (*A. sp. nov.* "Tapajós"). Morphologically, the distinct nominal and the three new species evidenced by the consensus are especially divergent considering hemipenial characters and meristic variation of male specimens, while the morphological variation of female specimens and the measurements of both sexes hamper their delimitation. Molecular-based analyses (mostly GMYC) also found some subdivisions not congruent considering morphological variation (within *A. carinicaudatus*, *A. collii* and *A. sp. nov.* "Tapajós"), which probably resulted from the heterogeneous amplitude of divergences within major clades in our sampling. This pattern is especially evident considering samples attributed to *A. carinicaudatus*, which according to

Species	1	2	3	4	5	6	7	8	9
1 <i>A. amazonius</i>	—	1.1	1.0	0.9	0.9	1.2	1.0	1.0	1.2
2 <i>A. angulatus</i>	14.5	1.7	1.0	1.0	1.0	1.3	1.3	1.2	1.1
3 <i>A. carinicaudatus</i>	8.9	13.6	3.4	1.0	0.9	1.1	1.0	1.0	1.0
4 <i>A. avilapiresae</i>	7.1	13.0	8.2	—	1.1	0.9	1.1	1.1	1.0
5 <i>A. collii</i>	7.2	12.3	7.7	8.7	1.9	1.3	1.0	1.0	1.2
6 <i>A. theodorusi</i>	9.4	15.0	9.0	5.2	10.2	—	1.2	1.4	1.0
7 <i>A. "Jurua"</i>	8.3	14.4	9.6	9.0	9.1	9.8	—	1.0	1.3
8 <i>A. "Southwest"</i>	7.1	13.5	9.5	8.8	7.6	11.2	9.3	—	1.3
9 <i>A. "Tapajós"</i>	8.7	13.0	9.4	4.6	9.5	5.7	10.3	10.7	0.4

TABLE 2 Mean uncorrected pairwise genetic distances (lower diagonal) and standard deviations (upper diagonal) within the *Alopoglossus angulatus* group, considering a fragment of the mitochondrial gene ND4. Intraspecific distances, when applicable, are highlighted in bold at central diagonal. Values are presented in percentage (%)

the applied criterion would represent three distinct CS, but given the overall morphological homogeneity among these CS, and awaiting the availability of new data, we consider them as representatives of DCL within *A. carinicaudatus*.

Mean interspecific genetic distances among delimited taxa ranged from $4.6 \pm 1.0\%$ (between *Alopoglossus avilapiresae* and *A. sp. nov.* "Tapajos") to $11.2 \pm 1.4\%$ (between *A. sp. nov.* "Southwest" and *A. theodorusi*) (Table 2). Maximum mean interspecific genetic distance increase to up to $15.0 \pm 1.3\%$ when we consider both major clades within the *A. angulatus* group (Western Amazonia clade and *A. angulatus*). Intraspecific distances reached a maximum of 3.4% for *A. carinicaudatus*, but were mostly below 2.0% (Table 2).

In light of the combined molecular and morphological evidence, we formally describe the three well-supported new species. We also noticed that the morphological variation of specimens of these CCS fits in the *A. amazonius* diagnosis provided by Ribeiro-Júnior, Choueri, et al. (2020), and therefore we also redefine *A. amazonius* sensu stricto.

3.4 | Taxonomic and systematic account

Reptilia: Squamata

Gymnophthamoidea Fitzinger, 1826

Alopoglossidae Goicoechea et al., 2016

Alopoglossus Boulenger, 1885

***Alopoglossus gansorum* sp. nov.**

(Figures 1 and 2 [*Alopoglossus* Southwest]; Figures 3–8, 16; Tables 2–5, S2)

LSID: <http://zoobank.org/urn:lsid:zoobank.org:act:A1986198-1941-4E25-83C3-32ABAD75A46C>

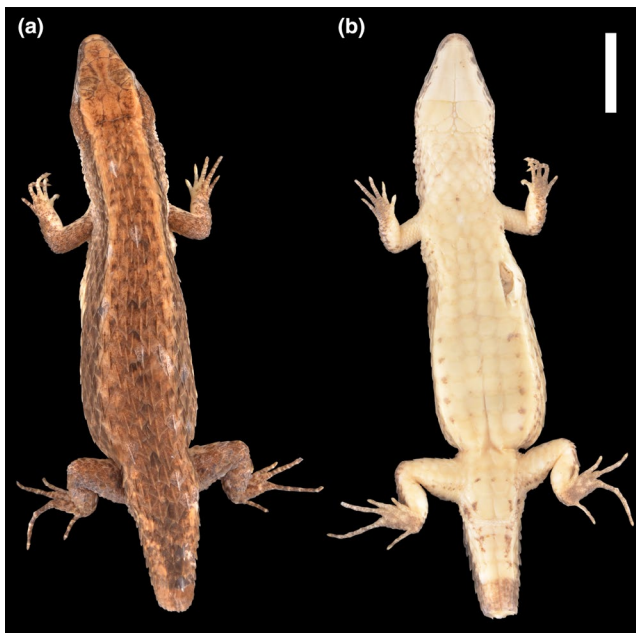


FIGURE 3 (a) Dorsal and (b) ventral views of the holotype of *Alopoglossus gansorum* sp. nov. (INPA-H 34819). Scale bar: 10 mm

Alopoglossus aff. *atriventris* Waldez et al. (2013: 309, Figure 4f).
Alopoglossus angulatus "Southwest" Ribeiro-Júnior, Choueri, et al. (2020: 6–8, 37–39; figures 2, 3, 20).

Holotype. INPA-H 34819, adult female, collected at Igarapé do Jacinto, Tapauá, Amazonas state, Brazil ($-5.69, -63.21$), by Alexandre Almeida and Luciana Frazão (Figures 3 and 4).

Paratypes. INPA-H 14001 (female), INPA-H 14003 (female), INPA-H 14005 (male), INPA-H 14007 (female), all collected on 2004 at Lago Ayapuá, Reserva de Desenvolvimento Sustentável Piagaçu-Purus, Anori, Amazonas, Brazil ($-4.36, -62.15$), by Fabiano Waldez; INPA-H 34770, male, collected at Reserva Biológica do Abufari, Tapauá, Amazonas, Brazil ($-5.28, -62.94$), by Alexandre Almeida and Luciana Frazão; INPA-H 34780, male, collected at Igarapé do Jacinto, Tapauá, Amazonas, Brazil ($-5.71, -63.22$), by Alexandre Almeida and Luciana Frazão; CZPB-RP 179, collected at Turiaçu, trilha oeste (at the 2500 m from the beginning of the trail), Tapauá, Amazonas, Brazil ($-4.97, -62.98$), by Deyla Oliveira, Juliana Vieira, Luciana Frazão-Luiz, Sergio Marques and Vinícius Carvalho; CZPB-RP 180,

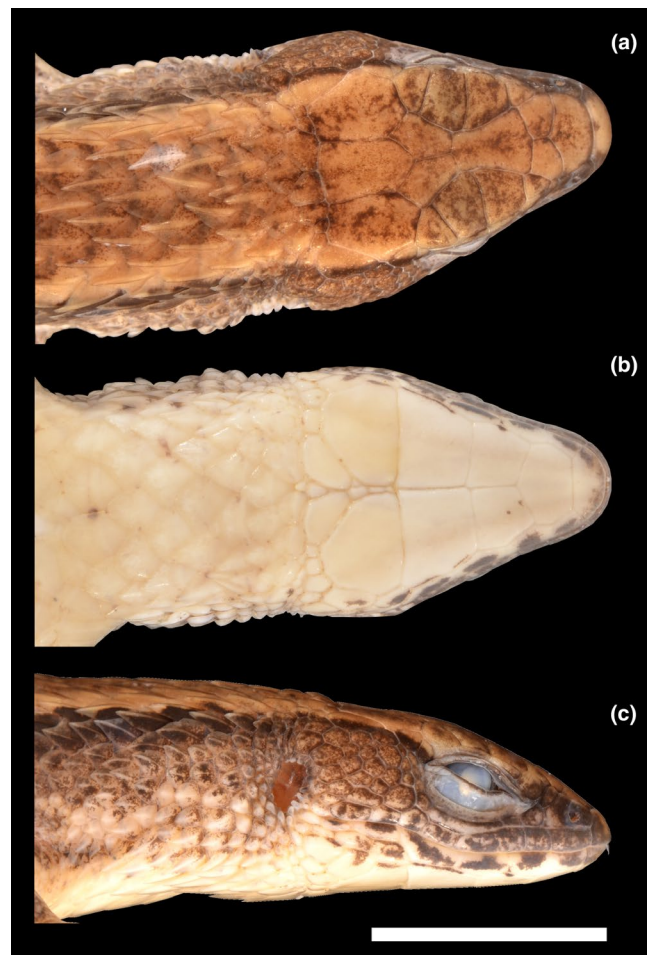


FIGURE 4 (a) Dorsal, (b) ventral and (c) lateral views of the head and neck of the holotype of *Alopoglossus gansorum* sp. nov. (INPA-H 34819). Scale bar: 10 mm



FIGURE 5 (a) Paratype of *Alopoglossus gansorum* sp. nov. (INPA-H 14005), with four pairs of chin shields and the fourth pair separated from gulars by two large scales; (b) holotype of *Alopoglossus indigenorum* sp. nov. (INPA-H 25543), with four pairs of chin shields and the fourth pair separated from gulars by two small scales; (c) paratype of *Alopoglossus tapajosensis* sp. nov. (INPA-H 41382), with three pairs of chin shields; (d) paratype of *Alopoglossus gansorum* sp. nov. (INPA-H 14005), with supratemporals separated from each other by one temporal scale; (E) holotype of *Alopoglossus indigenorum* sp. nov. (INPA-H 25543) and (f) paratype of *Alopoglossus tapajosensis* sp. nov. (INPA-H 41382), with supratemporals in contact with each other, forming a straight suture

collected at Turiaçu, trilha leste (1000 m), Tapauá, Amazonas, Brazil (−4.98, −62.96), by Deyla Oliveira, Juliana Vieira, Luciana Frazão-Luiz and Sérgio Marques.

Type specimens included in the molecular analyses. CZPB-RP 179 (paratype); CZPB-RP 180 (paratype); INPA-H 34770 (paratype); INPA-H 34780 (paratype).

Referred Specimens. MPEG 15861, collected at Rio Urucu, E. do Porto Urucu, próximo RUC-2/Petrobras, Coari, Amazonas, Brazil

(−4.85, −65.27); MPEG 17134, collected at Fazenda Eduardo Sá, sul da Fazenda Netinho, 12 km S de Tefé, Igarapé Curupira, Tefé, Amazonas, Brazil (−3.43, −64.73); specimen photographed at Floresta Estadual de Canutama, Canutama, Amazonas, Brazil (−6.49, −64.57), by Vinícius Carvalho.

Diagnosis. *Alopoglossus gansorum* sp. nov. is distinguished from all other species of *Alopoglossus* by the combination of the following characters: (1) non-granular, keeled, imbricate scales on medial and posterior sides of neck, varying from phylloid to



FIGURE 6 Living specimens of *Alopoglossus gansorum* sp. nov.: (a) paratype INPA-H 14005, photo: Fabiano Waldez; (b, c) paratype CZPB-RP 179, photo: Sergio Souza; (d) specimen from Canutama, photo: Vinícius Carvalho

micronate with almost rounded posterior margins, in 11–14 transverse rows; (2) four pairs of chin shield scales; (3) laterally to the fourth pair of chin shields, two large well-developed scales separating the third pair of chin shields from gular scales; (4) smooth scales along midventral gular region, with almost rounded posterior margins; (5) smooth scales on anterior temporal region; (6) feebly pointed distally scales on posterior temporal region; (7) smooth first supratemporal scale; (8) feebly keeled distally second supratemporal scale (smooth aspect), with an almost flat aspect, just slightly folding laterally toward the temporal region; (9) supratemporal scales separated from each other by a temporal scale, or touching each other with acute contact margins; (10) 20–23 total number of femoral pores in males.

Alopoglossus gansorum sp. nov. is also distinguished from other species of *Alopoglossus* by the combination of the following hemipenial characters: (11) progressive widening of the sulcus spermaticus; (12) sulcus spermaticus running in the frontal face of the base of the lobes; (13) sulcate face with a fine area parallel to the sulcus spermaticus without ornaments; (14) hemipenial body and base ornamented by 24 transversal flounces covering almost the complete organ; (15) lobes with pointed distal ends; and (16) absence of hemipenial body distal expansion.

Comparisons with other species. *Alopoglossus gansorum* sp. nov. differs from *A. atriventris*, *A. buckleyi*, *A. copii*, *A. embera*, *A. festae*, *A. lehmanni* and *A. viridiceps* (in parentheses) in having non-granular, keeled, imbricate scales on medial and posterior sides of neck (vs. granular in *A. atriventris* and *A. buckleyi*; mostly granular in *A. embera*, *A. festae*, *A. lehmanni* and *A. viridiceps*; conical with apparent bare skin between conical scales in *A. copii*); it also differs from *A. embera*, *A. festae* and *A. viridiceps* in not having gulars arranged in two longitudinal rows (vs. a double longitudinal row of widened gular scales), and from *A. lehmanni* in having dorsal scales rhomboidal, in oblique rows (vs. dorsal scales hexagonal with parallel lateral edges, in transverse rows).

From species of the *A. angulatus* group, *A. gansorum* sp. nov. differs from *A. andeanus*, *A. angulatus*, *A. avilapiresae*, *A. carinicaudatus*, *A. collii*, *A. tapajosensis* sp. nov., and *A. theodorusi* in having four pairs of chin shields (vs. three pairs of chin shields; Figure 5a,c). From species having four pairs of chin shields, *A. gansorum* sp. nov. differs from *A. amazonius*, *A. indigenorum* sp. nov., and *A. meloi* in having supratemporal scales separated from each other by a temporal scale, or touching each other with acute contact margins (vs. supratemporal scales in contact with each other, forming an evident, straight suture between them; Figure 5d,e). *Alopoglossus gansorum* sp. nov. also differs from *A. amazonius*, and *A. meloi* in having smooth temporal scales (vs. keeled), and feebly keeled distally second supratemporal scale, with smooth and flat aspect, just slightly folding laterally toward the temporal region (vs. strongly keeled second supratemporal scale, clearly folding laterally toward the temporal region); and from *A. meloi* in having 11–14 transverse rows of scales on the sides of the neck (vs. 6–8), and smooth scales on midventral gular region, with almost rounded posterior margins (vs. keeled, phylloid gular scales). *Alopoglossus gansorum* sp. nov. also differs from *A. indigenorum* sp. nov. in having, laterally to the fourth pair of chin shields, two large well-developed scales separating the third pair of chin shields from gular scales (vs. two small scales separating the third pair of chin shields from gular scales, or even third pair in short contact with gular scales; Figure 5a,b).

Based on hemipenial characters, *A. gansorum* sp. nov. is distinguished from *A. copii* in having a lobular base branched in two lobes (vs. lobular base not bifurcated), an area without ornaments in the distal region of the lateral and asulcate faces (vs. ornamented distal areas in lateral and asulcate faces), progressive widening of the sulcus spermaticus (vs. no changes in the widening of the sulcus spermaticus), a fine area parallel to the sulcus spermaticus without ornaments (vs. sulcate face completely covered with flounces), and 24 transversal flounces covering almost the complete organ (vs. 21 in *A. copii*). *A. gansorum* sp. nov. differs from *A. atriventris*, *A. buckleyi* and *A. festae* in having 24 transversal flounces that cover almost the complete organ (vs. 25–30 transversal flounces in *A. atriventris*, 37 in *A. buckleyi*, and 12 in *A. festae*), sulcus spermaticus running in the frontal face of the base of the lobes (vs. sulcus spermaticus running in the medial faces of the lobes), lobes with pointed distal ends (vs. lobes with rounded distal ends), progressive widening of the sulcus spermaticus (vs. no changes in the widening of the sulcus

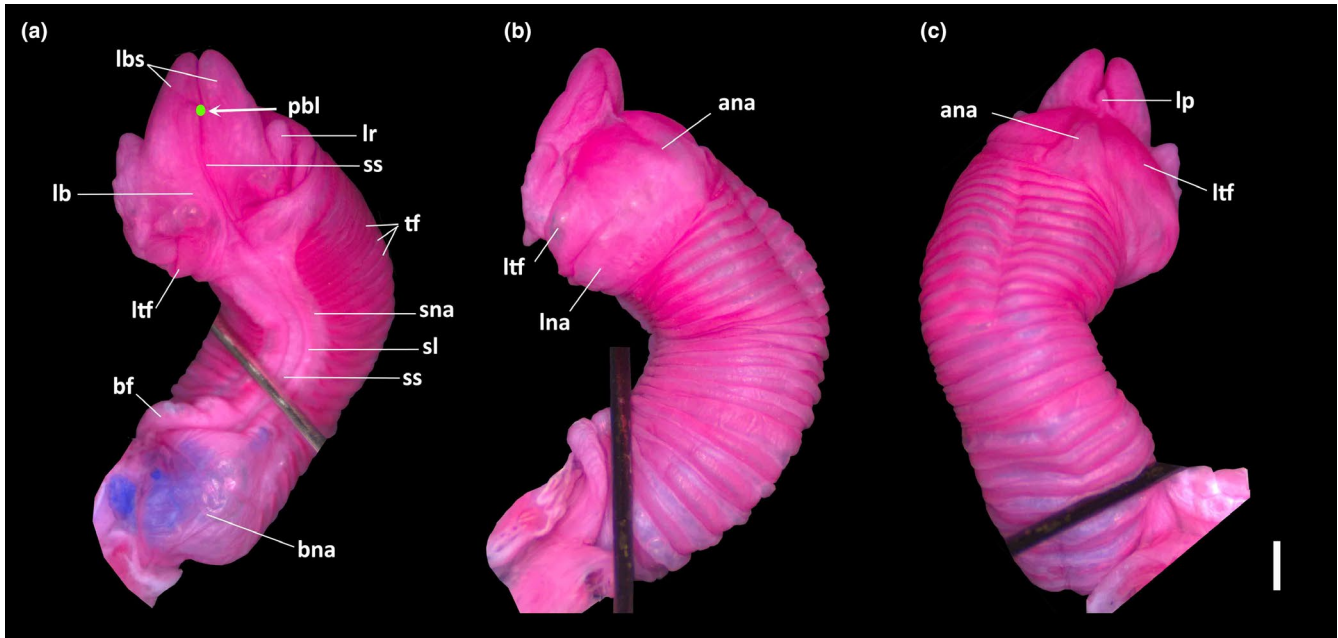


FIGURE 7 (a) Asulcate, (b) lateral, and (c) asulcate faces of the hemipenis of the paratype of *Alopoglossus gansorum* sp. nov. (INPA-H 14005). Scale bar: 1 mm. Green dot marks the lobes bifurcation point. ana, assulcate naked area; bf, base fold; bna, sulcate base naked area; lb, lobular base; lbs, lobes; lna, lateral naked area; lp, lobular protuberance; lr, lobular ridges; ltf, lateral transversal fold; pbl, lobes bifurcation point; sl, sucral lips; sna, sulcate naked area; ss, sulcus spermaticus; tf transversal flouces

spermaticus), and absence of hemipenial body distal expansion (vs. presence of a distal body expansion); it also differs from *A. atriventrtris* and *A. buckleyi* in having an area without ornaments in the distal region of the lateral and asulcate faces (vs. ornamented distal areas in lateral and asulcate faces). *Alopoglossus gansorum* sp. nov. differs from *A. angulatus*, *A. avilapiresae*, and *A. indigenorum* sp. nov. in having a progressive widening of the sulcus spermaticus (vs. no changes in the widening of the sulcus spermaticus), and 24 transversal flouces covering almost the complete organ (vs. 12–14 transversal flouces, in *A. angulatus*; 16 in *A. avilapiresae*; 21–22 in *A. indigenorum* sp. nov.); it also differs from *A. angulatus* and *A. indigenorum* sp. nov. in having a fine area parallel to the sulcus spermaticus without ornaments (vs. a decreasing ornamented area on the sides of the sulcus spermaticus, in *A. angulatus*; sulcate face completely covered with flouces, in *A. indigenorum* sp. nov.).

Description of the holotype. Female; body cylindrical, snout rounded, neck almost as wide as head and anterior part of body, limbs well developed, broken tail (Figure 3).

Rostral hexagonal, in broad contact with frontonasal, but also contacting first supralabial and nasal. Viewed dorsally, the rostral is about four times as wide as long. Frontonasal pentagonal, about twice as wide as long (wider posteriorly), anteriorly in contact with rostral, laterally with nasal and posteriorly with prefrontals. Prefrontals irregularly trapezoidal, wider than long, with a long medial suture with each other medially; laterally in contact with loreal and first supraocular, and touching nasal; posteriorly in contact with frontal. Frontal irregularly hexagonal, longer than wide (distinctly wider anteriorly); laterally in contact with first, second,

and third supraoculars; posteriorly in contact with frontoparietals. Frontoparietals irregularly pentagonal, longer than wide (wider posteriorly), with a long medial suture with each other medially; laterally in contact with third and fourth supraoculars; posteriorly in contact with interparietal and parietal. Interparietal pentagonal, lateral borders slightly opening toward neck (wider posteriorly), about twice as long as wide. A pair of irregularly heptagonal parietals, distinct wider medioanteriorly; parietals distinct wider than interparietal on anterior region, and narrower than it on the posterior region; anteriorly in contact with fourth supraocular, and laterally with first and second enlarged supratemporals, and one temporal (between the enlarged supratemporals). Parietal and interparietals of approximately similar length, forming a slightly undulating (almost straight) posterior head margin; interparietal posterior margin reaches slightly beyond parietals posterior margins (almost indistinct). Occipitals absent, but a pair of small, irregular in shape, imbricate, feebly keeled scales bordering each parietal posteriorly. Four supraoculars; first (anteriormost) smallest, contacting loreal, prefrontal, frontal, first superciliary, and second supraocular; second and third supraoculars largest, approximately similar in size, wider than long; second supraocular in contact with frontal, first and second superciliaries, and first and third supraoculars; third supraocular in contact with frontal, frontoparietal, third superciliary (touching second superciliary), and second and fourth supraoculars; fourth supraocular in contact with frontoparietal, parietal, third, fourth and fifth superciliaries, third supraocular, and first enlarged supratemporal. Five superciliaries; first largest, irregularly trapezoidal, slightly longer than tall; second, third, and fourth elongated (second and third about 3–4 times longer than tall, and fourth about twice as long as tall), fifth irregularly

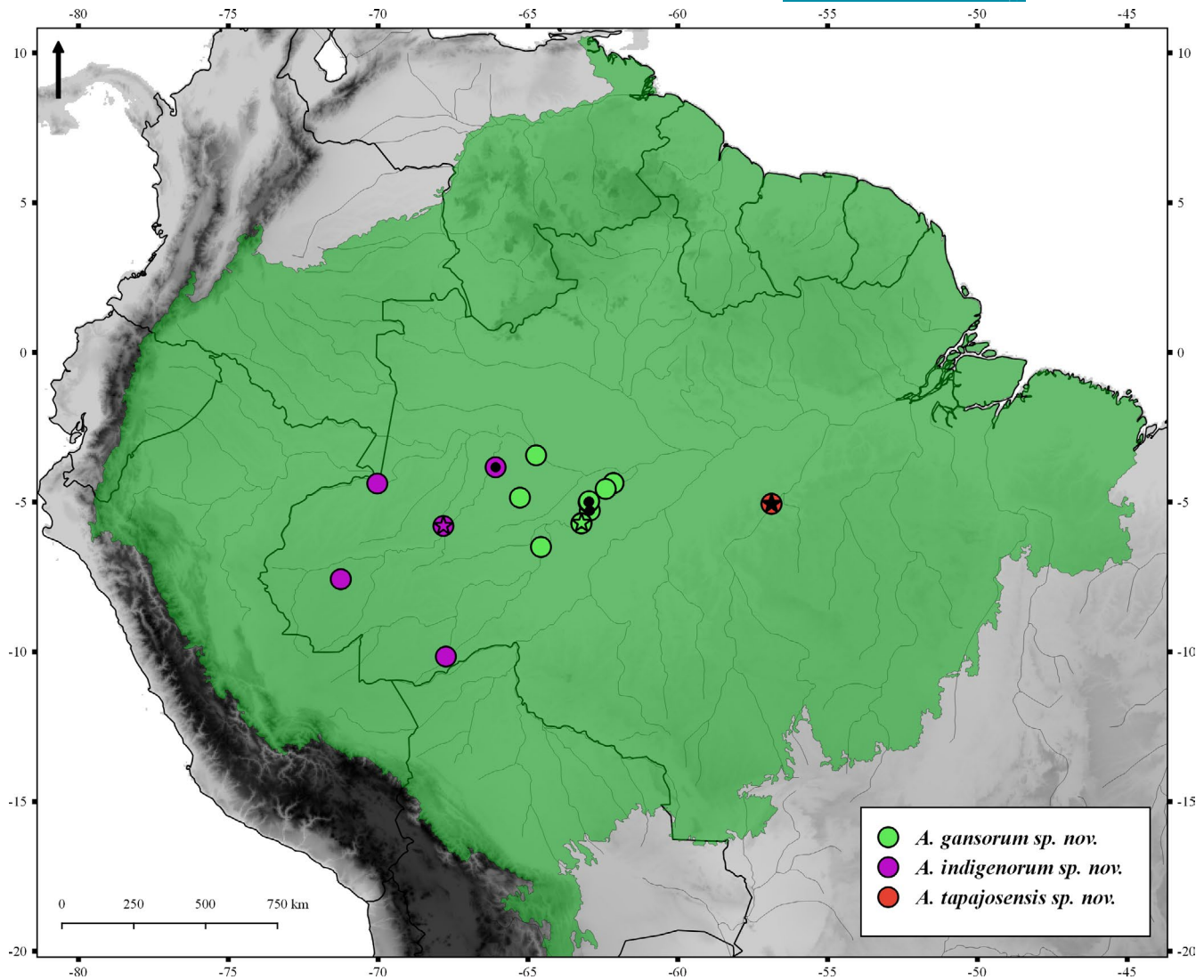


FIGURE 8 Distributional records of the three new species of *Alopoglossus* described here. Symbols with star denote type localities; black filled symbols represent samples included in the molecular analyses

triangular; first (anteriormost) in contact with loreal, first and second supraoculars and second superciliary; second in contact with second supraocular (touching third supraocular), and first and third superciliaries; third in contact with third and fourth supraoculars, and second and fourth superciliaries; fourth in contact with fourth supraocular, and third and fifth superciliaries; fifth in contact fourth supraocular, first enlarged supratemporal, fourth superciliary, and upper postocular (five very small scales between fifth superciliary, postoculars, and palpebrals, bordering eyes posteriorly, on the right side, and four on the left side, one of them larger than others). Three suboculars; first about twice as long as tall, contacting frenocular, third supralabial and second subocular; second longest, about eight times longer than tall, contacting third, fourth, fifth and sixth supralabials on the left side, third, fourth, and fifth supralabials on the right, and first and third suboculars; third irregularly pentagonal, as long as tall, slightly larger than first subocular, contacting sixth supralabial on the left side and fifth on the right, second subocular, the lower postocular, and one enlarged temporal. One almost indistinct

preocular between first supraocular, first superciliary, loreal, frenocular, and first subocular on the left side and two on the right. Two postoculars continuous with third subocular on the left side and three on the right; on each side postoculars are subequal in size, but on the left side taller than long, and on the right as tall as long. Lower eyelid with semitransparent disk of four large palpebrals on the left side and three on the right. Nasal divided, irregularly pentagonal, about twice as long as tall. Nostril in the mediolower part of nasal, directed posterodorsally. Loreal rectangular, contacting nasal, prefrontal, first supraocular, first superciliary and frenocular. Frenocular irregularly pentagonal, contacting loreal, nasal, second and third supralabials on the left side and only the second one on the right, and first subocular. Eight supralabials on the left side and seven on the right, third, fourth and fifth under the orbital region on the left side, and third and fourth on the right; first five supralabials on the left side, and first four on the right side irregularly rectangular, longer than tall (first and third longest on the left side, and third longest on the right side); sixth, seventh and eighth supralabials on the left

TABLE 3 Summary of quantitative analyses of meristic characters and measurements between groups of specimens with four pairs of chin shields

Meristics	<i>A. amazonius</i> (n = 33)	<i>A. meloi</i> (n = 23)	<i>A. "Jurua"</i> (n = 5)	<i>A. "Southwest"</i> (n = 10)
Dorsals*	mel	ama; sou	NA	mel
Ventrals*	mel, jur, sou	ama	Ama	ama
Midbody*	sou	NA	NA	ama
Postoculars	NA	NA	NA	NA
Scales on sides of neck*	mel	ama; jur; sou	mel	mel
Scales between 3rd pair of chin shields*	NA	sou	NA	mel
Scales between 4th pair of chin shields*	mel	ama; sou	NA	mel
Gulars	NA	NA	NA	NA
Lamellae under 4th finger*	sou	NA	NA	ama
Lamellae under 4th toe	NA	NA	NA	NA
Femoral pores in males*	NA	jur	mel; sou	jur
Measurements	(n = 8)	(n = 6)	(n = 4)	(n = 9)
Snout-vent length	NA	NA	NA	NA
Axilla-groin length	NA	NA	NA	NA
Head depth*	jur	NA	ama	NA
Head width	NA	NA	NA	NA
Head length	NA	NA	NA	NA
Neck length	NA	NA	NA	NA
Forelimb length	NA	NA	NA	NA
Hind limb length	NA	NA	NA	NA
Shank length*	jur	NA	ama	NA

Note: Tukey HSD comparisons: the first three letters of each group of specimens (or species, in *A. amazonius* and *A. meloi*) indicate significant differences in pairwise analyses. Supraoculars, superciliaries, suboculars, pairs of chin shields, supralabials, and infralabials were not included in analyses due to absence of variance found in two or more species.

n = total number of specimens studied; NA = pairwise comparisons not significant different from any species; NI = not included due to small sample size.

*Significant differences in one-way ANOVA ($p < 0.05$).

side, and fifth, sixth and seventh on the right side pentagonal; fourth supralabial smallest on the left side, and sixth on the right. Absence of a distinct post-supralabial scale. Temporals polygonal, juxtaposed, smooth on anterior and medial regions and feebly pointed distally on posterior region; most of them large, varying from as tall as wide to slightly longer than tall (medial temporal scales slightly smaller than others). Two enlarged supratemporal scales bordering the parietal, widely separated from each other by one temporal scale; first supratemporal irregularly triangular, smooth; second supratemporal largest, polygonal, longer than wide, feebly keeled distally (almost indistinct; smooth aspect). Viewed dorsally, the second supratemporals have an almost flat aspect, just slightly folding laterally toward the temporal region. Ear opening vertically oval, with anterior margin strongly denticulate. Tympanum recessed into a short auditory meatus. Except for second supratemporals and a few temporals feebly keeled distally, all dorsal and lateral head scales smooth and juxtaposed. Parietals and interparietal with feeble lateral ridges. Scales on nape irregular in shape, feebly keeled distally, smaller than dorsal scales. One transverse row of feebly keeled, granular scales

bordering ear opening posteriorly. Scales on sides of neck distinctly smaller than dorsals, keeled, imbricate, in 11-12 transverse rows; scales on anterior region feebly tuberculate with almost rounded posterior margins, disposed in regular transverse rows; scales on posterior region varying from phylloid to almost rounded posterior margins, disposed in irregular transverse rows. A distinctive area with granular scales much shorter than neck scales surrounds the area of arm insertion.

Mental trapezoidal, about twice as wide as long, with convex anterior margin. Postmental heptagonal, wider than long. Four pairs of chin shields; first two pairs in broad contact medially and with second, third and fourth infralabials; scales of the third pair irregularly hexagonal, separated from each other by four small scales, from infralabials by large scales, and from gulars by the fourth pair of chin shields, two large and one small scales on the left side of it and two large scales on the right side of it; scales of the fourth pair separated posteriorly from each other by two small scales; scales of the fourth pair in direct contact with gulars. Six infralabials, all longer than tall; second, third, fifth about twice as long as first, and fourth about

TABLE 4 Summary of the variation in meristic characters among species with four pair of chin shield, and among species of the *Alopoglossus avilapiresae* group

	Species with four pairs of chin shields				A. avilapiresae group			
	A. amazonius (n = 33)	A. gansorum sp. nov. (n = 10)	A. indigenorum sp. nov. (n = 5)	A. meloi (n = 23)	A. avilapiresae (n = 64)	A. tapajosensis sp. nov. (n = 2)	A. theodorusi (n = 6)	
Dorsals	27-31 (29.1 ± 1.4)	26-29 (27.7 ± 1)	25-29 (27 ± 1.6)	24-28 (25.8 ± 1.4)	23-30 (27.7 ± 1.7)	26; 27	25-28 (26.2 ± 1)	
Ventrals	17-19 (17.7 ± 0.7)	16-17 (16.6 ± 0.5)	16-17 (16.4 ± 0.5)	15-18 (15.9 ± 1)	14-18 (16.3 ± 0.9)	16; 18	16-17 (16.8 ± 0.4)	
Midbody	15-21 (18.9 ± 2.1)	19-22 (21 ± 1)	20-22 (20.8 ± 0.8)	19-21 (20.2 ± 0.8)	19-22 (20.6 ± 0.8)	20	20-22 (21 ± 0.9)	
Supraoculars	4	4	4	4-5 (4 ± 0.2)	4	4	4	
Superciliaries	5-6 (5.1 ± 0.3)	5	4-6 (4.9 ± 0.6)	5-7 (5.1 ± 0.4)	4-5 (5 ± 0.2)	5	5	
Suboculars	3	3	3	3	2-3 (3 ± 0.2)	3	3-4 (3.2 ± 0.4)	
Postoculars	2-3 (2.1 ± 0.3)	1-3 (2.3 ± 0.6)	1-2 (1.8 ± 0.4)	1-3 (2 ± 0.5)	2-3 (2.3 ± 0.5)	2	2-3 (2.2 ± 0.4)	
Supralabials	6-8 (7 ± 0.5)	7-8 (7.1 ± 0.3)	7-8 (7.1 ± 0.3)	7-8 (7.5 ± 0.5)	7-8 (7.1 ± 0.3)	7	7	
Infralabials	6	6-7 (6.2 ± 0.4)	6-7 (6.1 ± 0.3)	6	6-7 (6 ± 0.2)	6	6	
Scales on sides of neck	11-12 (11.5 ± 0.5)	11-14 (11.8 ± 0.8)	11-15 (12.7 ± 1.2)	6-8 (7.3 ± 0.6)	10-13 (11.4 ± 0.8)	10	9-10 (9.7 ± 0.5)	
Pairs of chin Shields	4	4	4	4	3	3	3	
Scales between 3 rd pair of chin shields	1-3 (1.6 ± 0.7)	2-3 (2.6 ± 0.5)	1-2 (1.4 ± 0.5)	0-3 (1.3 ± 0.6)	1-7 (4.2 ± 1.9)	2; 5	2-6 (2.8 ± 0.7)	
Scales between 4 th pair of chin shields	1-4 (2.6 ± 1.1)	1-4 (2.1 ± 1.1)	1-3 (1.6 ± 0.9)	0-2 (0.5 ± 0.7)	-	-	-	
Gulars	7-9 (8.2 ± 0.7)	7-8 (7.4 ± 0.5)	7-8 (7.6 ± 0.5)	7-9 (8 ± 0.3)	7-10 (8.6 ± 0.8)	9	7-9 (8.2 ± 0.7)	
Lamellae under 4 th finger	13-15 (14 ± 0.7)	14-18 (15.8 ± 1.4)	14-18 (15.7 ± 1.5)	14-16 (14.9 ± 0.9)	12-18 (14.3 ± 1.3)	15	13-15 (14 ± 0.9)	
Lamellae under 4 th toe	18-23 (20.2 ± 1.7)	18-23 (21 ± 1.4)	21-23 (21.4 ± 0.7)	18-23 (20.8 ± 1.4)	17-23 (19.9 ± 1.6)	19	19-23 (21.5 ± 1.8)	
Femoral pores in males	21-24 (22.5 ± 2.1)	20-23 (22 ± 1.7)	25-28 (26.5 ± 1.7)	20-23 (21.7 ± 1.3)	23-29 (25.7 ± 1.7)	22	22	

Note: Counts are presented as minimum-maximum (mean ± standard deviation). Counts for scales around the tail, number of loreal and frenocular scales presented similar values among specimens and species (n = 12; n = 1; n = 1; respectively).
n = total number of specimens studied.

TABLE 5 Summary of the variation in measurements among species with four pairs of chin shields, and among species of the *Alopoglossus avilapiresae* group

	Species with four pairs of chin shields						<i>A. avilapiresae</i> group		
	<i>A. amazonius</i> (n = 8)	<i>A. gansorum</i> sp. nov. (n = 9)	<i>A. indigenorum</i> sp. nov. (n = 4)	<i>A. meloi</i> (n = 6)	<i>A. avilapiresae</i> (n = 26)	<i>A. tapajosensis</i> sp. nov. (n = 2)	<i>A. theodorusi</i> (n = 6)		
Snout-vent length	34.6–62 (51.2 ± 9.1)	30.9–61.6 (47.5 ± 10.6)	54.6–59.4 (57.7 ± 2.7)	38.6–57.2 (46 ± 7.7)	36.1–58.7 (50 ± 7)	48.2; 56.7	33.8–59.6 (44.8 ± 8.8)		
Axilla–groin length	16.6–30.7 (25.2 ± 5.2)	14–28.6 (21.8 ± 5.5)	25–28.8 (27.2 ± 1.9)	16.4–27.8 (20.3 ± 4.1)	14.7–30.4 (23.3 ± 4.3)	27.1; 21	15.3–28.1 (21.6 ± 4.5)		
Head depth	4.1–7.5 (6 ± 1.1)	4.3–7.5 (5.8 ± 1.2)	6.9–7.5 (7.1 ± 0.3)	5–7.1 (5.9 ± 0.7)	4.4–7.1 (6 ± 0.7)	6.5; 5.6	5–6.2 (5.4 ± 0.4)		
Head width	5.2–9.8 (8.2 ± 1.6)	5.6–10.3 (8 ± 1.6)	9.4–10.1 (9.8 ± 0.4)	6.2–9.5 (7.2 ± 1.2)	5.8–9.4 (7.7 ± 0.9)	8.1; 7.6	6–9.1 (7.4 ± 1)		
Head length	7.7–13.5 (10.9 ± 1.6)	7.7–13.9 (10.9 ± 2.1)	12.4–13.3 (12.9 ± 0.5)	8.6–12.5 (10.5 ± 1.4)	8.5–13.3 (11 ± 1.3)	11.1; 10	7.8–11.5 (9.5 ± 1.2)		
Neck length	5.1–9.6 (7.5 ± 1.6)	5.1–9 (7.4 ± 1.5)	7.8–9.2 (8.7 ± 0.7)	5.7–11.5 (7.5 ± 2.2)	5.4–9.8 (7.5 ± 1)	8; 7.3	5–8.8 (7.1 ± 1.2)		
Forelimb length	8.8–17 (13.9 ± 2.6)	9–17 (13 ± 2.8)	15	10.5–17.5 (12.6 ± 2.6)	6.7–18.8 (11.9 ± 2.7)	15.3; 13.3	10.1–15.5 (12.9 ± 2)		
Hind limb length	15.4–27 (22.8 ± 4.1)	12–28 (19.8 ± 4.8)	25–26 (25.3 ± 0.6)	16.3–32.2 (21.6 ± 5.9)	11.2–25.5 (18.6 ± 4.8)	25; 23.6	16.4–25.2 (20.3 ± 3.1)		
Shank length	5.2–7.8 (6.5 ± 0.8)	5–10.1 (8 ± 1.7)	9.6–10 (9.7 ± 0.2)	6.3–10.7 (7.7 ± 1.7)	5.4–8.7 (7.2 ± 1)	7.8	5.5–7.9 (6.7 ± 0.8)		
Tail length	57.3–82.3 (76.9 ± 16.6; n = 8)	48–88 (68.3 ± 19.7; n = 3)	96–101 (98.3 ± 2.5; n = 4)	71.5–97 (82 ± 13.3; n = 3)	50.3–97 (78.2 ± 15.2; n = 16)	110.6 (n = 1)	69.4 (n = 1)		

Note: Measurements are presented as minimum–maximum (mean ± standard deviation). Only intact and non-regenerated tails were considered. n = total number of specimens measured.

three times longer than first; sixth smallest; suture between third and fourth below center of eye. Absence of a distinct post-infralabial scale. Gular scales slightly smaller than dorsals, imbricate, differentiated in size (but not in shape) toward collar; except by lateralmost scales (varying from feebly to strongly keeled, phylloid), gular scales smooth, with almost rounded posterior margins; anteriormost transverse row feebly pointed distally; scales on medial and posterior gular regions wider and larger than scales on anterior gular region; gular scales in seven transverse rows. Posterior row of gular scales (collar) with 10 smooth scales, smaller than preceding rows; lateral collar scales regularly organized in transverse row; medial collar scales irregular in shape and irregularly disposed obliquely/transversally. Absence of gular fold.

Dorsal scales rhomboid, strongly keeled and mucronate, imbricate and disposed in oblique rows; 29 scales along a middorsal line from parietals to the level of hind limbs. Scales on flanks similar in shape and size to dorsals. Twenty-two scales around midbody. Ventral scales smooth, imbricate; anterior ventral scales with irregular posterior margins; medial and posterior ventral scales varying from almost straight to rounded posterior margins; 16 transverse rows and four longitudinal rows between collar and preanals. Seven smooth scales in preanal plate (four anterior ones, two posteriors, and one small lateral on the left side); posterior scales slightly larger than anterior ones; anterior scales larger than preceding ventral scales. Preanal and femoral pores absent (female). Dorsal limb scales rhomboid, imbricate, strongly keeled, and mucronate; ventral scales on upper forelimbs and posterior aspect of thighs keeled, imbricate, feebly tuberculate with rounded posterior margins; ventral scales on lower forelimbs and hind limbs smooth, varying from rounded to triangular posteriorly. Five clawed digits on each limb. Lamellae under fingers single, transversely enlarged and smooth, with 14 under the fourth finger; lamellae under toes divided (except the 2–4 terminal ones on toes), with 20 under the left fourth toe, and 18 under the right fourth toe. Scales on tail keeled, slightly mucronate, imbricate, arranged in transverse rows (not counted; broken tail) and in 12–14 longitudinal rows at the base of the tail; scales in the two paravertebral rows wider than long near the base of the tail. Keels mostly sharp on tail (except on ventral surface), forming four dorsal, two lateral (on each side) and two ventrolateral distinct longitudinal ridges. Ventral scales at the base of tail smooth, with irregular posterior margins.

Measurements of the holotype (in millimeters). SVL = 60.8; AGL = 28.0; HD = 7.5; HW = 10.3; HL = 13.8; NL = 9.0; FL = 16.0; HLL = 22.0; ShL = 9.4; TL = 11.0 + (broken).

Coloration of the holotype in preservative. Dorsal surface of head, body and base of tail light brown; dorsal surfaces of head and neck densely speckled with very small dark-brown dots, mainly concentrated on scale's sutures, but also on supraocular region and bordering parietals/interparietal, and forming an inconspicuous longitudinal stripe from rostral to the suture between frontoparietals; dorsal surfaces of body and limbs densely speckled

with very small and large dark-brown dots; on the posterior dorsal surface between hind limbs and base of tail, the dark-brown dots merge to form an inconspicuous dark-brown medial band. Lateral aspect of head, neck, body and tail light brown densely speckled with very small dark-brown dots, becoming cream ventrally; on the anterolateral surface of head, flanks, and on lateral surface of base of tail the very small dark-brown almost cover the entire surface. A continuous dark-brown line extending posteriorly from the lateral surface of rostral and nostril, passing through the eyelids, first and fifth superciliaries, supratemporals, dorsolaterally on neck, flanks, above hind limbs insertion, and reaching laterally the tail; the dark-brown line bordered dorsally by a cream stripe from posterior corner of eye to base of tail (inconspicuous from medial surface of body to between hind limbs; wider, but also inconspicuous, on the base of tail). A dashed cream line extending posteriorly from the supralabials under the eye, passing through the lower part of the ear opening and neck, above the forelimbs insertion, ventrolaterally on flanks, and reaching the anterior surface of hind limbs. Ventral surface cream, with scattered, small, irregular dark-brown spots on gular region, ventrolateral surface of body, limbs and tail.

Coloration in life. Paratype INPA-H 14005, an adult male, from Lago Ayapuá, Reserva de Desenvolvimento Sustentável Piagaçu-Purus, Anori, Amazonas state, Brazil (−4.36, −62.15) (Figure 6a): dorsal surfaces of head, body, limbs and tail light brown; from nape and along middorsal surface, to the base of tail, large black dots forming an irregular longitudinal series of dots; on the posterior dorsal surface of body, between the hind limbs and the base of the tail, the black dots merge to form an inconspicuous wide, black medial band. Lateral surface of head light brown, with a continuous dark-brown line extending from the nostril to above the ear opening, and a continuous dark-brown line extending from below the eye to below the ear opening; lateral surfaces of neck and body black; a continuous white stripe extending posteriorly from the supralabials under the eye, passing through the lower part of the ear opening and neck, above the forelimbs, and reaching ventrolaterally the flanks. Iris vividly orange.

Paratype CZPB-RP 179, an adult male, from Reserva Biológica Abufari, comunidade Turiaçu, Tapauá, Amazonas state, Brazil (−4.97, −62.98) (Figure 6b,c), and specimen from Floresta Estadual de Canutama, Canutama, Amazonas state, Brazil (−6.49, −64.57) (Figure 6d): dorsal surfaces of head and body light brown, and dorsal surfaces of limbs dark-brown; speckled black dots can be seen on head, neck and limbs. Lateral surfaces of head, neck and flank black; a continuous white stripe extending posteriorly from the supralabials under the eye, passing through the lower part of the ear opening and neck, above the forelimbs, and reaching ventrolaterally the flanks. Iris vividly red in CZPB-RP 179, and vividly orange in the specimen from Canutama. CZPB-RP 179 with ventral surfaces of head, gular and body white with black dots; on head, dots are mainly concentrated on sutures of scales, and on gular and body mainly on anterior and lateral margins of the scales; posterior surface of body,

preanal plate, hind limbs and tail orange, with a few sparse, small black dots (Figure 6c).

Variation. All specimens have frontoparietals with long, straight medial suture in contact with each other, except INPA-H 14001 (juvenile) that has a relatively short but straight medial suture. Specimen INPA-H 14007 has one postocular on one side and two on the other side (all other specimens have 2–3 postoculars); only the holotype (INPA-H 34819) has eight supralabials on one side (all other specimens have seven supralabials on both sides). INPA-H 14003 has supratemporals touching each other, with acute contact margins on both sides; MPEG 15861 has supratemporals touching each other on the right side, with acute contact margins (left side with supratemporals separated from each other by one temporal scale). INPA-H 14001 and INPA-H 34780 (juveniles) have parietals and interparietal without lateral ridges (smooth). INPA-H 14001 has third pair of chin shields separated from each other by one small scale anteriorly, one large scale posteriorly, and contacting each other on medial region (all other specimens have third pair of chin shield complete separated from each other); fourth pair of chin shield either completely separated from each other by large/small scales or separated from each other only posteriorly; scales of the fourth pair of chin shields and large scales laterally to them either in direct contact with gulars or separated from them by small scales. All specimens (juveniles and adults) have smooth gular scales with rounded posterior margins (except lateralmost scales, varying from feebly to strongly keeled); ventral scales smooth with irregular posterior margins, varying from almost straight to rounded. Preanal and femoral pores are absent in females. In males, the femoral pores are arranged in a continuous, well-separated series on each side; two pores on each side are in the preanal position; each pore is between two scales; total number of pores 20–23 (INPA-H 34780: 20 pores; INPA-H 14005 and INPA-H 34770: 23 pores). Tables 3 and 4 present a summary of the variation in meristic characters and measurements, respectively. Table S2 presents a summary of the measurements in males and females.

Variation in coloration in preservative: on dorsal surface of head, speckled very small dark-brown dots forming an inconspicuous longitudinal stripe from rostral to either frontoparietal suture or prefrontal–frontal suture. Large dark-brown dots forming a mid-dorsal series of dots from the nape to the base of tail, or only from hind limbs to the base of tail. In males, anterolateral surface of head, upper temporal region, and upper flank light brown densely speckled with very small dark-brown dots; lower temporal region, lateral surface of neck and medial surface of flanks black; ventralmost lateral surface of head, neck and flanks (below the cream line) black with scattered cream large dots; from second pair of chin shields to collar, very small black spots covering almost all scales; all ventral scales covered anteriorly and laterally by very small black spots.

Hemipenial description. Hemipenis of the paratype INPA-H 14005 (Figure 7): The hemipenis is cylindrical and slightly bilobed. The sulcus spermaticus is single, centrolineal, and has thick sulcal lips.



FIGURE 9 (a) Dorsal and (b) ventral views of the holotype of *Alopoglossus indigenorum* sp. nov. (INPA-H 25543). Scale bar: 10 mm

The hemipenial base and body are ornamented by transversal flounces and do not show any calcareous structures. The lobular region is defined by two thick folds, one on each side, extending transversely over the distal regions of the sulcate and lateral faces, from the laterals of the sulcus spermaticus to the sides of the distal region of the asulcate face. Between these transversal folds, in the central axis of the organ, arise a base distally bifurcated originating the lobes. The hemipenial lobes are short, have broad bases, and pointed distal ends, and between them, there is a small protuberance in the asulcate face. In the lobes' bases, there are some ridges and bulges in the sulcate and lateral faces, but its partial eversion avoids the detailed description of the morphology of this region. In the base of the organ, the sulcus spermaticus is narrow and covered by a thick fold of tissue. The sulcus is widening as it runs toward the distal part of the organ. Once reaching the lobular region, the thickness of the sulcal lips decreases, and the sulcus course drastically narrows to pass between the transverse folds of the lobular region. The sulcus spermaticus and the sulcal lips continue further until reaching the point of bifurcation of the lobes. The hemipenial body and base are ornamented by 24 transversal flounces that cover almost the complete organ. The base's sulcate face is naked, while flounces cover the lateral and asulcate faces. The three faces of the body are ornamented, but also show three naked areas, (1) in the sulcate face, between the tips of the transversal flounces and the sulcal lips; (2) in the distal region of the lateral faces, below the transversal fold

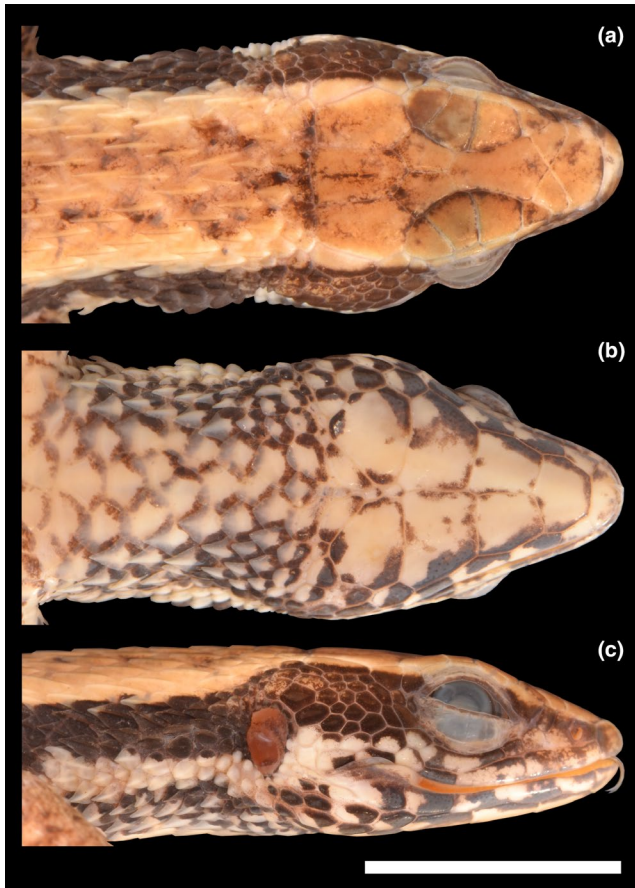


FIGURE 10 (a) Dorsal, (b) ventral and (c) lateral views of the head and neck of the holotype of *Alopoglossus indigenorum* sp. nov. (INPA-H 25543). Scale bar: 10 mm

that bounded the lobular region; and (3) in the distal region of the asulcate face, a triangular-shaped area that contacts the base of the asulcate face of the lobes.

Etymology. The specific epithet in genitive plural refers to Carl Gans and the Gans family. Members of the Carl Gans family run the Gans Collections and Charitable Fund, a private foundation established by Carls Gans to offer grants to students or researchers working in collection-based research. Their efforts in continuing and perpetuating Carl Gans' legacy in taxonomy have allowed the discovering of considerable species diversity in the main ecoregions around the globe, from the Sahara Desert to the Amazonia. The uncovered species diversity and new descriptions supported by the Gans Fund become crucial tools in conservation policies. The foundation also helps to keep alive and active taxonomy initiatives, a field in general biology often neglected by governments and policy decisions. This study and many others were only possible thank to the Gans Collections and Charitable Fund.

Distribution and habitat. *Alopoglossus gansorum* sp. nov. is distributed in southwestern Amazonia, between the lower Juruá and Madeira river basins (south of the Amazon River), and is endemic to the state of Amazonas, Brazil (Figure 8). In the Reserva de Desenvolvimento

Sustentável Piagaçu-Purus, Waldez et al. (2013) sampled flooded and non-flooded forests, and *A. gansorum* sp. nov. was only found in non-flooded forest. Vinicius Carvalho recorded it active in leaf litter of non-flooded, during the day, in the Floresta Estadual de Canutama, Amazonas, Brazil. The presence of most of its distribution range in protected areas, suggests a Least Concern conservation status.

***Alopoglossus indigenorum* sp. nov.**

(Figures 1 and 2 [*Alopoglossus* Juruá]; Figures 5, 8–11, 16, S3; Tables 2–5, S2)

LSID: <http://zoobank.org/urn:lsid:zoobank.org:act:86AD12AD-7694-4FA4-9949-5986546B0C81>

Alopoglossus angulatus Pantoja and Fraga (2012: 362, 366, appendix 4A).

Holotype. INPA-H 25543, adult male, collected in April 2007 at Reserva de Desenvolvimento Sustentável Uacari, Carauari, Amazonas, Brazil (−5.79, −67.82), by Fabiano W. S. Guimarães (Figures 9 and 10).

Paratype. INPA-H 39953, adult male, collected on 16 July 2018 at Reserva Extrativista do Baixo Juruá, Juruá, Amazonas state, Brazil (−3.83, −66.08), by Leandro J. C. L. Moraes, Raíssa N. Rainha and Alan F. S. Oliveira.

Type specimens included in the molecular analyses. INPA-H 39953 (paratype).

Referred Specimens. INPA-H 30243 and INPA-H 30244, male and female, respectively, collected at Reserva Extrativista do Rio Gregório, Ipixuna, Amazonas, Brazil (−7.60, −71.20), by Rafael de Fraga and Davi Pantoja; MPEG 15991, male, collected at Benjamin Constant, Amazonas, Brazil (−4.37, −70.03); specimen photographed at Senador Guimard, Acre (−10.16, −67.74), by Paulo Melo-Sampaio.

Diagnosis. *Alopoglossus indigenorum* sp. nov. is distinguished from all other species of *Alopoglossus* by the combination of the following characters: (1) non-granular, keeled, imbricate scales on medial and posterior sides of neck, varying from phylloid to mucronate with almost rounded posterior margins, in 11–15 transverse rows; (2) four pairs of chin shield scales; (3) laterally to the fourth pair of chin shields, two small scales separating the third pair of chin shields from gular scales, or even the third pair in short contact with gular scales; (4) scales along midventral gular region varying from smooth to feebly keeled, and from having irregular posterior margins, to mucronate or phylloid; (5) smooth scales on anterior temporal region; (6) smooth or feebly keeled distally scales on posterior temporal region; (7) smooth first supratemporal scale; (8) feebly keeled distally second supratemporal scale (smooth aspect), with an almost flat aspect, just slightly folding laterally toward the temporal region; (9) supratemporal scales in contact with each other, forming an evident, straight suture between them; (10) 25–28 total number of femoral pores in males.

Alopoglossus indigenorum sp. nov. is also distinguished from other species of *Alopoglossus* by the combination of the following

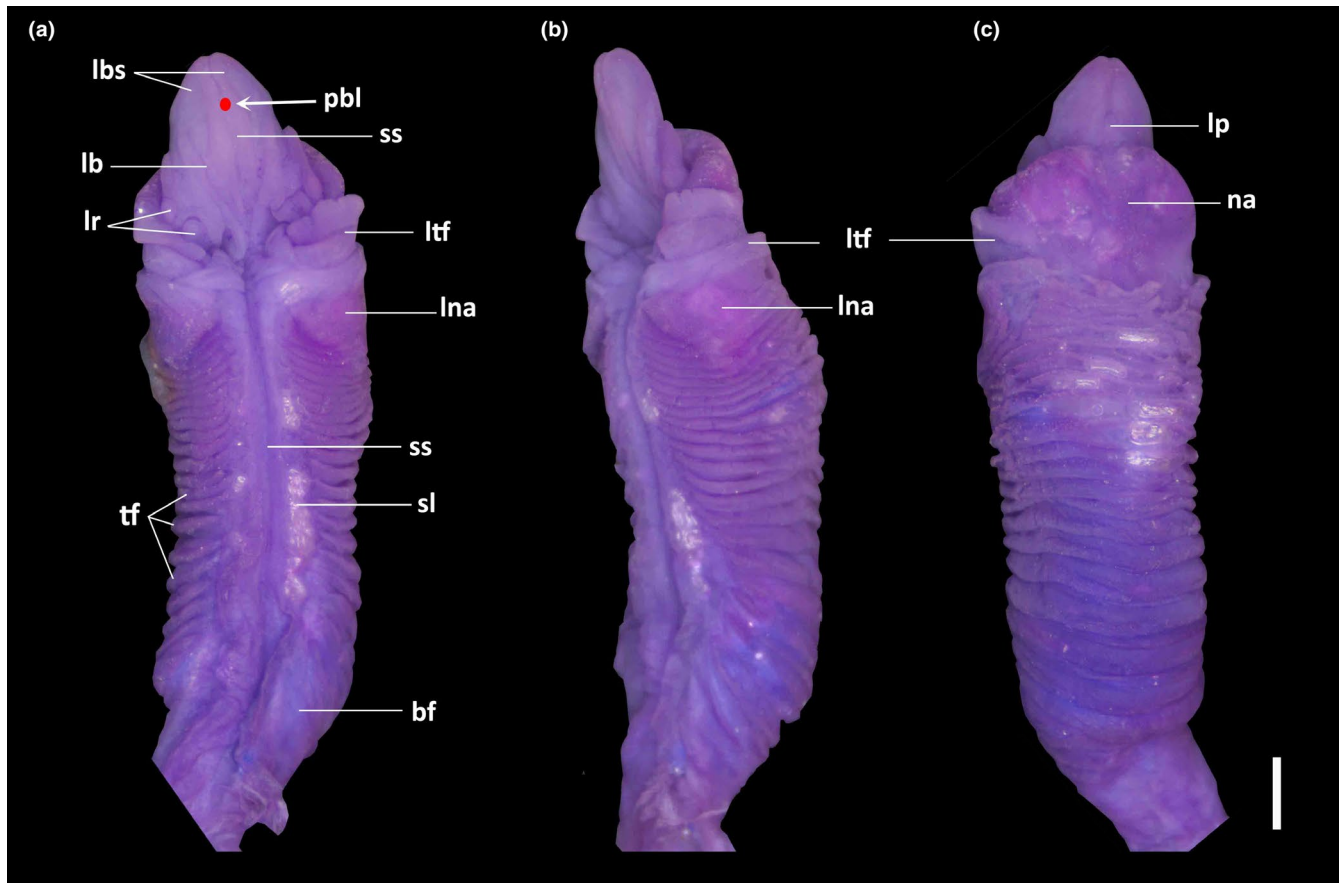


FIGURE 11 (a) Asulcate, (b) lateral, and (c) asulcate faces of the hemipenis of the holotype of *Alopoglossus indigenorum* sp. nov. (INPA-H 25543). Scale bar: 1 mm. Red dot marks the lobes bifurcation point. na, assulcate naked area; bf, base fold; lb, lobular base; lbs, lobes; lna, lateral naked area; lp, lobular protuberance; lr, lobular ridges; ltf, lateral transversal fold; pbl, lobes bifurcation point; sl, sulcus spermaticus; tf, transversal flouces

hemipenial characters: (11) no changes in the widening of the sulcus spermaticus; (12) sulcus spermaticus running in the frontal face of the base of the lobes; (13) sulcate face of the body totally covered by transversal flouces; (14) hemipenial body and base ornamented by 21–22 transversal flouces, covering almost the complete organ; (15) lobes with pointed distal ends; and (16) absence of hemipenial body distal expansion.

Comparisons with other species. *Alopoglossus indigenorum* sp. nov. differs from *A. atriventris*, *A. buckleyi*, *A. copii*, *A. embera*, *A. festae*, *A. lehmanni* and *A. viridiceps* (in parentheses) in having non-granular, keeled, imbricate scales on medial and posterior sides of neck (vs. granular in *A. atriventris* and *A. buckleyi*; mostly granular in *A. embera*, *A. festae*, *A. lehmanni* and *A. viridiceps*; conical with apparent bare skin between conical scales in *A. copii*); it also differs from *A. embera*, *A. festae* and *A. viridiceps* in not having gulars arranged in two longitudinal rows (vs. a double longitudinal row of widened gular scales), and from *A. lehmanni* in having dorsal scales rhomboidal, in oblique rows (vs. dorsal scales hexagonal with parallel lateral edges, in transverse rows).

From species of the *A. angulatus* group, *A. indigenorum* sp. nov. differs from *A. andeanus*, *A. angulatus*, *A. avilapiresae*, *A. carinicaudatus*,

A. collii, *A. tapajosensis* sp. nov., and *A. theodorusi* in having four pairs of chin shields (vs. three pairs of chin shields; Figure 5b,c), and from species with four pairs of chin shields, *A. indigenorum* sp. nov. differs from *A. amazonius*, *A. gansorum* sp. nov., and *A. meloi* in having, laterally to the fourth pair of chin shields, two small scales separating the third pair of chin shields from gular scales, or even the third pair in short contact with gular scales (vs. two large well-developed scales separating the third pair of chin shields from gular scales; Figure 5a,b). *Alopoglossus indigenorum* sp. nov. also differs from *A. gansorum* sp. nov. in having supratermporal scales in contact with each other, forming an evident, straight suture between them (vs. supratermporal scales separated from each other by a temporal scale, or touching each other with acute contact margins; Figure 5d,e); from *A. amazonius*, and *A. meloi* in having smooth scales on anterior temporal region (vs. keeled), feebly keeled distally second supratermporal scale, with smooth aspect, slightly folding laterally toward the temporal region (vs. strongly keeled second supratermporal scale, clearly folding laterally toward the temporal region), and 25–28 total number of femoral pores in males (vs. 21–24 in *A. amazonius*; 20–23 in *A. meloi*); it also differs from *A. meloi* in having smooth scales on midventral gular region, varying from almost rounded or irregular posterior margins, to mucronate or phylloid (vs. keeled, phylloid

gular scales), and 11–15 transverse rows of scales on the sides of the neck (vs. 6–8).

Based on hemipenial characters, *A. indigenorum* sp. nov. is distinguished from *A. copii* in having lobular base branched in two lobes (vs. lobular base not bifurcated), and an area without ornaments in the distal region of the lateral and asulcate faces (vs. ornamented distal areas in lateral and asulcate faces). *Alopoglossus indigenorum* sp. nov. differs from *A. atriventris*, *A. buckleyi* and *A. festae* in having sulcus spermaticus running in the frontal face of the base of the lobes (vs. sulcus spermaticus running in the medial faces of the lobes), absence of hemipenial body distal expansion (vs. presence of distal body expansion), lobes with pointed distal ends (vs. lobes with rounded distal ends), and 21–22 transversal flounces that cover almost the complete organ (vs. 25–30, in *A. atriventris*; 37 in *A. buckleyi*; 12 in *A. festae*); it also differs from *A. atriventris* and *A. buckleyi* in having an area without ornaments in the distal region of the lateral and asulcate faces (vs. ornamented distal areas in lateral and asulcate faces). *Alopoglossus indigenorum* sp. nov. differs from *A. angulatus*, *A. avilapiresae*, and *A. gansorum* sp. nov. in having a complete sulcate face covered with flounces (vs. a decreasing ornamented area on the sides of the sulcus spermaticus, in *A. angulatus*; a fine area parallel to the sulcus spermaticus without ornaments, in *A. avilapiresae* and *A. gansorum* sp. nov.), and 21–22 transversal flounces covering almost the complete organ (vs. 12–14, in *A. angulatus*; 16, in *A. avilapiresae*; 24, in *A. gansorum* sp. nov.); it also differs from *A. gansorum* sp. nov. in having a constant widening of the sulcus spermaticus (vs. a progressive widening of the sulcus spermaticus).

Description of the holotype. Male, body cylindrical, snout rounded, neck almost as wide as head and anterior part of body, limbs well developed, long tail (tip of tail regenerated) (Figure 9).

Rostral hexagonal, in broad contact with frontonasal, but also contacting first supralabial and nasal. Viewed dorsally, the rostral is about three times as wide as long. Frontonasal pentagonal, about 1.5 as wide as long (wider posteriorly), anteriorly in contact with rostral, laterally with nasal and posteriorly with prefrontals and touching frontal. Prefrontals irregularly triangular, slightly wider than long, separated from each other by an almost indistinct contact between rostral and frontal (prefrontals almost touching each other); laterally in contact with nasal, loreal and first supraocular; posteriorly in contact with frontal. Frontal irregularly hexagonal, longer than wide (distinctly wider anteriorly); laterally in contact with first, second, and third supraoculars; posteriorly in contact with frontoparietals. Frontoparietals irregularly pentagonal, longer than wide (wider posteriorly), with a long medial suture with each other medially; laterally in contact with third and fourth supraoculars; posteriorly in contact with interparietal and parietal. Interparietal pentagonal, lateral borders slightly opening toward neck (wider posteriorly), about twice longer than wide. A pair of irregularly hexagonal parietals, distinct wider medioanteriorly; parietals distinct wider than interparietal on anterior region, and narrower than it on the posterior region; anteriorly in contact with fourth supraocular, and laterally with first and second enlarged supratemporals. Parietal and interparietals

of approximately similar length, forming a slightly undulating (almost straight) posterior head margin; interparietal posterior margin reaches slightly beyond parietals posterior margins. Occipitals absent, but two small, irregular in shape, imbricate, feebly keeled scales bordering parietals posteriorly (two on each side), and one bordering parietal. Four supraoculars; first (anteriormost) smallest, contacting loreal, prefrontal, frontal, first superciliary, and second supraocular; second supraocular largest, longer than wide, contacting frontal, first and second superciliaries (and touching third), and first and third supraoculars; third supraocular slightly smaller than second one, wider than long, contacting frontal, frontoparietal, third superciliary, and second and fourth supraoculars; fourth supraocular in contact with frontoparietal, parietal, third, fourth and fifth superciliaries, third supraocular, and first enlarged supratemporal. Five superciliaries; first (anteriormost) largest, irregularly trapezoidal, slightly longer than tall; second, third, and fourth elongated (second slightly longer than third one, about 3–4 times longer than tall; third about 2.5–3 times longer than tall; fourth similar in length to third one or slightly shorter than it), fifth irregularly trapezoidal; first superciliary in contact with loreal, first and second supraoculars, second superciliary, and touching frenocular; second in contact with second supraocular, and first and third superciliaries; third in contact with second, third and fourth supraoculars, and second and fourth superciliaries; fourth in contact with fourth supraocular, and third and fifth superciliaries; fifth in contact fourth supraocular, first enlarged supratemporal, fourth superciliary, and upper postocular (one elongated scale on the right side between fifth superciliary, postoculars, and palpebrals, bordering eyes posteriorly, and two scales as wide as long on the left side). Three suboculars; first about 1.5 times longer than tall, contacting frenocular, second and third supralabials and second subocular; second longest, about seven times longer than tall, contacting third, fourth and fifth supralabials, and first and third suboculars; third irregularly pentagonal, longer than tall, similar in size or slightly smaller than first subocular, contacting fifth supralabial, second subocular, the lower postocular, and one enlarged temporal. One elongated preocular between first superciliary, frenocular, and first subocular. Two postoculars continuous with third subocular; on the left side postoculars slightly taller than long, similar in size among them, and on the right side the lower one about twice taller than long, and twice the size of upper one. Lower eyelid with semitransparent disk of 3–4 large palpebrals. Nasal divided, irregularly pentagonal, about twice as long as tall. Nostril in the mediolower part of nasal, directed posterodorsally. Loreal rectangular, contacting nasal, prefrontal, first supraocular, first superciliary and frenocular. Frenocular irregularly pentagonal, contacting loreal, nasal, second supralabial, and first subocular. Seven supralabials; third, fourth and fifth under the orbital region; first four supralabials irregularly rectangular, longer than tall (third longest); fifth, sixth and seventh polygonal; fourth supralabial shortest. Absence of a distinct post-supralabial scale. Temporals polygonal, juxtaposed, smooth or feebly keeled distally on medial and posterior regions, and smooth on anterior region; most of them large, varying from longer than tall (posterior ones) to taller than long (anterior ones); medial temporal

scales distinct smaller than others, varying from longer than tall to taller than long. Two enlarged supratemporal scales bordering the parietal in contact with each other and forming a straight suture between them; first supratemporal irregularly triangular, smooth; second supratemporal largest, irregularly hexagonal, longer than wide, feebly keeled only distally (smooth aspect). Viewed dorsally, the second supratemporals have an almost flat aspect, just slightly folding laterally toward the temporal region. Tympanum recessed into a short auditory meatus. Except for posteriormost temporals and posterior margin of the second supratemporals (feebly keeled distally), all dorsal and lateral head scales smooth and juxtaposed. Parietals and interparietal with feeble lateral ridges. Scales on nape irregular in shape, keeled distally, smaller than dorsal scales. One transverse row of keeled, granular scales bordering ear opening posteriorly. Scales on sides of neck distinctly smaller than dorsals, keeled, varying from subimbricate anteriorly to imbricate posteriorly, in 12–13 transverse rows; scales on anterior region feebly tuberculate, and scales on medial and posterior regions varying from mucronate to phylloid; on anterior, medial and posterior regions scales are disposed in regular transverse rows. A distinctive area with granular scales much shorter than neck scales surrounds the area of arm insertion.

Mental trapezoidal, about twice as wide as long, with convex anterior margin. Postmental heptagonal, wider than long. Four pairs of chin shields; first two pairs in broad contact medially and with second, third and fourth infralabials; scales of the third pair irregularly hexagonal, separated from each other by two small, irregular in shape, flat and juxtaposed scales; third pair of chin shields separated from gulars by the fourth pair of chin shields and two small, imbricate scales on the right left of the fourth pair, and by one on the right side of the fourth pair; scales of the fourth of pair of chin shields separated from each other by four small scales, and in direct contact with gulars. Six infralabials, all longer than tall; second, third, fourth and fifth similar in size and length, and about 1.5–2 times longer than first one; sixth shortest; suture between third and fourth below center of eye. Absence of a distinct post-infralabial scale. Gular scales slightly smaller than dorsals, imbricate, differentiating in size toward collar; except by lateralmost rows (varying from feebly to strongly keeled, from mucronate to phylloid), gular scales smooth, varying from almost rounded or irregular posterior margins, to mucronate or phylloid; scales on anterior and medial regions feebly pointed distally; scales on medioposterior region larger than scales on anterior region; gular scales in eight transverse rows. Posterior row of gular scales (collar) with 10 smooth scales, varying from similar in size to slightly smaller than preceding rows; lateral collar scales regularly organized in a transverse row; collar scales irregular in shape (laterals phylloid; medials with almost rounded or irregular posterior margins). Absence of gular fold.

Dorsal scales rhomboid, strongly keeled and mucronate, imbricate and disposed in oblique rows; 29 scales along a middorsal line from parietals to the level of hind limbs. Scales on flanks similar in shape and size to dorsals. Twenty-two scales around midbody. Ventral scales smooth, imbricate, with irregular posterior margins

(varying from almost straight to rounded); 17 transverse rows and four longitudinal rows between collar and preanals. Eight smooth scales in preanal plate (four anterior ones, two posteriors, and two laterals), varying from with irregular posterior margins to feebly pointed distally; anterior ones similar in size among them, similar in size to lateral ones, and posterior ones distinctly larger than them; anterior ones distinctly smaller than preceding ventral scales. A continuous, well-separated series of femoral pores on each side; each pore between two or three scales; two pores on each side in preanal position; total number of pores 25, with 12 on the left side and 13 on the right side. Dorsal limb scales rhomboid, imbricate, strongly keeled, and varying from mucronate to phylloid; ventral scales on upper forelimbs and posterior aspect of thighs keeled, imbricate, feebly tuberculate with rounded posterior margins; ventral scales on lower forelimbs feebly keeled, mucronate, and on hind limbs smooth, mucronate. Five clawed digits on each limb. Lamellae under fingers single, transversely enlarged and smooth, with 14 under the fourth finger; lamellae under toes divided (except the 2–4 terminal ones), with 21 under the fourth toes. Scales on tail keeled, imbricate, varying from mucronate to phylloid, arranged in transverse rows (not counted; tip of tail regenerated) and in 14–16 longitudinal rows at the base of the tail; scales in the two paravertebral rows wider than long near the base of the tail and longer than wide posteriad it. Keels mostly sharp on tail (except on anterior ventral surface, varying from smooth to feebly keeled), forming two dorsal, three lateral (on each side) and two ventrolateral distinct longitudinal ridges; on posterior ventral surface of tail, four distinct longitudinal ridges formed by strongly keeled scales.

Measurements of the holotype (in millimeters). SVL = 59.5; AGL = 28.0; HD = 6.9; HW = 10.1; HL = 13.4; NL = 7.8; FL = 15.0; HLL = 25.0; ShL = 9.7; TL = 96.0 (tip of tail regenerated).

Coloration of the holotype in preservative. Dorsal surface of head, body and tail light brown; dorsal surfaces of head and neck densely speckled with very small dark-brown dots, except on dorsal surfaces of supratemporal scales; on rostral, prefrontals, supraoculars, frontoparietals and parietals the small dark-brown are concentrated on scales sutures; on dorsal surface of neck the small dark-brown form large, sparse dark-brown dots; from the posterior surface of interparietal/parietals, along neck and body, to the base of tail, the large dark-brown dots form an inconspicuous longitudinal series of dots, and between the posterior surface of body and base of tail the dots are larger, forming an inconspicuous longitudinal dark-brown medial band; posterior dorsal surface of body densely speckled with very small dark-brown dots; dorsal surface of limbs densely speckled with very small dark-brown dots, large dark-brown dots, and cream dots. Lateral aspect of head, neck, body and tail light brown densely speckled with very small dark-brown dots, becoming cream ventrally; from rostral and nostril, passing through temporal, neck, flanks, and reaching the base of tail, the dark-brown dots almost cover the entire surface, forming a continuous wide dark-brown band; the dark-brown band bordered dorsally by a cream dorsolateral stripe,

conspicuous from the posterior corner of eyes to the anterior surface of body, inconspicuous or formed by a longitudinal series of cream dots posteriorly. A conspicuous cream line extending posteriorly from the supralabials under the eye, passing through the lower part of the ear opening and neck, above the forelimbs insertion, flanks, to the anterior surface of hind limbs, bordered ventrally by an inconspicuous dark-brown stripe. Ventral surface cream, with large dark-brown spots on lateral head and on margins of scales, almost covering the gular region (except by midventral region, in which dots are concentrated on margins of scales), and on anterior body (in which dots are concentrated on anterior and lateral margin of the scales); posterior ventral surface of body with a few black dots on margins of scales; hind limbs, preanal plate and anterior surface of tail almost homogeneous cream, with a few sparse, small black dots; posterior surface of tail densely speckled with very small dark-brown dots.

Variation. Specimen INPA-H 39953 has the contact between frontoparietals forming a long suture, while INPA-H 30244 and MPEG 15991 have the contact between frontoparietals forming a short suture, and INPA-H 30243 and the holotype INPA-H 25543 have frontoparietals separated from each other by the contact between frontonasal and frontal. All specimens have supratemporals in contact with each other and forming a straight suture between them. Specimen INPA-H 30244 has first superciliary and first supraocular fused. Holotype INPA-H 25543 and specimen INPA-H 30244 have the third pair of chin shields completely separated from each other by two small scales, while all other specimens have the third pair of chin shields only separated by each other posteriorly, by one small scale; except by the holotype INPA-H 25543, with the fourth pair of chin shields completely separated from each other by two small scales, all other specimens have the fourth pair of chin shields only separated from each other posteriorly by 1–3 small scales; laterally to the fourth pair of chin shields, two small scales on each side separate the third pair of chin shields from the gular scales (specimen MPEG 15991 has the third pair of chin shields in direct contact with gular scales in one side, and separated from them by two small scales on the other side); scales of the fourth pair of chin shields and small scales laterally to them either in direct contact with gulars, or separated from them by small scales. All specimens have smooth scales along midventral gular region, with the anterior and medial ones feebly pointed distally; all specimens have smooth ventral scales, varying from almost straight to rounded. Preanal and femoral pores are absent in females; in males, total number of pores 25–28. Tables 3 and 4 present a summary of the variation in meristic characters and measurements, respectively. Table S2 presents a summary of the measurements in males and females.

Variation in coloration in preservative: Rostral, prefrontals, supraoculars, frontoparietals and parietals with small dark-brown dots concentrated on scales sutures in males, but sparse (not on sutures) along the dorsal surface of head in females; dorsal surface of supra-temporal scales with speckled very small dark-brown dots or absent of them. Large dark-brown dots inconspicuously forming a middorsal

series of dots from the nape to the base of tail, or only from hind limbs to the base of tail (even between hind limbs, it is inconspicuous, not forming a wide black longitudinal band). In males, lateral aspect of head, neck, body and base of tail densely speckled with very small dark-brown dots forming a continuous wide dark-brown band, or from rostral and nostril, passing through the eyelids, first and fifth superciliaries, upper temporals, upper neck, upper and lowermost flanks, reaching the base of tail, a longitudinal narrow dark-brown stripe (similar can be observed in females, but less speckled with dark-brown dots). The conspicuous cream line extending posteriorly from the supralabials under the eye, passing through the lower part of the ear opening and neck, above the forelimbs insertion, flanks, to the anterior surface of hind limbs, bordered ventrally by an inconspicuous dark-brown stripe, is evident in both males and females. Ventral surface of head, neck, body, limbs, preanal plate, and anterior tail homogeneous cream in females. In males, ventral surface of head either densely covered by large black dots or black dots concentrated on ventrolateral surface and third and fourth pairs of chin shields; gular region densely covered by black dots (except on midventral region, in which black dots are disposed on anterior and lateral margins of the scales); anterior body surface either densely covered by black dots or they are concentrated mainly on ventrolateral region; posterior dorsal surface of body, limbs, preanal plate, and anterior tail either homogeneously cream, or with sparse small black dots.

Hemipenial description. Hemipenis of the holotype INPA-H 25543 (Figure 11) and hemipenis of the paratype INPA-H 30243 (Figure S3): The hemipenis is cylindrical and slightly bilobed. The sulcus spermaticus is single, centrolateral, and has thick sulcal lips. The base and body are ornamented by transversal flounces and do not show any calcareous structures. The lobular region is defined by two thick folds, one on each side, extending transversely over the distal regions of the sulcate and lateral faces, from the laterals of the sulcus spermaticus to the sides of the distal region of the asulcate face. Between these transversal folds, in the central axis of the organ, arise a base distally bifurcated originating the lobes. The hemipenial lobes are short, have broad bases, and pointed distal ends, and between them, there is a small protuberance in the asulcate face. There are some ridges and bulges in the sulcate and lateral faces of the lobes' bases, but the partial eversion of them avoids the detailed description of the morphology of this region. In the base of the organ, the sulcus spermaticus is narrow and covered by a thick fold of tissue. There are no changes in the width of the sulcus throughout its course, but once reaching the lobular region, the thickness of the sulcal lips decreases. The sulcus spermaticus pass between the transverse folds of the lobular region and continue further until reaching the point of bifurcation of the lobes. The hemipenial body and base are ornamented by 21–22 transversal flounces that cover almost the complete organ. The base's sulcate face is naked, while flounces cover the lateral and asulcate faces. The body is ornamented in the three faces. In the sulcate face, there is no naked area, the transversal flounces cover the whole face, and

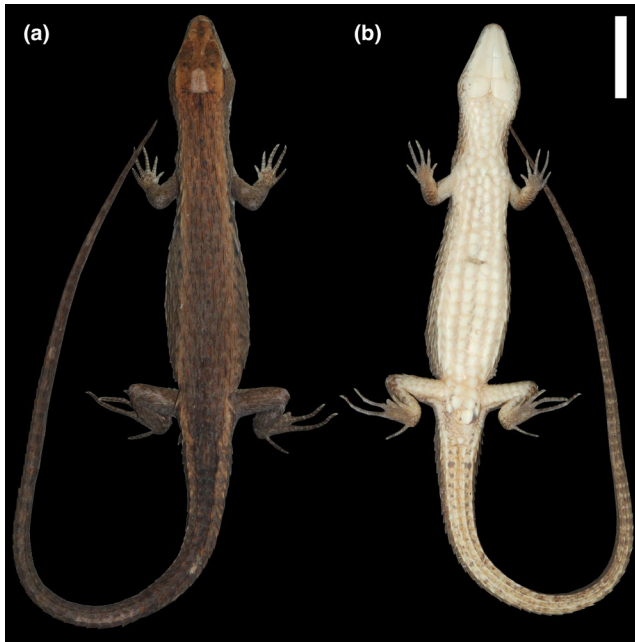


FIGURE 12 (a) Dorsal and (b) ventral views of the holotype of *Alopoglossus tapajosensis* sp. nov. (INPA-H 41383). Scale bar: 10 mm

their tips reach the sulcal lips. In the lateral faces, the regions under the transversal folds of the lobular region do not show ornaments, as well as the contiguous triangular-shaped distal area of the asulcate face that contacts the base of the asulcate face of the lobes.

Etymology. The specific epithet in genitive plural refers to the indigenous people, native inhabitants of the region. In the occurrence area of the new species, there is the highest density of isolated indigenous people in the world, and estimates suggest they spoke about 30 different and unique languages. However, their isolation, culture, and languages are under threat of extinction due to dispossession of lands, loggers, animal traffickers, and discriminatory actions by recent political decisions in Brazil.

Remarks. Besides distinctiveness mentioned above between *A. indigenorum* sp. nov. and *A. amazonius* (temporals, supratemporals, scales separating the third pair of chin shields from gular scales, and femoral pores in males), *A. indigenorum* sp. nov. has lower mean of number of dorsal and ventral scales than *A. amazonius* (25–29, mean = 27, of dorsals, and 16–17, mean = 16, of ventrals; vs. 27–31, mean = 29, of dorsals, and 17–19, mean = 18, of ventrals in *A. amazonius*), and higher mean of midbody scales (20–22, mean = 21; vs. 15–21, mean = 19, in *A. amazonius*).

Distribution and habitat. *Alopoglossus indigenorum* sp. nov. is distributed in southwestern Amazonia, between the southern side of the upper-middle Amazon River and the upper Purus river system (Acre River), occurring in the state of Amazonas and Acre, Brazil (Figure 8). Specimens were found active in leaf litter, in non-flooded and flooded forests, during the day (specimens collected by

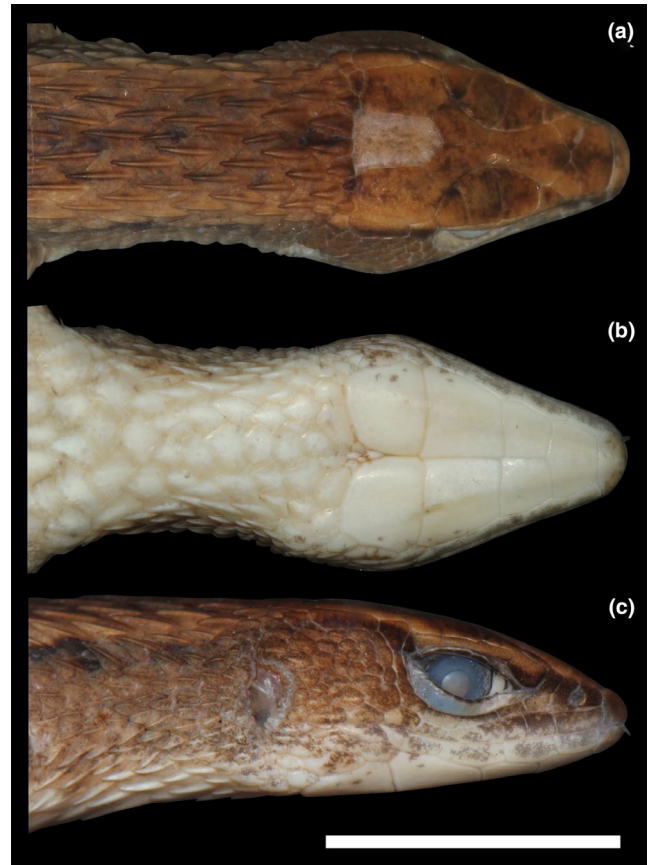


FIGURE 13 (a) Dorsal, (b) ventral and (c) lateral views of the head and neck of the holotype of *Alopoglossus tapajosensis* sp. nov. (INPA-H 41383). Scale bar: 10 mm

our team, and the ones mentioned in Pantoja & Fraga, 2012). The wide distribution range of *A. indigenorum* sp. nov., most of it inside protected areas, suggests a Least Concern conservation status.

***Alopoglossus tapajosensis* sp. nov.**

(Figures 1 and 2 [*Alopoglossus* Tapajos]; Figures 5, 8, 12–16; Tables 2, 4, 5)

LSID: <http://zoobank.org/urn:lsid:zoobank.org:act:37C70B7A-7AB9-493F-A63A-26B94B477A1D>

Alopoglossus angulatus Moraes et al. (2020: 696, 699, figures 25.6–25.8), part

Holotype. INPA-H 41383, adult female, collected on 22 July 2012 at the west bank of the middle Tapajós River, Itaituba, Pará, Brazil (−5.06, −56.87), by Ana B. Barros, Dante Pavan and Leandro J. C. L. Moraes (Figures 12–14).

Paratype. INPA-H 41382, adult male, collected on 11 December 2012 at the west bank of the middle Tapajós River, Itaituba, Pará, Brazil (−5.05, −56.87), by Dante Pavan and Leandro J. C. L. Moraes (Figure 15).

Type specimens included in the molecular analyses. INPA-H 41383 (holotype); INPA-H 41382 (paratype).



FIGURE 14 Living specimen of *Alopoglossus tapajosensis* sp. nov., holotype INPA-H 41383, photo: Leandro Moraes

Diagnosis. *Alopoglossus tapajosensis* sp. nov. is distinguished from all other species of *Alopoglossus* by the combination of the following characters: (1) non-granular, keeled, imbricate scales on medial and posterior sides of neck, varying from phylloid to mucronate with almost rounded posterior margins, in 10 transverse rows; (2) three pairs of chin shield scales; (3) third pair of chin shields in broad contact with each other anteromedially, and separated from each other on the posteriormost portions by small, imbricate scales; (4) smooth scales along midventral gular region; (5) feebly keeled scales on anterior temporal region; (6) strongly keeled scales on posterior temporal region; (7) smooth first supratemporal scale; (8) strongly keeled distally second supratemporal, clearly folding laterally toward the temporal region; (9) supratemporal scales in contact with each other, forming a long, straight suture between them; (10) 22 total number of femoral pores in males.

Comparisons with other species. *Alopoglossus tapajosensis* sp. nov. differs from *A. atriventris*, *A. buckleyi*, *A. copii*, *A. embera*, *A. festae*, *A. lehmanni* and *A. viridiceps* (in parentheses) in having non-granular, keeled, imbricate scales on medial and posterior sides of neck (vs. granular in *A. atriventris* and *A. buckleyi*; mostly granular in *A. embera*, *A. festae*, *A. lehmanni* and *A. viridiceps*; conical with apparent bare skin between conical scales in *A. copii*). It also differs from *A. embera*, *A. festae* and *A. viridiceps* in not having gulars arranged in two

longitudinal rows (vs. a double longitudinal row of widened gular scales), and from *A. lehmanni* in having dorsal scales rhomboidal, in oblique rows (vs. dorsal scales hexagonal with parallel lateral edges, in transverse rows).

From species of the *A. angulatus* group, *Alopoglossus tapajosensis* sp. nov. differs from *A. amazonius*, *A. gansorum* sp. nov., *A. indigenorum* sp. nov., and *A. meloi* in having three pairs of chin shields (vs. four pairs of chin shields; Figure 5a–c). *Alopoglossus tapajosensis* sp. nov. differs from *A. andeanus* and *A. carinicaudatus* in having 10 transverse rows of scales on sides of neck (vs. 11–12); it also differs from *A. andeanus* in having 22 femoral pores in males (vs. 24–28), and by absence of a distinct, enlarged medial pair of preular scales; and from *A. carinicaudatus* in having smooth scales on the medial gular region (vs. strongly keeled). *Alopoglossus tapajosensis* sp. nov. differs from *A. collii* in having 10 transverse scale rows on the sides of neck (vs. 8–9), feebly keeled scales on the anterior temporal region (vs. strongly keeled), and smooth ventral scales (vs. ventrals bluntly pointed, varying from smooth to feebly keeled). *Alopoglossus tapajosensis* sp. nov. differs from *A. angulatus* in having prefrontals widely separated from each other by the contact between frontonasal and frontal (vs. prefrontals with a wide contact with each other medially), scales of the third pair of chin shields in broad contact with each other anteriorly (vs. scales of the third pair of chin shields completely separated from each other by small scales), feebly keeled scales on anterior temporal region (vs. strongly keeled), and 10 transverse rows of scales on the sides of the neck (vs. 6–9). *Alopoglossus tapajosensis* sp. nov. differs from *A. avilapiresae* in having prefrontals widely separated from each other by the contact between frontonasal and frontal (vs. prefrontals with a long contact with each other medially), and in having 22 femoral pores in males (vs. 23–29). *Alopoglossus tapajosensis* sp. nov. differs from *A. theodorusi* in having feebly keeled scales on the anterior temporal region (vs. smooth), strongly keeled scales on the posterior temporal region (vs. feebly keeled, but with general aspect smooth), smooth scales on the medial gular region (vs. feebly pointed), and imbricate scales separating the posteriormost portions of the scales of the third pair of chin shields (vs. granular scales separating the second half portion [posterior] of the scales of the third pair of chin shields).

Description of the holotype. Female, body cylindrical, snout rounded, neck almost as wide as head and anterior part of body, limbs well developed, long tail (Figure 12).

Rostral hexagonal, in broad contact with frontonasal, but also contacting first supralabial and nasal. Viewed dorsally, the rostral is about three times as wide as long. Frontonasal irregularly hexagonal, about 1.5 as wide as long (wider posteriorly), anteriorly in contact with rostral, laterally with nasal and posteriorly with prefrontals frontal. Prefrontals irregularly trapezoidal (almost triangular), as wide as long, widely separated from each other by the contact between frontonasal and frontal; laterally in contact with nasal, loreal and first supraocular; posteriorly in contact with frontal. Frontal irregularly heptagonal (anteriorly curly bracket shaped), longer than



FIGURE 15 (a) Dorsal and (b) ventral views of the paratype of *Alopoglossus tapajosensis* sp. nov. (INPA-H 41382). Scale bar: 10 mm

wide (distinctly wider anteriorly); laterally in contact with first, second, and third supraoculars; posteriorly in contact with frontoparietals. Frontoparietals irregularly pentagonal, longer than wide (wider posteriorly), with a long medial suture with each other medially; laterally in contact with third and fourth supraoculars; posteriorly in contact with interparietal and parietal. Interparietal pentagonal, lateral borders slightly opening toward neck (slightly wider posteriorly), about twice as long as wide. A pair of irregularly hexagonal parietals, distinct wider medioanteriorly; parietals distinct wider than interparietal on anterior region, and narrower than it on the posterior region; anteriorly in contact with fourth supraocular, and laterally with first and second enlarged supratemporals. Parietal and interparietals of approximately similar length, forming a slightly undulating (almost straight) posterior head margin; interparietal posterior margin reaches slightly beyond parietals posterior margins. Occipitals absent, but two small, irregularly shaped, imbricate, strongly keeled scale bordering parietals posteriorly (one on each side). Four supraoculars; first (anteriormost) smallest, contacting loreal, prefrontal,

frontal, first superciliary, and second supraocular; second supraocular wider than long, contacting the frontal, first and second superciliaries, and the first and third supraoculars; third supraocular similar in size to the second one, wider than long, contacting frontal, frontoparietal, second, third and fourth superciliaries, and second and fourth supraoculars; fourth supraocular larger than first and smaller than second and third supraoculars, contacting frontoparietal, parietal, fourth and fifth superciliaries, third supraocular, and first enlarged supratemporal. Five superciliaries; first (anteriormost) largest, irregularly trapezoidal, longer than tall; second, third, and fourth elongated, second slightly longer than third one, about 3–4 times longer than tall, and fourth slightly shorter than third); fifth triangular; first superciliary in contact with loreal, first and second supraoculars, and second superciliary; second in contact with second and third supraoculars, and first and third superciliaries; third in contact with third supraocular, and second and fourth superciliaries; fourth in contact with third and fourth supraoculars, and third and fifth superciliaries; fifth in contact fourth supraocular, first enlarged supratemporal,

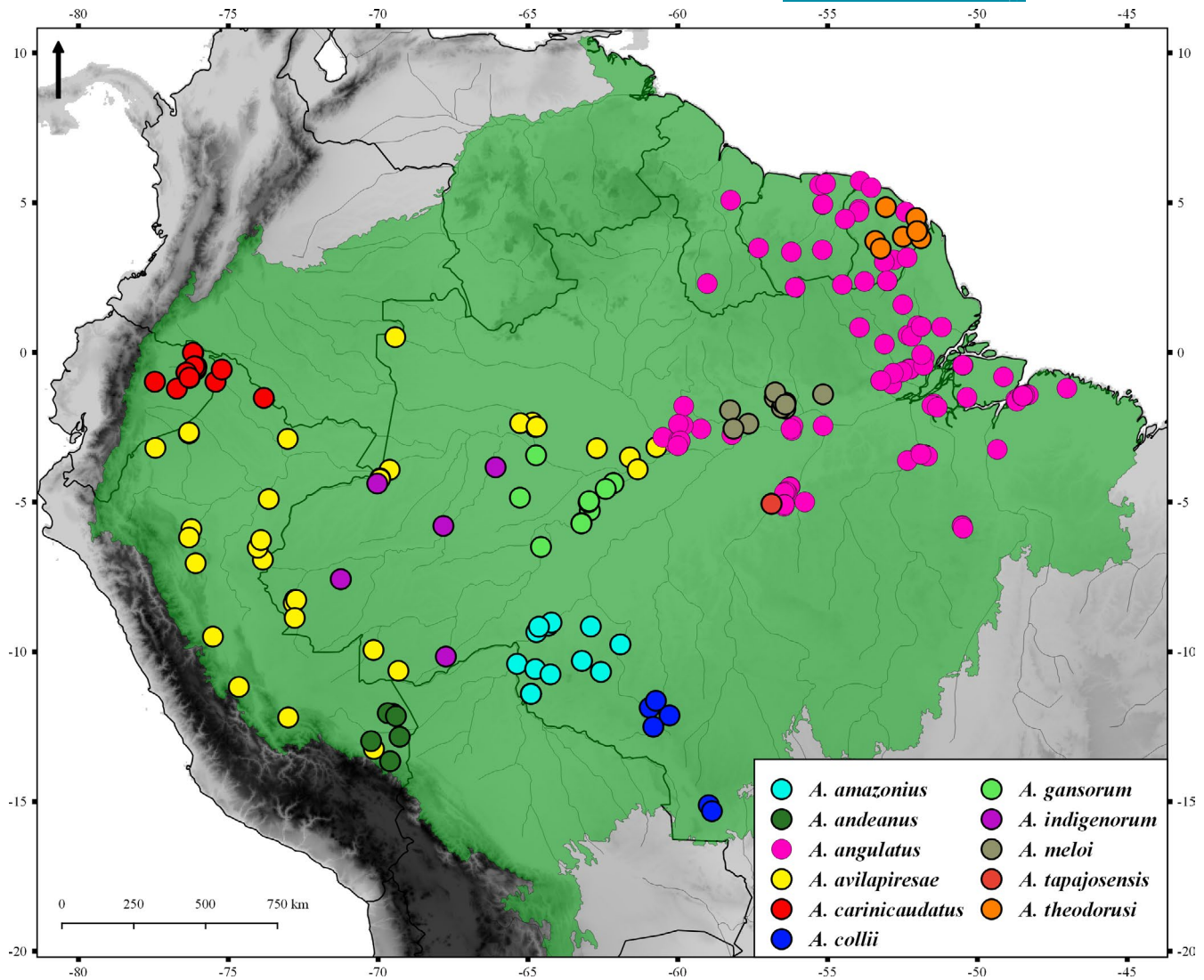


FIGURE 16 Distributional records of the 11 species of the *Alopoglossus angulatus* group

fourth superciliary, and touching upper postocular (two elongated scale between fifth superciliary, postoculars, and palpebrals, bordering eyes posteriorly). Three suboculars; first about twice longer than tall, contacting frenocular, second and third supralabials and second subocular; second longest, about seven times longer than tall, contacting third, fourth and fifth supralabials, and first and third suboculars; third irregularly pentagonal, slightly longer than tall, slightly larger than first subocular, contacting fifth supralabial, second subocular, the lower postocular, and one enlarged temporal. One elongated preocular between first superciliary, frenocular, and first subocular. Two postoculars continuous with third subocular, taller than long; upper one about three times taller than long, and larger than lower one; lower postocular about twice taller than long. Lower eyelid with semitransparent disk of five large palpebrals. Nasal divided, irregularly pentagonal, about twice as long as tall. Nostril in the mediolower part of nasal, directed posterodorsally. Loreal rectangular, contacting nasal, prefrontal, first supraocular, first superciliary and frenocular. Frenocular irregularly pentagonal, contacting loreal, nasal, and second supralabial. Seven supralabials; third, fourth

and fifth under the orbital region; first four supralabials irregularly rectangular, longer than tall (second slightly longer than tall, third longest); fifth, sixth and seventh polygonal; fourth supralabial shortest. Absence of a distinct post-supralabial scale. Temporals irregularly polygonal, juxtaposed, varying from feebly keeled on anterior region to feebly or strongly keeled on medial and posterior regions; most of them small on anterior and medial regions, as long as tall or slightly taller than long; larger temporals on antero-lower and postero-upper regions, varying from longer than tall to as tall as long. Two enlarged supratemporal scales bordering the parietal in contact with each other and forming a long straight suture between them; first supratemporal irregularly hexagonal (triangular shaped), smooth; second supratemporal largest, irregularly heptagonal, longer than wide, strongly keeled distally. The second supratemporals clearly folding laterally toward temporal region. Tympanum recessed into a short auditory meatus. Except for temporals and the second supratemporals, all dorsal and lateral head scales smooth and juxtaposed. Parietals and interparietal with feeble lateral ridges. Scales on nape irregular in shape, strongly keeled, smaller than dorsal scales.

One transverse row of keeled, granular scales bordering ear opening posteriorly. Scales on sides of neck distinctly smaller than dorsals, strongly keeled, imbricate, phylloid, in 10 transverse rows; scales on anterior region smaller than scales on medial and posterior regions; on anterior, medial and posterior regions scales are disposed in regular transverse rows. Granular scales much shorter than neck scales surround the area of arm insertion.

Mental trapezoidal, about twice as wide as long, with convex anterior margin. Postmental heptagonal, wider than long. Three pairs of chin shields; first two pairs in broad contact medially and with second, third and fourth infralabials; scales of the third pair irregularly hexagonal in contact with each other anteriorly, but separated from each other by five small, imbricate scales posteriorly, and separated from infralabials by large scales laterally; third pair almost straight medially and posteriorly, in direct contact with gulars. Six infralabials, all longer than tall; first, second, fourth and fifth similar in size length, about 2.5–3 times longer than tall one; third slightly longer than others; sixth shortest; suture between third and fourth below center of eye. Absence of a distinct post-infralabial scale. Gular scales slightly smaller than dorsals, imbricate, differentiating in size toward collar; anteriormost transverse row with large, smooth, scales, with almost rounded posterior margins; medial and posterior gular scales smooth, slightly larger than anterior ones, varying from almost rounded or irregular posterior margins, to mucronate or phylloid, wider and longer than lateral gular scales; lateral gular scales varying from feebly to strongly keeled, from mucronate to phylloid; gular scales in nine transverse rows. Posterior row of gular scales (collar) with nine smooth scales, varying from similar in size to slightly smaller than preceding rows; collar scales regularly organized in a transverse row; collar scales irregular in shape, varying from phylloid to almost rounded posterior margins. Absence of gular fold.

Dorsal scales rhomboid, strongly keeled and mucronate, imbricate and disposed in oblique rows; 26 scales along a middorsal line from parietals to the level of hind limbs. Scales on flanks similar in shape and size to dorsals. Twenty scales around midbody. Ventral scales smooth, imbricate; scales along the midventral portion varying from mucronated (bluntly pointed on anterior region) to almost rounded (on medial and posterior regions); ventrolateral scales varying from smooth to pointed distally; 18 transverse rows and four longitudinal rows between collar and preanals. Eight scales in preanal plate (four anterior ones, two posteriors, and two laterals); anteromedial ones similar in size among them, smooth, larger or similar in size to preceding ventral scales; anterolateral ones the smallest, longer than wide, feebly keeled distally; two laterals feebly keeled distally, slightly larger than anterolateral ones; two largest scales on posterior region, smooth. Preanal and femoral pores absent (female). Dorsal limb scales rhomboid, imbricate, strongly keeled; ventral scales on upper forelimbs and posterior aspect of thighs keeled, imbricate, feebly tuberculate with rounded posterior margins; ventral scales on lower forelimbs feebly keeled, mucronate, and on hind limbs varying from smooth to feebly keeled, from mucronate to phylloid. Five clawed digits on each limb. Lamellae under fingers

single, transversely enlarged and smooth, with 15 under the fourth finger; lamellae under toes divided (except the 4–6 terminal ones), with 19 under the fourth toes. Cutted second toe of the right feet. Scales on tail keeled, imbricate, varying from mucronate to phylloid, arranged in transverse rows (not counted) and in 12–15 longitudinal rows at the base of the tail; scales in the two paravertebral rows wider than long near the base of the tail and longer than wide posteriorly. Keels mostly sharp on tail (except on anteriormost ventral surface, feebly keeled), forming two dorsal, three lateral (on each side) and four ventrolateral distinct longitudinal ridges.

Measurements of the holotype (in millimeters). SVL = 56.7; AGL = 27.1; HD = 6.5; HW = 8.1; HL = 11.1; NL = 8.0; FL = 15.3; HLL = 25.0; ShL = 7.8; TL = 110.6.

Coloration of the holotype in preservative. Dorsal surface of head, body and tail light brown; dorsal surfaces of head and neck densely speckled with very small dark-brown dots, except on dorsal surfaces of supratemporal scales; on rostral, frontonasals, prefrontals, and frontal the small dark-brown dots are concentrated on middorsal surface, on supraoculars they are on scales sutures, and on frontoparietals, parietals and interparietal they are sparsely speckled on the scales; on dorsal surface of neck the small dark-brown form large, sparse dark-brown dots; from the posterior surface of interparietal/parietals, along neck and body, to the base of tail, the large dark-brown dots form an inconspicuous longitudinal series of dots, and between the posterior surface of body and base of tail the dots are larger, forming an inconspicuous longitudinal dark-brown medial band; posterior dorsal surface of body densely speckled with very small dark-brown dots; dorsal surface of limbs densely speckled with very small dark-brown and large dark-brown dots. Lateral aspect of head, neck, body and tail light brown densely speckled with very small dark-brown dots, becoming cream ventrally; on the anterolateral surface of head, flanks, and on lateral surface of base of tail the very small dark-brown almost cover the entire surfaces, but not forming a wide black lateral band. A continuous dark-brown line extending posteriorly from the lateral surface of rostral and nostril, passing through the eyelids, first and fifth superciliaries, supratemporals, dorsolaterally on neck, flanks, above hind limbs insertion, and reaching laterally the tail; the dark-brown line bordered dorsally by a cream stripe from posterior corner of eye to base of tail (conspicuous along all body). A rather inconspicuous ventrolateral cream line extending from the supralabials under the eye, passing through the lower part of ear opening and neck, ventrolaterally on flanks, anterior and posterior surfaces of hind limbs (interrupted above the limbs), to the tail. Ventral surface cream, with few, small and sparse dark-brown spots on lateral head and on preanal plate; ventral surface of tail densely speckled with small dark-brown dots.

Coloration of the holotype in life. Holotype INPA-H 41383, adult female (Figure 14), presenting differences between specimen in preservative (above) and in life: dorsal surfaces of head, body, limbs and tail dark brown; small dots speckled on head are black;

the longitudinal series of dots from the posterior surface of interparietal/parietals to the base of tail is not evident in life as in preservative, due to the darker background coloration of the dorsal surface of neck and body. Lateral aspect of head, neck, body and tail light dark brown, becoming cream ventrally; anterolateral surface of head almost covered by black dots. The continuous dark-brown line extending posteriorly from the lateral surface of rostral reaching laterally the tail is black in life, and not evident posteriorly the shoulders as in preservative; the cream stripe bordering dorsally the dark line is evident from the head to the shoulders and on the base of tail, inconspicuous along body. The ventrolateral cream line, from the supralabials under the eye to the tail, is not evident in life as in preservative. Iris vividly orange.

Variation. Only one other specimen of *Alopoglossus tapajosensis* sp. nov., the paratype INPA-H 41382 (male), is known. Little variation in meristic characters is found. It has the third pair of chin shields in broad contact with each other medially, with two small, imbricate scales separating each other only on their posteriormost portion. It has a continuous, well-separated series of femoral pores on each side; each pore between two or three scales; two pores on each side in preanal position; total number of pores 22, 11 on each side. Measurements of the paratype (in millimeters): SVL = 48.2; AGL = 21.0; HD = 5.6; HW = 7.6; HL = 10.0; NL = 7.3; FL = 13.3; HLL = 23.6; ShL = 7.8; TL = 16.7 + 69.0 (broken). Tables 3 and 4 present a summary of the variation in meristic characters and measurements, respectively.

Coloration in preservative of the paratype INPA-H 41382 (male) (Figure 15): Dorsal surface of head, body and tail light brown; dorsal surfaces of head and neck densely speckled with very small dark-brown dots, except on lateral surfaces of rostral, frontonasal, prefrontal, and frontal scales and dorsal surfaces of supratemporal scales; on rostral, frontonasals, prefrontals, and frontal the small dark-brown are concentrated on middorsal surface, on supraoculars they cover almost the entire surface of the scales, and on frontoparietals, parietals and interparietal they are sparsely speckled on the scales; on dorsal surface of neck the small dark-brown form large dark-brown dots; dorsal surface of body densely speckled with very small and large dark-brown dots; from the posterior surface of interparietal/parietals, along neck to anterior body surface, the dark-brown dots merge to form an conspicuous dark-brown medial band, and on posterior body surface they are speckled, sparse, forming large dots or not; on the base of tail, the small dark-brown almost cover the entire dorsal surface; dorsal surface of limbs densely speckled with very small and large dark-brown dots. Lateral aspect of head, neck, body and tail light brown densely speckled with very small dark-brown dots (almost covering the entire surfaces), becoming cream ventrally. The dark-brown lateral surfaces bordered dorsally by a conspicuous cream dorsolateral stripe, from the posterior corner of eyes to the dorsolateral surface of the tail; the cream dorsolateral stripe conspicuous and wider on head, above limbs, and base of tail. A conspicuous white line extending posteriorly from the supralabials under the eye, passing through the lower part of the ear opening and neck, above

the forelimbs insertion, ventral surface of flank, anterior and posterior surfaces of hind limbs, and on ventral surface of the tail; it is bordered ventrally by a conspicuous dark-brown stripe. Ventral surface white; large dark-brown dots on ventrolateral surface of head, and on the third pair of chin shields they are concentrated on scale sutures; on ventral surfaces of neck, body and preanal plate, the dark-brown dots are on anterior and lateral margins of all scales; on ventral surfaces of limbs, dark-brown dots scattered; on ventral surface of limbs, large dark-brown dots forming two longitudinal series of dots.

Etymology. The specific epithet is masculine and refers to the fact that this species is currently known only for the Tapajós River basin, in Brazilian Amazonia.

Remarks. Besides the distinctiveness mentioned above between *Alopoglossus tapajosensis* sp. nov. and its closest related species *A. theodorusi* (temporals, gulars, and scales separating the third pair of chin shields), *A. tapajosensis* sp. nov. has interparietal and parietals similar in length, while interparietal in *A. theodorusi* is shorter than parietals. The third pair of chin shields in *A. tapajosensis* sp. nov. forms a longer suture in contact with each other medially than the scales of the third pair in *A. theodorusi*. The general shape of the scales of the third pair of chin shields also differs between them, with *A. tapajosensis* sp. nov. having almost straight mediolateral and posterior margins, while *A. theodorusi* has rounded posterior margins.

Distribution and habitat. *Alopoglossus tapajosensis* sp. nov. is only known from two localities, ~1 km apart, on the west bank of the middle Tapajós River, south of the Amazon River, occurring in the state of Pará, Brazil (Figure 8). The region was standardized surveyed in 2012/2013 at 11 sampling localities on both banks of the Tapajós River and its affluent Jamanxim River (see Moraes et al., 2016 for additional details). Only these two specimens of *A. tapajosensis* sp. nov. were collected in a single sampling unit, a trail crossing a large portion of periodically flooded forest. The holotype was found active during the day in the leaf litter of the flooded forest, and the paratype was collected in a pitfall trap located at a non-flooded forest, but bordering the limit of the water in the flooded season. Mining had, up to the years 2012/2013, been intensively practiced in the region and habitat where both specimens were found. A hydroelectricity power plant is also planned to be constructed in the same area, endangering the species. Then, conservation status of it deserves attention, and its population status should be monitored.

3.5 | Redefinition of *A. amazonius* sensu stricto, based on the new taxonomic arrangement of the species with four pairs of chin shields

3.5.1 | Referred specimens

UMMZ 56853, holotype, male, collected at Vila Murтинho, Nova Mamoré, Rondônia (−10.40, −65.36) (see Figures 8 and 9 in

Ribeiro-Júnior, Choueri, et al., 2020: 17–18); INPA-H 40747, male, collected at Jirau-D, Porto Velho, Rondônia, Brazil (−9.34, −64.72); MPEG 20511–12, collected at Guajará-Mirim, Rondônia, Brazil (−10.57, −64.76); MPEG 31439, male, collected at Jamari, Rondônia, Brazil (−9.15, −62.9); UFRO-H 002394/SA12891, UFRO-H 002399/SA14360, and UFRO-H 002400/SA14423, females, collected at Lote D, Ilha São Patrício, Porto Velho, Rondônia, Brazil (−9.11, −64.32); UFRO-H 002405/SA16632, collected at Lote D, Ilha São Patrício, Porto Velho, Rondônia, Brazil (−9.12, −64.32); MZUSP 64339–40, collected at Santa Cruz da Serra, Rondônia, Brazil (−10.67, −62.57); MZUSP 67737–38, collected at Cachoeira de Nazaré, Rio Machado, Vale do Anari, Rondônia, Brazil (−9.75, −61.92); MZUSP 89342–44, collected at Cacaúlândia, Rondônia, Brazil (−10.3, −63.2); MZUSP 89965, collected at Serra dos Pacaás Novos, Nova Mamoré, Rondônia (−10.75, 64.25).

3.5.2 | Diagnosis

Alopoglossus amazonius sensu stricto is distinguished from all other species of *Alopoglossus* by the combination of the following characters: (1) non-granular, keeled, imbricate, phylloid scales on medial and posterior sides of neck, in 11–12 transverse rows; (2) four pairs of chin shield scales; (3) laterally to the fourth pair of chin shields, two large scales separating the third pair of chin shields from gular scales; (4) scales along midventral gular region varying from smooth to feebly keeled, and from mucronate or phylloid to having irregular posterior margins; (5) keeled scales on anterior temporal region; (6) keeled scales on posterior temporal region; (7) feebly keeled first supratemporal scale; (8) strongly keeled second supratemporal scale, clearly folding laterally toward the temporal region; (9) supratemporal scales in contact with each other, forming an evident, straight suture between them; (10) 21–24 total number of femoral pores in males.

3.5.3 | Comparisons with other species

Alopoglossus amazonius sensu stricto differs from *A. atriventris*, *A. buckleyi*, *A. copii*, *A. embera*, *A. festae*, *A. lehmanni* and *A. viridiceps* (in parentheses) in having non-granular, keeled, imbricate scales on medial and posterior sides of neck (vs. granular in *A. atriventris* and *A. buckleyi*; mostly granular in *A. embera*, *A. festae*, *A. lehmanni* and *A. viridiceps*; conical with apparent bare skin between conical scales in *A. copii*); it also differs from *A. embera*, *A. festae* and *A. viridiceps* in not having gulars arranged in two longitudinal rows (vs. a double longitudinal row of widened gular scales), and from *A. lehmanni* in having dorsal scales rhomboidal, in oblique rows (vs. dorsal scales hexagonal with parallel lateral edges, in transverse rows).

From species of the *A. angulatus* group, *A. amazonius* differs from *A. andeanus*, *A. angulatus*, *A. avilapiresae*, *A. carinicaudatus*, *A. collii*, *A. tapajosensis* sp. nov., and *A. theodorusi* in having four pairs of chin shields (vs. three pairs of chin shields). From species with four pairs of chin shields, *A. amazonius* differs from *A. gansorum* sp. nov. in having supratemporal scales in contact with each other, forming an evident,

straight suture between them (vs. supratemporal scales separated from each other by a temporal scale, or touching each other with acute contact margins); from *A. indigenorum* sp. nov. in having keeled scales on anterior temporal region (vs. smooth), strongly keeled second supratemporal scale, clearly folding laterally toward the temporal region (vs. feebly keeled distally second supratemporal scale, with a smooth aspect, slightly folding laterally toward the temporal region), in having, laterally to the fourth pair of chin shields, two large well-developed scales separating the third pair of chin shields from gular scales (vs. two small scales separating the third pair of chin shields from gular scales, or even the third pair in short contact with gular scales), and in having 21–24 total number of femoral pores in males (vs. 25–28). *Alopoglossus amazonius* differs from *A. meloi* in having 11–12 transverse rows of scales on the sides of the neck (vs. 6–8), scales on midventral gular region varying from smooth to feebly keeled, and from mucronate or phylloid to having irregular posterior margins (vs. scales keeled, phylloid), and having higher mean of dorsal and ventral scales (27–31, mean =29, of dorsals, and 17–19, mean =18, of ventrals; vs. 24–28, mean =26, of dorsals, and 15–18, mean =16, of ventrals in *A. meloi*).

3.5.4 | Variation

All specimens have frontoparietals in contact with each other, forming a straight suture between them, except the holotype UMMZ 56853 that has frontoparietals only touching each other, forming an acute contact margin. Specimen MPEG 31439 has six superciliaries and three postoculars, while all other specimens have five and two, respectively. Specimen INPA-H 40747 has seven infralabials on one side and six on the other. The third pair of chin shields can be either completely separated from each other by 2–3 small scales or separated only posteriorly by one scale. Specimen UFRO-H 002399/SA14360 has the fourth pair of chin shields partially separated from each other posteriorly by one scale, while other species have fourth pair of chin shields completely separated from each other by 3–4 scales. Scales of the fourth pair of chin shields and large scales laterally to them either in direct contact with gulars, or separated from them by small scales. Specimen UFRO-H 002399/SA14360 has gular scales in seven transverse rows. Preanal and femoral pores are absent in females. In males, the femoral pores are arranged in a continuous, well-separated series on each side; two pores on each side are in the preanal position; each pore is between two scales; total number of pores 21–24. Tables 3 and 4 present a summary of the variation in meristic characters and measurements, respectively. Table S2 presents a summary of the variation in measurements between males and females. Variations in coloration in preservative are the same presented in Ribeiro-Júnior, Choueri, et al. (2020).

3.5.5 | Distribution and habitat

Alopoglossus amazonius is distributed in southwestern Amazonia, in the upper Madeira river basin. Most of the occurrence localities

are on the eastern riverbank, but the species is also recorded in the western riverbank, near to the river margin, as well as in fluvial islands (Figure 16). Specimens were recorded active during the day in the leaf litter, in non-flooded forests, patches of forest within savannas, and flooded forest in fluvial islands (Ribeiro-Júnior, Choueri, et al., 2020). Although currently considered as endemic from Brazil, this species might also occur in similar habitats in adjacent Bolivia.

Alopoglossus amazonius is only known to occur in one of the most threatened areas in the Brazilian Amazonia. In the upper Madeira River, two large hydroelectric power stations were recently constructed, and may be at least in part responsible for the homogenization of occurrence of *A. amazonius* on both riverbanks and fluvial islands. Dam filling affected both up and downstream seasonal flooding regime, and potentially the effect of this large river as a geographical barrier for some species. The river course below the dams experienced (and continues experiencing) extended periods of lower water level, potentially improving species dispersion between banks (U. Suendel personal observation). However, hypotheses about the historical and/or ecological mechanisms involved in the distribution of this species and how these recent anthropic changes have affected it remains to be tested.

4 | DISCUSSION

Our study confirmed the occurrence of hidden diversity in the *A. angulatus* group, despite recent taxonomic elucidations within this taxon. Seven species were described/resurrected from *A. angulatus* in the last few years (Ribeiro-Júnior, 2018; Ribeiro-Júnior, Choueri, et al., 2020; Ribeiro-Júnior, Meiri, et al., 2020; Figure 16), and we discovered and described another three here. It is also noteworthy that the DCL found here as part of *A. carinicaudatus* intraspecific variation. They deserve taxonomic assessment. Further analysis of their morphological variations may provide evidence to support their descriptions as new species. The combined results of our studies and pervasive taxonomic shortfalls (Hortal et al., 2015) indicate how far we are from achieving a better resolution of Amazonian species diversity. The investigation of different evolutionary lines of evidence, and an effective integration of them (Miralles & Vences, 2013), are fundamental to uncover hidden diversity in this region. A detailed refinement of morphological characters traditionally considered as diagnostics can reveal subtle divergences, such as those that proved fundamental in advancing taxonomic knowledge for *Alopoglossus* (see Ribeiro-Júnior, 2018: 34–35, and Ribeiro-Júnior, Choueri, et al., 2020: 261–262).

The presence of non-granular, phyloid, imbricate scales on the medial and posterior sides of neck seems to be a synapomorphy of the *A. angulatus* group, while granular scales on the sides of the neck are plesiomorphic characters. In contrast, the presence of four pairs of chin shields seems to have independently evolved in deeply divergent clades (i.e., in *A. viridiceps* [from the *A. festae* group], *A. buckleyi* and *A. atriventris*, and in six species of the *A. angulatus* group [*A. amazonius*, *A. indigenorum* sp. nov., *A. meloi*, and *A. gansorum* sp. nov.]). *Alopoglossus collii* is the only species with three pairs of chin shields

in a clade that comprises of species with four pairs of chin shields (*A. amazonius*, *A. indigenorum* sp. nov. and *A. gansorum* sp. nov.). This suggests a possible character reversal. Similarly, although *A. collii* is phenetically divergent from other species in this clade, molecular relationships of species in this group are overall poorly supported. Thus, we argue that a genomic-level assessment of phylogenetic relationships and species boundaries is urgently needed for this species group, before the evolutionary coding of the morphological traits can be addressed. This evident shortfall reinforces the notion that using the morphological characters formerly diagnosing *Alopoglossus* species (i.e., before the latest taxonomic revisions) can lead to premature taxonomic decisions.

We presented the first detailed hemipenial descriptions for *Alopoglossus*, which allows us to discuss their taxonomic value in taxonomic decisions involving alopoglossids. Previously, hemipenial descriptions for *Alopoglossus* was limited to that presented by Nunes (2011), which broadly described the hemipenes with a focus in comparisons among Gymnophthalamoidea genera. In this study, Nunes (2011) outlined two groups of *Alopoglossus* species based on hemipenial morphology. The first one included *A. atriventris*, *A. buckleyi*, and *A. festae*, and it was characterized by a distal body expansion showing a “Y” shape, lobes with a rounded distal end, and a sulcus spermaticus running on the medial faces of the lobes. In this group, *A. festae* has the most divergent hemipenis, and could be considered as a third distinct morphological group. The second group included *A. angulatus* and *A. copii*, species that share a hemipenis with less accentuated distal body expansion, an area without ornaments in the distal region of the lateral and asulcate faces that define the lobular region, and sharp lobular projections (Nunes, 2011). Under descriptions of these morphological subgroups, hemipenial morphology of *A. indigenorum* sp. nov. and *A. gansorum* sp. nov. fit in the second group, as expected given the phylogenetic proximity to *A. angulatus*.

Based on the combined information on hemipenial morphology described in our study and available in the literature (Harris, 1994; Nunes, 2011; Peloso & Ávila-Pires, 2010), we suggest that hemipenial morphology, together with external morphological characters, could distinguish the genera *Alopoglossus* and *Ptychoglossus*. According to Harris (1994) and Nunes (2011), *Ptychoglossus* species present two types of hemipenial lobular ornamentations. The first one has lobes as projection of the body (not clearly expanded and distinct), with symmetric lobular ornamentation (six small appendices, as in *P. brevifrontalis*, Nunes, 2011: Plate 6). The second one has distinct and expanded lobes, but with asymmetric ornamentation (lobular tip divided by the sulcus spermaticus into two parts of very different sizes, as in *P. myersi*, Nunes, 2011: Plate 9). *Alopoglossus* species are easily distinguished from these groups in having hemipenes with distinct and expanded lobes, with symmetrical lobular ornamentations (*A. gansorum* sp. nov., Figure 7). In *Alopoglossus*, the number of lobes is either one (*A. copii*, Nunes, 2011: Plate 4) to two (*A. gansorum* sp. nov. and *A. indigenorum* sp. nov., Figure 6, and *A. buckleyi*, Nunes, 2011: Plate 3). In addition, some species of *Alopoglossus* (e.g., *A. atriventris* and *A. buckleyi*) show a distal expansion of the hemipenis body, a feature not shared with any *Ptychoglossus* species.

Morales et al. (2020) included hemipenial morphology data in their phylogenetic study, but did not provide descriptions or figures of the hemipenes that could allow us to incorporate their results in our comparisons. The three hemipenial synapomorphies presented by Morales et al. (2020: 7, 15) to support a monophyletic clade comprising of *A. angulatus* and *A. copii* are questionable. For example, authors mentioned: 1) hemipenis not distally forked (character 77, status 0), but we found that the distal part of the hemipenis branches into two lobes in *A. angulatus* group and is not forked in *A. copii*; 2) the presence of odd projections on the distal part of the hemipenis (character 79, status 1). We could not evaluate this because what constitute “odd projections” in Morales et al. (2020) is not defined. Unfortunately, there are still few hemipenes described for *Alopoglossus* (7/18 species), but existing evidence suggests that a taxonomically comprehensive resolution of this characteristic can certainly help elucidating decisions involving the systematics and taxonomy of alopoglossids. Therefore, taxonomic changes regarding higher levels of alopoglossids should be suggested with caution. While such fine resolution is not achieved, we suggest that available data do not support synonymizing *Ptychoglossus* with *Alopoglossus*. We therefore formally recognize them as distinct genera.

Amazonia is characterized by some of the highest species richness of reptiles Squamata on Earth (Gumbs et al., 2020; Rabosky et al., 2019; Roll et al., 2017), and its diversity is heterogeneously distributed across this region (Ribeiro-Júnior & Amaral, 2016b). In Brazilian Amazonia, high lizard richness were recorded along the lower courses of Trombetas, Negro and Japurá rivers, the middle courses of Tapajós and Madeira rivers, and the upper courses of Juruá, Madeira and Amazon rivers (Ribeiro-Júnior & Amaral, 2016b). The environmental heterogeneity present in this ecosystem is postulated as one of the main drivers of the species richness spatialization (Ávila-Pires, 1995; Ribeiro-Júnior, 2015a, 2015b; Ribeiro-Júnior & Amaral, 2016a, 2016b, 2017; Silva & Sites, 1995). The diversification of *A. angulatus* group in Amazonia seems to reflect this assumption, as most diverse regions for this group are congruent with overall lizard hotspots (Ribeiro-Júnior & Amaral, 2016b). Two eastern distributed species (*A. meloi* and *A. theodorusi*) are geographically constrained to the lower Trombetas River and easternmost Guiana Shield, respectively (Ribeiro-Júnior, Meiri, et al., 2020). *Alopoglossus tapajosensis* sp. nov. is only known from a restricted area in the middle Tapajós river basin, as well as *A. gansorum* sp. nov. is restricted to the lower Purus River, and *A. amazonius* and *A. collii* to the upper Madeira River. *Alopoglossus indigenorum* sp. nov., however, has a wider distribution encompassing some southwestern Amazonia river basins. The association between the *Alopoglossus* species and environmental heterogeneity still needs to be elucidated. Further, biogeographical and macroecological analyses can help on our understanding of the historical and ecological mechanisms shaping such a diversity.

ACKNOWLEDGMENTS

We thank the following curators and personnel from museums and institutions who granted access to specimens and tissue samples:

N. Vidal (MNHN), E. Dondorp (RMNH), P. Venegas (CORBIDI), D. Frost, D. Kizirian (AMNH), J. Losos (MCZ), R. Heyer, K. Tighe (USNM), H. Zaher, C. Castro-Mello (MZUSP), G. Colli, I. Arantes (UNB), R. Vogt, F. Werneck, A. Silva, V. Carvalho, R. Fraga, A. Lima (INPA), T. Ávila-Pires, A. Prudente, F. Sarmiento (MPEG), S. Morato, J. Moura-Leite (MHNCI), M. Menin (UFAM), J. D. Lima and J. R. Lima (IEPA). We thank Alan F. S. Oliveira, Albedi Andrade Jr., Ana B. Barros, Elizângela S. Brito, Jerriane O. Gomes, José Cassimiro, José M. Guellere, Luis Storti, Mauro Hoffman, Raíssa N. Rainha, and Tainá F. D. Rodrigues for their help during field expeditions. We also thank F. Waldez and S. Souza for sending photographs of animals in life, I. Fernandes for sending photographs of specimens housed at INPA, and Erez Maza (Steinhardt Museum of Natural History, Tel Aviv, Israel) for helping with loans. Some of the field expeditions were financially and logistically supported by CNEC WorleyParsons Engenharia S.A (middle Tapajós River), the Instituto de Desenvolvimento Sustentável Mamirauá, Instituto Chico Mendes de Conservação da Biodiversidade (ICMBio), and Gordon and Betty Moore Foundation (lower Juruá River). This work was supported by the Gans Collections and Charitable Fund Inc. [grant], the Rector scholarship (Tel Aviv University; M.A.R.-J. postdoctoral fellowship), and the Alexander and Eva Lester Fund scholarship (I. Meier Segals Garden for Zoological Research; M.A.R.-J. postdoctoral fellowship), Conselho Nacional de Desenvolvimento Científico e Tecnológico (CNPq; research and productivity fellowships #313055/2015-7 to L.J.C.L.M., and #425571/2018-1 and #305535/2017-0 to F.P.W.), Fundação de Amparo à Pesquisa do Estado do Amazonas (FAPEAM; research fellowships #062.00665/2015, #062.01110/2017 and #062.00962/2018 to F.P.W, and POSGRAD fellowship #002/2016 to E.L.C.), Partnerships for Enhanced Engagement in Research from the U.S. National Academy of Sciences and U.S. Agency of International Development (F.P.W PEER NAS/USAID AID-OAA-A-11-00012, cycle 3), L'Oréal-Unesco For Women in Science Program (F.P.W. Brazil/ABC 2016, IRT 2017), and Coordenação de Aperfeiçoamento de Pessoal de Nível Superior (CAPES/PNPD postdoctoral fellowship to V.T.C.). Lastly, we also thank the editor Martin Husemann, the editor-in-chief Elisabeth Haring, and two anonymous reviewers for their contributions in the earlier version of this article.

CONFLICT OF INTEREST

The authors declare no conflict of interest.

ORCID

Marco Antônio Ribeiro-Júnior  <https://orcid.org/0000-0002-0863-6121>

REFERENCES

- Arévalo, E., Davis, S. K., & Sites, J. W. Jr (1994). Mitochondrial DNA sequence divergence and phylogenetic relationships among eight chromosome races of the *Sceloporus grammicus* complex (Phrynosomatidae) in Central Mexico. *Systematic Biology*, 43, 387–418. <https://doi.org/10.1093/sysbio/43.3.387>

- Ávila-Pires, T. C. S. (1995). Lizards of Brazilian Amazonia (Reptilia: Squamata). *Zoologische Verhandlungen*, 299, 1–706.
- Ayala, S. C., & Harris, D. M. (1984). A new microteiid lizard (*Alopoglossus*) from the Pacific rain forest of Colombia. *Herpetologica*, 40, 154–158.
- Barrett, J. C., Fry, B., Maller, J. D., & Dally, M. J. (2005). Haploview: Analysis and visualization of LD and haplotype maps. *Bioinformatics*, 21, 263–265.
- Bouckaert, R., Heled, J., Kühnert, D., Vaughan, T., Wu, C.-H., Xie, D., Suchard, M. A., Rambaut, A., & Drummond, A. J. (2014). BEAST 2: A software platform for bayesian evolutionary analysis. *PLoS Computational Biology*, 10, e1003537. <https://doi.org/10.1371/journal.pcbi.1003537>
- Boulenger, G. A. (1885). *Catalogue of the lizards in the British Museum (Natural History). Volume II, Iguanidae, Xenosauridae, Zonuridae, Anguillidae, Anniellidae, Helodermatidae, Varanidae, Xantusiidae, Teiidae, Amphisbaenidae, Second edition*: Trustees of the British Museum.
- Boulenger, G. A. (1890). First report on additions to the lizard collection in the British Museum (Natural History). *Proceedings of the Zoological Society of London*, 1890, 77–86.
- Castoe, T. A., Doan, T. M., & Parkinson, C. L. (2004). Data partitions and complex models in Bayesian analysis: The phylogeny of gymnophthalmid lizards. *Systematic Biology*, 53, 448–469. <https://doi.org/10.1080/10635150490445797>
- Clark, K., Karsch-Mizrachi, I., Lipman, D. J., Ostell, J., & Sayers, E. W. (2016). GenBank. *Nucleic Acids Research*, 44, D67–D72. <https://doi.org/10.1093/nar/gkv1276>
- Cope, E. D. (1876). Report on the reptiles brought by Professor James Orton from the middle and upper Amazon, and western Peru. *Journal of the Academy of Natural Sciences of Philadelphia*, 8, 159–183.
- de Oliveira, D. P., de Carvalho, V. T., & Hrbek, T. (2016). Cryptic diversity in the lizard genus *Plica* (Squamata): Phylogenetic diversity and Amazonian biogeography. *Zoologica Scripta*, 45, 630–641. <https://doi.org/10.1111/zsc.12172>
- Dowling, H. G., & Savage, J. M. (1960). A guide to the snake hemipenis: A survey of basic structure and systematic characteristics. *Zoologica*, 45, 17–28.
- Duellman, W. E. (1973). Descriptions of new lizards from the upper Amazon Basin. *Herpetologica*, 29, 228–231.
- Ezard, T., Fujisawa, T., & Barraclough, T. G. (2009). SPLITS: SPecies' Limits by threshold statistics, R package version 1.0-19. <http://R-Forge.R-project.org/projects/splits/>
- Fitzinger, L. J. F. J. (1826). *Neue Classification der Reptilien nach ihren Natürlichen Verwandtschaften nebst einer Verwandtschafts-Tafel und einem Verzeichnisse der Reptilien-Sammlung des K.K. Zoologisch Museum's zu Wien*. : J.G. Heubner.
- Fouquet, A., Cassini, C., Haddad, C. F. B., Pech, N., & Rodrigues, M. T. (2014). Species delimitation, patterns of diversification and historical biogeography of a Neotropical frog genus; *Adenomera* (Anura, Leptodactylidae). *Journal of Biogeography*, 41, 855–870. <https://doi.org/10.1111/jbi.12250>
- Fouquet, A., Gilles, A., Vences, M., Marty, C., Blanc, M., & Gemmill, N. J. (2007). Underestimation of species richness in Neotropical frogs revealed by mtDNA analyses. *PLoS One*, 2, e1109. <https://doi.org/10.1371/journal.pone.0001109>
- Fujisawa, T., & Barraclough, T. G. (2013). Delimiting species using single-locus data and the Generalized Mixed Yule Coalescent (GMYC) approach: A revised method and evaluation on simulated datasets. *Systematic Biology*, 62, 707–724. <https://doi.org/10.1093/sysbio/syt033>
- Funk, W. C., Caminer, M., & Ron, S. R. (2012). High levels of cryptic species diversity uncovered in Amazonian frogs. *Proceedings of the Royal Society B*, 279, 1806–1814. <https://doi.org/10.1098/rspb.2011.1653>
- Geurgas, S. R., & Rodrigues, M. T. (2010). The hidden diversity of *Coleodactylus amazonicus* (Sphaerodactylidae, Gekkota) revealed by molecular data. *Molecular Phylogenetics and Evolution*, 54, 583–593. <https://doi.org/10.1016/j.ympev.2009.10.004>
- Goicoechea, N., Frost, D. R., De la Riva, I., Pellegrino, K. C. M., Sites, J., Rodrigues, M. T., & Padial, J. M. (2016). Molecular systematics of teiid lizards (Teioidea/Gymnophthalmoidea: Squamata) based on the analysis of 48 loci under tree-alignment and similarity-alignment. *Cladistics*, 2016, 1–48. <https://doi.org/10.1111/cla.12150>
- Gumbs, R., Gray, C. L., Böhm, M., Hoffman, M., Grenyer, R., Jetz, W., Meiri, S., Roll, U., Owen, N. R., & Rosindell, J. (2020). Global priorities for conservation of reptilian phylogenetic diversity in the face of human impacts. *Nature Communications*, 11, 2616. <https://doi.org/10.1038/s41467-020-16410-6>
- Guo, P., Liu, Q., Zhu, F., Murphy, R. W., Zhong, G. H., Che, J., Wang, P., Xie, Y. L., & Malhotra, A. (2019). Multilocus phylogeography of the brown-spotted pitviper *Protobothrops mucrosquamatus* (Reptilia: Serpentes: Viperidae) sheds a new light on the diversification pattern in Asia. *Molecular Phylogenetics and Evolution*, 133, 82–91. <https://doi.org/10.1016/j.ympev.2018.12.028>
- Hammer, Ø., Harper, D. A. T., & Ryan, P. D. (2001). Past: Paleontological statistics software package for education and data analysis. *Palaeontologia Electronica*, 4, 1–9.
- Harris, D. M. (1994). Review of the teiid lizard genus *Ptychoglossus*. *Herpetological Monographs*, 8, 226–275. <https://doi.org/10.2307/1467082>
- Hortal, J., de Bello, F., Diniz-Filho, J. A. F., Lewinsohn, T. M., Lobo, J. M., & Ladle, R. J. (2015). Seven shortfalls that beset large-scale knowledge of biodiversity. *Annual Review of Ecology, Evolution, and Systematics*, 46, 523–549. <https://doi.org/10.1146/annurev-ecolsys-112414-054400>
- Katoh, K., & Standley, D. M. (2013). MAFFT Multiple sequence alignment software version 7: Improvements in performance and usability. *Molecular Biology and Evolution*, 30, 772–780.
- Kearse, M., Moir, R., Wilson, A., Stones-Havas, S., Cheung, M., Sturrock, S., Buxton, S., Cooper, A., Markowitz, S., Duran, C., Thierer, T., Ashton, B., Mentjies, P., & Drummond, A. (2012). Geneious Basic: An integrated and extendable desktop software platform for the organization and analysis of sequence data. *Bioinformatics*, 28, 1647–1649. <https://doi.org/10.1093/bioinformatics/bts199>
- Köhler, G., Diethert, H.-H., & Veselý, M. (2012). A contribution to the knowledge of the lizard genus *Alopoglossus* (Squamata: Gymnophthalmidae). *Herpetological Monographs*, 26, 173–188. <https://doi.org/10.1655/HERPMONOGRAPHS-D-10-00011.1>
- Kumar, S., Stecher, G., & Tamura, K. (2016). MEGA7: Molecular evolutionary genetics analysis version 7.0 for bigger datasets. *Molecular Biology and Evolution*, 33, 1870–1874. <https://doi.org/10.1093/molbev/msw054>
- Lanfear, R., Frandsen, P. B., Wright, A. M., Senfeld, T., & Calcott, B. (2017). PartitionFinder 2: New methods for selecting partitioned models of evolution for molecular and morphological phylogenetic analyses. *Molecular Biology and Evolution*, 34, 772–773. <https://doi.org/10.1093/molbev/msw260>
- Linnaeus, C. (1758). *Systema naturae per regna tria naturae, secundum classes, ordines, genera, species, cum characteribus, differentiis, synonymis, locis, Tomus I, Editio Decima, Reformata*. : Holmiae, Impensis Direct.
- Macey, J. R., Schulte, J. A. II, Ananjeva, N. B., Larson, A., Rastegar-Pouyani, N., Shammakov, S. M., & Papenfuss, T. J. (1998). Phylogenetic relationships among agamid lizards of the *Laudakia caucasia* species group: Testing hypotheses of biogeographic fragmentation and an area cladogram for the Iranian Plateau. *Molecular Phylogenetic & Evolution*, 10, 118–131. <https://doi.org/10.1006/mpev.1997.0478>
- Manzani, P. R., & Abe, A. S. (1988). Sobre dois métodos de preparo do hemipênis de Serpentes. *Memórias do Instituto Butantan*, 50, 15–20.

- Marques-Souza, S., Pellegrino, K. C. M., Brunes, T. O., Carnaval, A. C., Borges, M. L. O., Gallardo, C. C., & Rodrigues, M. T. (2019). Hidden in the DNA: How multiple historical processes and natural history traits shaped patterns of cryptic diversity in an Amazon leaf-litter lizard *Loxopholis osvaldoi* (Squamata: Gymnophthalmidae). *Journal of Biogeography*, 47, 501–515. <https://doi.org/10.1111/jbi.13748>
- Miller, M. A., Pfeiffer, W., & Schwartz, T. (2010). Creating the CIPRES Science Gateway for inference of large phylogenetic trees. *Proceedings of the Gateway Computing Environments Workshop (GCE)*, 1–8.
- Miralles, A., & Vences, M. (2013). New metrics for comparison of taxonomies reveal striking discrepancies among species delimitation methods in *Madascincus* lizards. *PLoS One*, 8, e68242. <https://doi.org/10.1371/journal.pone.0068242>
- Moraes, L. J. C. L., Pavan, D., Barros, M. C., & Ribas, C. C. (2016). The combined influence of riverine barriers and flooding gradients on biogeographical patterns for amphibian and squamates in south-eastern Amazonia. *Journal of Biogeography*, 43, 2113–2124. <https://doi.org/10.1111/jbi.12756>
- Moraes, L. J. C. L., Ribas, C. C., Pavan, D., & Werneck, F. P. (2020). Biotic and Landscape Evolution in an Amazonian Contact Zone: Insights from the Herpetofauna of the Tapajós River Basin, Brazil. In V. Rull, & A. C. Carnaval (Eds.), *Neotropical diversification: Patterns and processes* (pp. 683–712). Springer.
- Morales, C. M., Sturaro, M. J., Nunes, P. M. S., Lotzkat, S., & Peloso, P. L. V. (2020). A species-level total evidence phylogeny of the microteiid lizard family Alopoglossidae (Squamata: Gymnophthalmoidea). *Cladistics*, 36, 301–321. <https://doi.org/10.1111/cla.12407>
- Myers, C. W., Fuenmayor, G. R., & Jadin, R. C. (2009). New species of lizards from Auyantepui and La Escalera in the Venezuelan Guayana, with notes on “microteiid” hemipenes (Squamata: Gymnophthalmidae). *American Museum Novitates*, 3660, 1–31. <https://doi.org/10.1206/6571>
- Nunes, P. M. S. (2011). *Morfologia hemipeniana dos lagartos microteídeos e suas implicações nas relações filogenéticas da família Gymnophthalmidae (Teiioidea: Squamata) Volumes 1 and 2*. Unpublished PhD Thesis, Universidade de São Paulo, São Paulo.
- Nunes, P. M. S., Fouquet, A., Curcio, F. F., Kok, P. J. R., & Rodrigues, M. T. (2012). Cryptic species in *Iphisa elegans* Gray, 1851 (Squamata: Gymnophthalmidae) revealed by hemipenial morphology and molecular data. *Zoological Journal of the Linnean Society*, 166, 361–376. <https://doi.org/10.1111/j.1096-3642.2012.00846.x>
- O’Shaughnessy, A. W. E. (1881). An account of the collection of lizards made by Mr. Buckley in Ecuador, and now in the British Museum, with descriptions of the new species. *Proceedings of the Zoological Society of London*, 1881, 227–245. <https://doi.org/10.1111/j.1096-3642.1881.tb01282.x>
- Ortiz, D. A., Lima, A. P., & Werneck, F. P. (2018). Environmental transition zone and rivers shape intraspecific population structure and genetic diversity of an Amazonian rain forest tree frog. *Evolutionary Ecology*, 32, 359–378. <https://doi.org/10.1007/s10682-018-9939-2>
- Padial, J. M., Miralles, A. D., de la Riva, I., & Vences, M. (2010). The integrative future of taxonomy. *Frontiers in Zoology*, 7, 1–14. <https://doi.org/10.1186/1742-9994-7-16>
- Pantoja, D. L., & Fraga, R. (2012). Herpetofauna of the Reserva Extrativista do Rio Gregório, Juruá Basin, southwest Amazonia, Brazil. *Check List*, 8, 360–374. <https://doi.org/10.15560/8.3.360>
- Pellegrino, C. M., Rodrigues, M. T., Yonenaga-Yassuda, Y., & Sites, J. W. (2001). A molecular perspective on the evolution of microteiid lizards (Squamata, Gymnophthalmidae), and a new classification for the family. *Biological Journal of the Linnean Society*, 74, 315–338. <https://doi.org/10.1006/bjil.2001.0580>
- Peloso, P. L. V., & Ávila-Pires, T. C. S. (2010). Morphological variation in *Ptychoglossus brevifrontalis* Boulenger, 1912 and the status of *Ptychoglossus nicefori* (Loveridge, 1929) (Squamata, Gymnophthalmidae). *Herpetologica*, 66, 357–372. <https://doi.org/10.1655/09-048.1>
- Peloso, P. L. V., & Morales, C. H. (2017). Description of a new species of *Alopoglossus* Boulenger, 1885 from Western Colombia (Gymnophthalmoidea). *South American Journal of Herpetology*, 12, 89–98. <https://doi.org/10.2994/SAJH-D-16-00059.1>
- Peracca, M. G. (1904). Rettili ed anfibi. *Bollettino Dei Musei Di Zoologia Ed Anatomia Comparata Della R. Università Di Torino*, 19, 1–41. <https://doi.org/10.5962/bhl.part.11596>
- Pesantes, O. S. (1994). A method for preparing the hemipenis of preserved snakes. *Journal of Herpetology*, 28, 93–95. <https://doi.org/10.2307/1564686>
- Primack, R., & Corlett, R. (2005). *Tropical rain forests: An ecological and biogeographical comparison*. Blackwell Publishing.
- Puillandre, N., Lambert, A., Brouillet, S., & Achaz, G. (2012). ABGD, Automatic Barcode Gap Discovery for primary species delimitation. *Molecular Ecology*, 21, 1864–1877. <https://doi.org/10.1111/j.1365-294X.2011.05239.x>
- R Core Team (2013). *R: A language and environment for statistical computing*. R Foundation for Statistical Computing. <http://www.R-project.org/>
- Rabosky, D. L., von May, R., Grundler, M. C., & Davis Rabosky, A. R. (2019). The Western Amazonian richness gradient for squamate reptiles: Are there really fewer snakes and lizards in Southwestern Amazonian lowlands? *Diversity*, 11, 199. <https://doi.org/10.3390/d11100199>
- Rambaut, A., Suchard, M. A., Xie, D., & Drummond, A. J. (2018). Tracer version 1.7. <http://tree.bio.ed.ac.uk/software/tracer>
- Ribeiro-Júnior, M. A. (2015a). Catalogue of distribution of lizards (Reptilia: Squamata) from the Brazilian Amazonia. I. Dactyloidae, Hoplocercidae, Iguanidae, Leiosauridae, Polychrotidae, Tropicuridae. *Zootaxa*, 3983, 1–110. <https://doi.org/10.11646/zootaxa.3983.1.1>
- Ribeiro-Júnior, M. A. (2015b). Catalogue of distribution of lizards (Reptilia: Squamata) from the Brazilian Amazonia. II. Gekkonidae, Phyllodactylidae. *Sphaerodactylidae*. *Zootaxa*, 3981, 1–55.
- Ribeiro-Júnior, M. A. (2018). A new species of *Alopoglossus* lizard (Squamata, Alopoglossidae) from the Southern Guiana Shield, northeastern Amazonia, with remarks on diagnostic characters to the genus. *Zootaxa*, 4422, 25–40. <https://doi.org/10.11646/zootaxa.4422.1.2>
- Ribeiro-Júnior, M. A., & Amaral, S. (2016a). Catalogue of distribution of lizards (Reptilia: Squamata) from the Brazilian Amazonia. III. Anguidae, Scincidae, Teiidae. *Zootaxa*, 4205, 401–430. <https://doi.org/10.11646/zootaxa.4205.5.1>
- Ribeiro-Júnior, M. A., & Amaral, S. (2016b). Diversity, distribution, and conservation of lizards (Reptilia: Squamata) in the Brazilian Amazonia. *Neotropical Biodiversity*, 2, 195–421. <https://doi.org/10.1080/23766808.2016.1236769>
- Ribeiro-Júnior, M. A., & Amaral, S. (2017). Catalogue of distribution of lizards (Reptilia: Squamata) from the Brazilian Amazonia. IV. Alopoglossidae, Gymnophthalmidae. *Zootaxa*, 4269, 151–196. <https://doi.org/10.11646/zootaxa.4269.2.1>
- Ribeiro-Júnior, M. A., Choueri, E., Lobos, S., Venegas, P., Torres-Carvajal, O., & Werneck, F. (2020). Eight in one: Morphological and molecular analyses reveal cryptic diversity in Amazonian alopoglossid lizards (Squamata: Gymnophthalmoidea). *Zoological Journal of the Linnean Society*, 190, 227–270. <https://doi.org/10.1093/zoolinnean/zlz155>
- Ribeiro-Júnior, M. A., Gardner, T. A., & Ávila-Pires, T. C. S. (2008). Evaluating the effectiveness of herpetofaunal sampling techniques across a gradient of habitat change in a tropical forest landscape. *Journal of Herpetology*, 42, 733–749. <https://doi.org/10.1670/07-097R3.1>
- Ribeiro-Júnior, M. A., Meiri, S., & Fouquet, A. (2020). A new species of *Alopoglossus* Boulenger (1885) (Squamata, Alopoglossidae) from the lowlands of the eastern Guiana Shield, with assessment of the taxonomic status of *A. copii surinamensis*. *Journal of Herpetology*, 54, 427–445. <https://doi.org/10.1670/20-032>

- Ribeiro-Júnior, M. A., Silva, M. B., & Lima, J. D. (2016). A new species of *Bachia* Gray 1845 (Squamata: Gymnophthalmidae) from the eastern Guiana Shield. *Herpetologica*, 72, 148–156. <https://doi.org/10.1655/HERPETOLOGICA-D-15-00030>
- Roll, U., Feldman, A., Novosolov, M., Allison, A., Bauer, A. M., Bernard, R., Böhm, M., Castro-Herrera, F., Chirio, L., Collen, B., Colli, G. R., Dabool, L., Das, I., Doan, T. M., Grismer, L. L., Hoogmoed, M., Itescu, Y., Kraus, F., LeBreton, M., ... Meiri, S. (2017). The global distribution of tetrapods reveals a need for targeted reptile conservation. *Nature Ecology & Evolution*, 1, 1677–1682. <https://doi.org/10.1038/s41559-017-0332-2>
- Ronquist, F., Teslenko, M., van der Mark, P., Ayres, D. L., Darling, A., Höhna, S., Larget, B., Liu, L., Suchard, M. A., & Huelsenbeck, J. P. (2012). MrBayes 3.2: Efficient Bayesian phylogenetic inference and model choice across a large model space. *Systematic Biology*, 61, 539–542. <https://doi.org/10.1093/sysbio/sys029>
- Ruibal, R. (1952). Revisionary studies of some South American Teiidae. *Bulletin of the Museum of Comparative Zoology*, 106, 477–529.
- Ruthven, A. G. (1924). Description of a new lizard of the genus *Alopoglossus*. *Occasional Papers of the Museum of Zoology, University of Michigan*, 153, 1–3.
- Sabaj-Perez, M. H. (2016). Standard symbolic codes for institutional resource collections in herpetology and ichthyology: An online reference (v6.5). <http://www.asih.org/>
- Silva, M. B., Ribeiro-Júnior, M. A., & Ávila-Pires, T. C. S. (2018). A new species of *Tupinambis* Daudin, 1802 (Squamata: Teiidae) from Central South America. *Journal of Herpetology*, 52, 94–110. <https://doi.org/10.1670/16-036>
- Silva, N. J. Jr, & Sites, J. W. Jr (1995). Patterns of diversity of Neotropical Squamate reptile species with emphasis on the Brazilian Amazon and the conservation potential of indigenous reserves. *Conservation Biology*, 9, 873–901. <https://doi.org/10.1046/j.1523-1739.1995.09040873.x>
- Stamatakis, A. (2014). RAxML version 8: A tool for phylogenetic analysis and post-analysis of large phylogenies. *Bioinformatics*, 30, 1312–1313. <https://doi.org/10.1093/bioinformatics/btu033>
- Torres-Carvajal, O., & Lobos, S. E. (2014). A new species of *Alopoglossus* lizard (Squamata, Gymnophthalmidae) from the tropical Andes, with a molecular phylogeny of the genus. *ZooKeys*, 410, 105–120. <https://doi.org/10.3897/zookeys.410.7401>
- Uzzell, T. (1973). A revision of lizards of the genus *Prionodactylus* with a new genus for *P. leucostictus* and notes on the genus *Euspondylus* (Sauria, Teiidae). *Postilla*, 159, 1–67.
- Vacher, J.-P., Chave, J., Ficetola, F., Sommeria-Klein, G., Tao, S., Thébaud, C., Blanc, M., Camacho, A., Cassimiro, J., Colston, T. J., Dewynter, M., Ernst, R., Gaucher, P., Gomes, J. O., Jairam, R., Kok, P. J. R., Lima, J. D., Martinez, Q., Marty, C., ... Fouquet, A. (2020). Large scale DNA-based survey of Amazonian frogs suggest a vast underestimation of species richness and endemism. *Journal of Biogeography*, 47, 1781–1791. <https://doi.org/10.1111/jbi.13847>
- Vieites, D. R., Wollenberg, K. C., Andreone, F., Köhler, J., Glaw, F., & Vences, M. (2009). Vast underestimation of Madagascar's biodiversity evidenced by an integrative amphibian inventory. *Proceedings of the National Academy of Sciences of the United States of America*, 106, 8267–8272. <https://doi.org/10.1073/pnas.0810821106>
- Waldez, F., Menin, M., & Vogt, R. C. (2013). Diversidade de anfíbios e répteis Squamata na região do baixo rio Purus, Amazônia Central, Brasil. *Biota Neotropica*, 13, 300–316. <https://doi.org/10.1590/S1676-06032013000100029>
- Werneck, F. P., Gamble, T., Colli, G. R., Rodrigues, M. T., & Sites, J. W. Jr (2012). Deep diversification and long-term persistence in the South American 'dry diagonal': Integrating continentwide phylogeography and distribution modeling of geckos. *Evolution*, 66, 3014–3034. <https://doi.org/10.1111/j.1558-5646.2012.01682.x>
- Wiens, J. J., & Servedio, M. R. (2000). Species delimitation in systematics: Inferring diagnostic differences between species. *Proceedings of the Royal Society of London B*, 267, 631–636.
- Zaher, H. (1999). Hemipenial morphology of the South American Xenodontine snakes, with a proposal for a monophyletic Xenodontinae and a reappraisal of colubroid hemipenes. *Bulletin of the American Museum of Natural History*, 240, 1–168.
- Zaher, H., & Prudente, A. L. C. (2003). Hemipenes of *Siphlophis* (Serpentes, Xenodontinae) and techniques of Hemipenial preparation in snakes: A response to Dowling. *Herpetological Review*, 34, 302–307.

SUPPORTING INFORMATION

Additional supporting information may be found online in the Supporting Information section.

Figure S1. Bayesian phylogenetic tree (A) and haplotype network (B) inferred from a fragment of the nuclear DNA locus *PRLR*

Figure S2. Bayesian phylogenetic tree (A) and haplotype network (B) inferred from a fragment of the nuclear DNA locus *SNCAIP*

Figure S3. Hemipenis of the paratype of *Alopoglossus indigenorum* sp. nov. (INPA-H 30243)

Table S1. Accession numbers and complete information related to our molecular dataset

Table S2. Summary of the variation in measurements between males and females of *Alopoglossus amazonius*, *A. gansorum* sp. nov., and *A. indigenorum* sp. nov

List S1. Referred specimens

Data S1. Ribeiro-Junior_et_al_PRLR

Data S2. Ribeiro-Junior_et_al_SNCAIP

Data S3. Ribeiro-Junior_et_al_CYTB

Data S4. Ribeiro-Junior_et_al_ND4

Data S5. Ribeiro-Junior_et_al_concatenated_alignment

How to cite this article: Ribeiro-Júnior MA, Sánchez-Martínez PM, Moraes LJ, et al. Uncovering hidden species diversity of alopoglossid lizards in Amazonia, with the description of three new species of *Alopoglossus* (Squamata: Gymnophthalmidae). *J Zool Syst Evol Res*. 2021;00:1–35. <https://doi.org/10.1111/jzs.12481>

Uncovering hidden species diversity of alopoglossid lizards in Amazonia, with the description of three new species of *Alopoglossus* (Squamata: Gymnophthalmoidae)

Marco Antônio Ribeiro-Júnior, Paola María Sánchez-Martínez, Leandro João Carneiro de Lima Moraes, Uécson Suendel Costa de Oliveira, Vinícius Tadeu de Carvalho, Dante Pavan, Erik Henrique de Lacerda Choueri, Fernanda P. Werneck, & Shai Meiri

List of Supporting Information

Table S1. Accession numbers and complete information related to our molecular dataset.

Table S2. Summary of the variation in measurements between males and females of *Alopoglossus amazonius*, *A. gansorum* sp. nov., and *A. indigenorum* sp. nov.

List S1. Referred specimens.

Figure S1. Bayesian phylogenetic tree (A) and haplotype network (B) inferred from a fragment of the nuclear DNA locus *PRLR*.

Figure S2. Bayesian phylogenetic tree (A) and haplotype network (B) inferred from a fragment of the nuclear DNA locus *SNCAIP*.

Figure S3. Hemipenis of the paratype of *Alopoglossus indigenorum* sp. nov. (INPA-H 30243).

FASTA files:

Ribeiro-Junior_et_al_PRLR

Ribeiro-Junior_et_al_SINCAIP

Ribeiro-Junior_et_al_CYTB

Ribeiro-Junior_et_al_ND4

Ribeiro-Junior_et_al_concatenated_alignment

Table S1. Accession numbers and complete information related to sequences included in our dataset.

Taxon	Voucher	Type status	Locality	Country	Lat	Long	Cytb	ND4	PRLR (phased)	SINCAIP (phased)
<i>Alopoglossus amazonius</i>	CHUNB22682	---	Guajará-Mirim, Rondônia	Brazil	-10.80	-65.36	MN735116	MN735056	---	MN734822 / MN734823
<i>Alopoglossus angulatus</i>	MPEG21853	---	Acampamento Mutum, Juruti, Pará	Brazil	-2.60	-56.19	---	MN735074	MN734998 / MN734999	MN734878 / MN734879
<i>Alopoglossus angulatus</i>	MPEG28239	---	Acampamento Mutum, Juruti, Pará	Brazil	-2.60	-56.19	MN735134	MN735078	MN735006 / MN735007	MN734886 / MN734887
<i>Alopoglossus angulatus</i>	MPEG28502	---	Adutora, Juruti, Pará	Brazil	-2.45	-56.15	MN735135	MN735079	MN735008 / MN735009	MN734888 / MN734889
<i>Alopoglossus angulatus</i>	INPA-H26238	---	FLONA Trairão, Pará	Brazil	-4.56	-55.4	MN735123	---	MN734960 / MN734961	MN734834 / MN734835
<i>Alopoglossus angulatus</i>	INPA-H26239	---	FLONA Trairão, Pará	Brazil	-4.56	-55.4	MN735124	---	---	MN734836 / MN734837
<i>Alopoglossus angulatus</i>	MPEG27542	---	FLOTA Paru, Almeirim, Pará	Brazil	-0.94	-53.23	MN735131	MN735075	MN735000 / MN735001	MN734880 / MN734881
<i>Alopoglossus angulatus</i>	MPEG27543	---	FLOTA Paru, Almeirim, Pará	Brazil	-0.93	-53.22	MN735132	MN735076	MN735002 / MN735003	MN734882 / MN734883
<i>Alopoglossus angulatus</i>	MPEG29595	---	Ilha do Marajó, Rio Preto, Afuá, Pará	Brazil	-0.42	-50.48	MN735137	MN735081	MN735012 / MN735013	MN734890 / MN734891
<i>Alopoglossus angulatus</i>	MPEG29596	---	Ilha do Marajó, Rio Preto, Afuá, Pará	Brazil	-0.42	-50.48	MN735138	MN735082	MN735014 / MN735015	MN734892 / MN734893
<i>Alopoglossus angulatus</i>	MPEG29597	---	Ilha do Marajó, Rio Preto, Afuá, Pará	Brazil	-0.42	-50.47	MN735139	MN735083	MN735016 / MN735017	MN734894 / MN734895
<i>Alopoglossus angulatus</i>	MPEG29598	---	Ilha do Marajó, Rio Preto, Afuá, Pará	Brazil	-0.42	-50.47	MN735140	MN735084	MN735018 / MN735019	MN734896 / MN734897
<i>Alopoglossus angulatus</i>	MPEG29599	---	Ilha do Marajó, Rio Preto, Afuá, Pará	Brazil	-0.42	-50.47	MN735141	MN735085	---	MN734898 / MN734899
<i>Alopoglossus angulatus</i>	MPEG29601	---	Ilha do Marajó, Rio Preto, Afuá, Pará	Brazil	-0.42	-50.49	MN735142	MN735086	MN735022 / MN735023	MN734902 / MN734903
<i>Alopoglossus angulatus</i>	MPEG29602	---	Ilha do Marajó, Rio Preto, Afuá, Pará	Brazil	-0.42	-50.48	MN735143	MN735087	MN735024 / MN735025	MN734904 / MN734905
<i>Alopoglossus angulatus</i>	MPEG29603	---	Ilha do Marajó, Rio Preto, Afuá, Pará	Brazil	-0.42	-50.48	MN735144	MN735088	MN735026 / MN735027	MN734906 / MN734907
<i>Alopoglossus angulatus</i>	MPEG29604	---	Ilha do Marajó, Rio Preto, Afuá, Pará	Brazil	-0.42	-50.48	MN735145	MN735089	MN735028 / MN735029	MN734908 / MN734909
<i>Alopoglossus angulatus</i>	Ernst12124	---	Guyana	Guyana	5.15	-58.69	MN735121	---	---	MN734830 / MN734831
<i>Alopoglossus angulatus</i>	PG176	---	Awala	French Guiana	5.72	-53.91	---	MN735091	---	MN734914 / MN734915
<i>Alopoglossus angulatus</i>	BOHE10	---	Borne 4	French Guiana	2.37	-53.77	MN735111	MN735051	---	MN734810 / MN734811
<i>Alopoglossus angulatus</i>	MPEG29762	---	Rio Maracá, Mazagão, Amapá	Brazil	-0.17	-51.77	MN735146	MN735090	MN735030 / MN735031	MN734910 / MN734911
<i>Alopoglossus angulatus</i>	MPEG29468	---	São Luis, Itaituba, Pará	Brazil	-4.48	-56.24	MN735136	MN735080	MN735010 / MN735011	---

<i>Alopoglossus angulatus</i>	MPEG27609	---	REBIO Maicuru, Almeirin, Pará	Brazil	0.83	-53.93	MN735133	MN735077	MN735004 / MN735005	MN734884 / MN734885 MN734920 / MN734921 MN734916 / MN734917
<i>Alopoglossus angulatus</i>	INPA-H35839	---	Reserva Adolpho Ducke, Amazonas	Brazil	-2.95	-59.92	MN735147	MN735094	---	
<i>Alopoglossus angulatus</i>	PG314	---	Toponowini	French Guiana	3.09	-52.78	---	MN735092	---	
<i>Alopoglossus angulatus</i>	INPA-H20118	---	UTE Poço de Silves, Amazonas	Brazil	-2.85	-58.46	MN735122	---	MN734958 / MN734959	---
<i>Alopoglossus angulatus</i>	INPA-H41384	---	Trairão, Médio Rio Tapajós, margem Leste, Pará	Brazil	-5.07	-56.44	---	MN866498	---	---
<i>Alopoglossus angulatus</i>	INPA-H41385	---	Trairão, Médio Rio Tapajós, margem Leste, Pará	Brazil	-5.10	-56.44	---	MN866500	---	---
<i>Alopoglossus angulatus</i>	BPN2920	---	RAP BC 1, Waterfall trail	Suriname	2.46	-55.62	---	MN735052	---	MN734812/MN 734813
<i>Alopoglossus avilapiresae</i>	CORBIDI8321	---	La Convención, KP 50, Cuzco	Peru	-12.18	-73.00	---	MN735033	---	---
<i>Alopoglossus carinicaudatus</i>	QCAZ9530	---	Comunidad El Edén, margen S del Río Napo, Orellana	Ecuador	-0.49	-76.07	MN735109	MN735049	MN734950 / MN734951	---
<i>Alopoglossus carinicaudatus</i>	QCAZ9531	---	Comunidad El Edén, margen S del Río Napo, Orellana	Ecuador	-0.49	-76.07	MN735110	MN735050	MN734952 / MN734953	---
<i>Alopoglossus carinicaudatus</i>	QCAZ10735	---	Comunidad Oasis, Pad R, a 500 m de la orilla del río Napo, en orilla sur diagonal a Comunidad Pañacocha, Orellana	Ecuador	-0.46	-76.13	MN735095	MN735034	MN734924 / MN734925	---
<i>Alopoglossus carinicaudatus</i>	QCAZ5571	---	Estación Científica Yasuní, km9 vía Tivacuno, Parcela B, Orellana	Ecuador	-0.67	-76.397	MN735101	MN735040	MN734936 / MN734937	---
<i>Alopoglossus carinicaudatus</i>	QCAZ5572	---	Parque Nacional Yasuní, Estación Científica Yasuní PUCE, poza 1, Orellana	Ecuador	-0.67	-76.39	MN735102	MN735041	---	---
<i>Alopoglossus carinicaudatus</i>	QCAZ6362	---	Parque Nacional Yasuní, Estación Científica Yasuní PUCE, sendero Ceiba, Orellana	Ecuador	-0.67	-76.39	MN735104	MN735043	MN734940 / MN734941	---
<i>Alopoglossus carinicaudatus</i>	QCAZ11600	---	Parque Nacional Yasuní, Tambococha, Orellana	Ecuador	-0.97	-75.42	MN735096	MN735035	MN734926 / MN734927	---
<i>Alopoglossus carinicaudatus</i>	QCAZ5227	---	Parque Nacional Yasuní, vía Pompeya Sur-Iro, Sitio A16, Orellana	Ecuador	---	---	MN735100	MN735039	MN734934 / MN734935	---
<i>Alopoglossus carinicaudatus</i>	QCAZ5216	---	Parque Nacional Yasuní, vía Pompeya Sur-Iro, Sitio A33, Orellana	Ecuador	---	---	MN735098	MN735037	MN734930 / MN734931	---
<i>Alopoglossus carinicaudatus</i>	QCAZ5226	---	Parque Nacional Yasuní, vía Pompeya Sur-Iro, Sitio A35, Orellana	Ecuador	---	---	MN735099	MN735038	MN734932 / MN734933	---
<i>Alopoglossus carinicaudatus</i>	QCAZ5191	---	Parque Nacional Yasuní, vía Pompeya Sur-Iro, Sitio A38, Orellana	Ecuador	---	---	MN735097	MN735036	MN734928 / MN734929	---
<i>Alopoglossus carinicaudatus</i>	QCAZ7944	---	Parroquia Taracoa, Orellana	Ecuador	-0.57	-76.08	MN735105	MN735044	MN734942 / MN734943	---
<i>Alopoglossus carinicaudatus</i>	QCAZ9144	---	Vía Pompeya Sur-Iro, km 80, puente sobre el Río Beye, Orellana	Ecuador	-0.84	-76.30	MN735107	MN735047	MN734946 / MN734947	---
<i>Alopoglossus carinicaudatus</i>	QCAZ8915	---	Cononaco, Bataburo Lodge, Pastaza	Ecuador	-1.20	-76.71	---	MN735046	---	---
<i>Alopoglossus carinicaudatus</i>	QCAZ9526	---	A 2,5 km al S de Pañacocha, en el margen N del Río Napo, Sucumbios	Ecuador	-0.47	-76.06	MN735108	MN735048	MN734948 / MN734949	---
<i>Alopoglossus carinicaudatus</i>	QCAZ8489	---	Reserva de Producción Faunística	Ecuador	-0.01	-76.18	MN735106	MN735045	MN734944 /	---

			Cuyabeno, cabañas Neotropic. Laguna Grande, Sucumbios						MN734945	
<i>Alopoglossus carinicaudatus</i>	QCAZ5624	---	Reserva de Producción Faunística Cuyabeno, Saladero de Dantas, Sucumbios	Ecuador	-0.01	-76.17	MN735103	MN735042	MN734938 / MN734939	---
<i>Alopoglossus colli</i>	UFMT4105	Paratype	PCH Ombreiras, margem direita do rio Jauru, Mato Grosso	Brazil	-15.31	-58.86	---	MN735093	---	MN734918 / MN734919
<i>Alopoglossus colli</i>	CHUNB18038	Holotype	Pimenta Bueno, Rondônia	Brazil	-12.50	-60.81	MN735112	---	MN734954 / MN734955	MN734814 / MN734815
<i>Alopoglossus colli</i>	CHUNB18039	Paratype	Pimenta Bueno, Rondônia	Brazil	-12.50	-60.81	MN735113	MN735053	---	MN734816 / MN734817
<i>Alopoglossus colli</i>	CHUNB18040	Paratype	Pimenta Bueno, Rondônia	Brazil	-12.50	-60.81	MN735114	MN735054	---	MN734818 / MN734819
<i>Alopoglossus colli</i>	CHUNB18599	Paratype	Pimenta Bueno, Rondônia	Brazil	-12.50	-60.81	MN735115	MN735055	---	MN734820 / MN734821
<i>Alopoglossus gansorum</i> sp. nov.	INPA-H34780	Paratype	Igarapé do Jacinto, rio Purus, Amazonas	Brazil	-5.71	-63.21	MN735117	---	MN734956 / MN734957	MN734824 / MN734825
<i>Alopoglossus gansorum</i> sp. nov.	CZPB-RP179	Paratype	REBIO Abufari, comunidade Turiaçu, rio Purus, Amazonas	Brazil	-4.96	-62.97	MN735118	---	---	MN734826 / MN734827
<i>Alopoglossus gansorum</i> sp. nov.	INPA-H34770	Paratype	REBIO Abufari, comunidade Turiaçu, rio Purus, Amazonas	Brazil	-4.96	-62.96	MN735119	MN735057	---	MN734828 / MN734829
<i>Alopoglossus gansorum</i> sp. nov.	CZPB-RP180	Paratype	REBIO Abufari, comunidade Turiaçu, rio Purus, Amazonas	Brazil	-4.98	-62.96	MN735120	---	---	---
† <i>Alopoglossus indigenorum</i> sp. nov.	INPA-H39953	Paratype	Reserva Extrativista do Baixo Juruá, Amazonas	Brazil	-3.83	-66.08	---	MW916091	---	---
<i>Alopoglossus tapajosensis</i> sp. nov.	INPA-H41382	Paratype	Itaituba, Médio Rio Tapajós, margem Oeste, Pará	Brazil	-5.05	-56.87	---	MN866499	---	---
<i>Alopoglossus tapajosensis</i> sp. nov.	INPA-H41383	Holotype	Itaituba, Médio Rio Tapajós, margem Oeste, Pará	Brazil	-5.05	-56.87	---	MN866497	---	---
<i>Alopoglossus theodorusi</i>	MNHN-RA-2020.0020	Paratype	Armontabo	French Guiana	3.86	-52.48	---	---	---	MN734912 / MN734913
<i>Alopoglossus theodorusi</i>	MNHN-RA-2020.0019	Holotype	Maripa. St Georges	French Guiana	3.81	-51.88	---	MN735032	MN734922 / MN734923	MN734808 / MN734809
<i>Alopoglossus atriventris</i>	INPA-H28234	---	BR-319, Amazonas	Brazil	-6.99	-63.08	MN735126	MN735060	---	MN734840 / MN734841
<i>Alopoglossus atriventris</i>	INPA-H28239	---	BR-319, Amazonas	Brazil	-6.99	-63.08	MN735127	MN735062	MN734964 / MN734965	MN734844 / MN734845
<i>Alopoglossus atriventris</i>	INPA-H28233	---	BR-319, Amazonas	Brazil	-6.99	-63.08	MN735125	MN735059	---	MN734838 / MN734839
<i>Alopoglossus atriventris</i>	INPA-HT4625	---	Tapauá, rio Purus, igarapé do Jacinto, Amazonas	Brazil	-5.71	-63.20	MN735130	MN735067	MN734978 / MN734979	MN734858 / MN734859
<i>Arthrosaura reticulata</i>	LOMU74	---	Urucará, Amazonas	Brazil	---	---	---	MN735073	MN734996 / MN734997	MN734876 / MN734877

† New sequences.

Table S2. Summary of the variation in measurements between males and females of *Alopoglossus amazonius*, *A. gansorum*, and *A. indigenorum*. Measurements are presented as minimum–maximum (mean \pm standard deviation). Only intact and non-regenerated tails were considered.

	<i>A. amazonius</i>	<i>A. gansorum</i> sp. nov.	<i>A. indigenorum</i> sp. nov.
	(males n = 2) (females n = 6)	(males n = 3) (females n = 6)	(males n = 3) (female n = 1)
SVL (male)	33.8–45.5 (39.6 \pm 8.3)	30.9–61.6 (46.1 \pm 15.3)	54.6–59.4 (57 \pm 3.4)
SVL (female)	34.6–57 (51.1 \pm 8.7)	38.6–60.8 (48.2 \pm 9.2)	58.9
AGL (male)	15.1–21.6 (18.4 \pm 4.6)	14–28.6 (21 \pm 7.3)	25–27.9 (26.5 \pm 2)
AGL (female)	16.6–31 (26.2 \pm 5.2)	16.4–28 (22.1 \pm 5.1)	28.8
HD (male)	4.3–5 (4.7 \pm 0.5)	4.3–7.3 (5.7 \pm 1.5)	6.9–7 (7 \pm 0.1)
HD (female)	4.1–6 (5.5 \pm 0.8)	4.9–7.5 (5.9 \pm 1.1)	7.5
HW (male)	5.8–7.2 (6.5 \pm 1)	5.6–10.1 (7.9 \pm 2.2)	9.4–10.1 (9.7 \pm 0.5)
HW (female)	5.2–9.5 (8 \pm 1.5)	6.7–10.3 (8.1 \pm 1.5)	10
HL (male)	8.3–10.4 (9.3 \pm 1.5)	7.7–13.9 (10.8 \pm 3.1)	12.4–13.3 (12.9 \pm 0.7)
HL (female)	7.7–13.5 (10.5 \pm 1.9)	9.3–13.8 (11 \pm 1.8)	12.9
NL (male)	4.3–8.6 (6.4 \pm 3)	5.1–8.6 (6.7 \pm 1.8)	7.8–9 (8.4 \pm 0.8)
NL (female)	5.1–8.1 (7.5 \pm 1.2)	6–9 (8 \pm 1.4)	9.2
FL (male)	9–13 (11 \pm 2.8)	9–17 (12.7 \pm 4)	15
FL (female)	8.8–15 (13.4 \pm 2.4)	11–16 (13.2 \pm 2.4)	15
HLL (male)	14–22.8 (18.4 \pm 6.2)	12–28 (20 \pm 8)	25
HLL (female)	15.4–27 (21 \pm 3.8)	16–25 (19.8 \pm 3.5)	26

ShL (male)	5–5.2 (5.1 ± 0.1)	5–10 (7.8 ± 2.5)	9.7–10 (9.8 ± 0.2)
ShL (female)	5.4–8.5 (7.4 ± 1.3)	6.5–9.9 (8.1 ± 1.4)	9.6
TL (male)	81.66 (n = 1)	48 (n = 1)	96–98 (97 ± 1.4; n = 3)
TL (female)	57.3–110 (84.4 ± 26.4; n = 3)	55.1–88 (75 ± 17.5; n = 3)	101 (n = 1)

n = total number of specimens measured.

List S1. Referred specimens.

Alopoglossus andeanus: PERU: Madre de Dios Department: CORBIDI 13508, collected on 28 September 2013 by J. Malqui and G. Chávez, at El Parador, Inambari (12°58'47"S, 70°14'6.25"W), Tambopata; CORBIDI 17100, collected on 16 May 2013 by B. Crnobrna and H. Williams, at The Amazon Research and Conservation Center (ARCC), Las Piedras (12°2'43.86"S, 69°40'42.07"W), Tambopata; CORBIDI 17713, collected on 28 June 2016 by G. Chávez and A. Barboza, at Conseción Río Las Piedras, Las Piedras (12°8'38.04"S, 69°24'23"W), Tambopata; USNM 222340, collected on 5 November 1979 by R. McDiarmid, at ca. 30 km (airline) SSW of, Tambopata Reserve, Explorer's Inn (12°50'S, 69°17'W), Puerto Maldonado; USNM 247489, collected on 16 September 1984 by R. Cocroft, at ca. 30 km (airline) SSW of, Tambopata Reserve, Explorer's Inn (12°50'S, 69°17'W), Puerto Maldonado.

Alopoglossus angulatus: BRAZIL: State of Amapá: IEPA LT47, Cajari Extractive Reserve, A3 (0°33'57.8"S, 52°16'33.1"W), Laranjal do Jari municipality; IEPA Ac45, Cajari Extractive Reserve, Açaizal (0°33'27"S, 52°14'17"W), Laranjal do Jari municipality; IEPA Bj10, Bj61, Cajari Extractive Reserve, Bom Jardim (0°32'40"S, 52°17'09"W), Laranjal do Jari municipality; IEPA RS92, RS54b, RS115, RS176, Iratapuru Sustainable Development Reserve (0°16'35"N, 53°06'22.9"W), Laranjal do Jari municipality; IEPA 110, 114, 176, 218, 221, 245, Santo Antônio Hydroelectric Power Station (0°39'02.2"S, 52°30'23.9"W), Laranjal do Jari municipality; IEPA ST17, ST94, ST108, Santo Antônio Waterfall, Jari River (0°39'02.2"S, 52°30'23.9"W), Laranjal do Jari municipality; IEPA RS430, RS457, Cupixi River (0°34'45.8"N, 52°19'08.3"W), Pedra Branca do Amapari municipality; IEPA TQ26, Tumucumaque (1°35'44.7"N, 52°29'31.7"W), Serra do Navio municipality; MPEG 15127, collected on 18 November 1988, at margin of the Araguari River, end of Serra do Navio—Araguari highway (0°50'53.1"N, 51°11'46.2"W), Ferreira Gomes municipality, field number TCAP 973; MPEG 29762, collected on 20 October 2006 by C. Silva, at Mazagão municipality (0°10.3'S, 51°43.3'W); MPEG 797–99, 1921, collected by M. Moreira, at upper Maracá River (0°32'N, 52°12'W), Mazagão municipality; MPEG 15033, 15095, 15150–55, 15182–85, collected on 6–20 November 1988, at Serra do Navio municipality (0°53'36"N, 51°59'54"W); MPEG 19585, 19595, 19597–98, 19611, 19613, collected on 1–27 November 2000 by D. Silvano, B. Pimenta, and U. Galatti, at Amapari Project, 50 north line (0°51'47"N, 51°52'43"W), Serra do Navio municipality; MPEG 19608, collected on 24 November 2000 by D. Silvano, B. Pimenta, and U. Galatti, at Amapari Project, 400 south line (0°51'34"N, 51°52'34"W), Serra do Navio municipality; MZUSP 88450–55, collected on 15–19 June 2001

by M. Rodrigues and D. Pavan, at mouth of Camaipi Stream, Maracá River (0°04'22"S, 51°51'52"W), Mazagão municipality, field numbers MTR 6266, MTR 6267, MTR 6280, MTR 6287, MTR 6359, MTR 6352, respectively; MZUSP 78180, collected on 12 May 1992 by Exp. S. Kasahara, at Vila Nova (0°26'S, 51°48'W), Mazagão municipality, field number 92.6009. BRAZIL: State of Amazonas: AMNH 101947, collected on January–February 1966 by D. Cooper, at Manjuru River (4°S, 57°W), Itaituba municipality; INPA-H 1320, 18744–45, collected on 17 November 1993, 30 August 2004, and March 2003, by M. Martins, M. Pinto, and M. Pinto, at Adolpho Ducke Reserve (2°57'29.2"S, 59°55'38.7"W), Manaus municipality; INPA-H 789, collected on November 1993 by M. Martins, at Adolpho Ducke Reserve, Cuieiras River (2°50'04.2"S, 60°29'53.5"W), Manaus municipality; INPA-H 19794, collected on 10 February 2007 by V. Carvalho, at Federal University of Amazonas (3°05'59.4"S, 59°58'31.7"W), Manaus municipality; INPA-H 20948, collected on September 2008 by L. Brito Jr, at Ponta Negra (3°03'06.7"S, 60°05'57.6"W), Manaus municipality; INPA-H 9022, collected on November 1988 by G. Rebelo, at Tiradentes, Coroado (3°04'32.6"S, 59°58'39.3"W), Manaus municipality; INPA-H 147, 149, 202, collected between 21 April and 31 July 1987 by M. Martins, at Caititu Stream, Uatumã River, Balbina Hydroelectric Power Station (1°47'28.1"S, 59°48'10.3"W), Presidente Figueiredo municipality; INPA-H 20118, collected on 23 November 2007 by L. Bonora, R. Bernhard, and R. Melina, at Silves municipality (2°44'45.7"S, 58°11'48"W); MPEG 14018, 14277, 14405, 14416–17, collected between 7 January and 12 September 1985 by D. Peccinini-Seale, A. Lima, and T. Ávila-Pires, at Adolpho Ducke Reserve, 25 km north of Manaus (2°56'17.5"S, 59°58'12"W), Manaus municipality; MZUSP 10909, 76289, 79762, collected on 17 April 1962 and 2 October 1992 (last two specimens), at Ducke Reserve (2°57'13"S, 59°55'W), Manaus municipality; MZUSP 57637, collected on 16 December 1981, at Manaus municipality (3°07'S, 60°W); MZUSP 67052, collected on 1986 by B. Zimmerman, at INPA-WWF Reserves, central point (2°23'57"S, 59°58'51"W), Rio Preto da Eva municipality; MZUSP 66144–45, collected on January 1986 by M. Rodrigues, at INPA-WWF Reserves, Gavião (2°26'03"S, 59°48'56"W), Rio Preto da Eva municipality. BRAZIL: State of Pará: AAGARDA 6416, collected on 13–22 October 2012 by S. Mângia, at Maísa Farm (3°14'20"S, 49°20'23"W), Moju municipality; IEPA UHE445, UHE454, UHEIV204, TCD (0°63'12"S, 52°50'09.3"W), Almeirim municipality; INPA-H 26238–42, Trairão National Forest (4°59'35.3"S, 55°45'53.7"W), Trairão municipality; MPEG 29595–604, collected on 3–8 December 2009 by M. Ribeiro-Júnior and team, at Preto River, Marajó Island (0°25'47.8"S, 50°28'52.4"W), Afuá municipality, field numbers MAR 1478, MAR 1480,

MAR 1496, MAR 1479, MAR 1500, MAR 1526, MAR 1529, MAR 1565, MAR 1532, MAR 1568, respectively; MPEG 22764, collected on 15 September 2004 by T. Gardner and M. Ribeiro-Júnior, at área 95 (0°41'45"S, 52°48'32"W), Almeirim municipality, field number 2424; MPEG 27609, collected on 29 October 2008 by M. Hoogmoed and W. Rocha, at Maicuru Biological Reserve (0°50'N, 53°56.2'W), Almeirim municipality, field number CN 1563; MPEG 27542–43, collected on 8–10 December 2008 by M. Hoogmoed and A. Dangiolllela, at Paru State Forest (0°56.4'S, 53°13.7'W), Almeirim municipality, field numbers CN1601, CN1911; MPEG 24993, 25000–02, 25441, collected between 7 November 2007 and 15 January 2008 by J. Bernardi and C. Lima, at Tapuama, Belo Monte Hydroelectric Power Station (3°36'39"S, 52°20'26"W), Altamira municipality, field numbers BMW 31, BMW 17, BMW 28, BMW 46, BMW 139, respectively; MPEG 24909, 24916, collected on 7–10 November by M. Hoogmoed, A. Lima, and R. Rocha, at Caracol, Belo Monte Hydroelectric Power Station (3°27.6'S, 51°40'W), Anapu municipality, field numbers BML 211, BML 119; MPEG 19902, collected on 23 November 2001, at Barcarena municipality (1°34'20.5"S, 48°43'18.9"W), field number HERP 4656; MPEG 24290, collected on 20 October 2006 by F. Nunes and team, at Curupeté Stream (1°34'S, 48°45'W), Barcarena municipality, field number BAR 70; MPEG 19903, collected on 23 November 2001, at km 10, Vila do Conde–Abaetetuba highway (1°37'38.5"S, 48°41'18.1"W), Barcarena municipality, field number HERP 4657; MPEG 18125, collected on 5 January 1998, at Goeldi Museum (1°27'03.7"S, 48°26'42.9"W), Belém municipality; MPEG 15626, 19070, collected on 20 April 1989 and 14 February 2000, at Mocambo Reserve (1°26'30.7"S, 48°26'21.7"W), Belém municipality; MPEG 16670, collected on 23 April 1993, at Nina Ribeiro Street (1°27'07.21"S, 48°27'51.1"W), Belém municipality; MPEG 233, 1918, Utinga (1°25'13.6"S, 48°25'36.4"W), Belém municipality; MPEG 14733, collected on 27 November 1987 by D. Neto, at Caruaca River, Castanhal Ranch, Marajó Island (1°30'S, 50°21'W), Breves municipality, field number 24; MPEG 14985, collected on 3 October 1988 by M. Silva, at km 18, Capanema–Bragança highway (1°11'43"S, 47°0'51.6"W), Capanema municipality; MPEG 30020, collected on 28 March 2009 by M. Sturaro and J. Gomes, at Aldeia Nova (4°38'23.2"S, 56°17'26.2"W), Itaituba municipality, field number MJS 134; MPEG 29441, 29468, collected on 11 October 2009 and 11 August 2011 by M. Hoogmoed and J. Nascimento, and A. Dourado and team, at Amazonia National Park (4°37.5'S, 56°23.3'W), Itaituba municipality, field numbers MSH 7902, PRMT 15; MPEG 25041, 27838, 28502, 28577, collected between 25 February 2008 and 6 January 2011, at ALCOA, Adutora road (2°27'11"S, 56°09'10"W), Juruti municipality; MPEG 28576, collected on 5 January 2011 by M. Gordo, L. Frazão and F. Corrêa, at Guaraná

Stream (2°33'13"S, 59°13'33"W), Juruti municipality, field number JUR 1186; MPEG 21853, 28239, collected on 3 August 2004 and 27 July 2010, by G. Maschio and R. Silva, and Herp team, at Mutum (2°36'34"S, 56°11'46"W), Juruti municipality, field numbers ACP 04, JUR 1112; MPEG 28238, collected on 20 July 2010 by Herp team, at Prudente/Galiléia Stream (2°32'51"S, 56°13'32"W), Juruti municipality, field number JUR 1034; MPEG 17998, collected on 1 July 1997, at Tapirapé-Aquiri National Forest (5°46'26"S, 50°30'46"W), Marabá municipality, field number Salobo-87; MPEG 17997, collected on 1 December 1997 by U. Galatti, R. Rocha, and A. Barros, at camp in Tapirapé-Aquiri National Forest (5°48'06"S, 50°30'58"W), Marabá municipality, field number Salobo-286; MPEG 18022, collected on 1 December 1997 by U. Galatti, R. Rocha, and A. Barros, at Itacaiunas River, Tapirapé-Aquiri National Forest (5°52'20.4"S, 50°28'50.3"W), Marabá municipality; MPEG 21435, collected on 01 August 1997 by R. Yuki and team, at Pirelli Farm (1°24'57.7"S, 48°17'58.5"W), Marituba municipality, field number Pirelli-142; MPEG 16478, 16610, 19942, 20277, 20334, 20885–86, 20896, 20946, collected on ECFPn, Caxiuanã National Forest (1°44'15.5"S, 51°27'11"W), Melgaço municipality; MPEG 20933, collected on 2 April 1998 by J. Bernardi and R. Rocha, at Arauá River, ECFPn, Caxiuanã National Forest (1°45'58.2"S, 51°31'22.7"W), Melgaço municipality; MPEG 21738, 21747, 21796, collected between 26 November 2003 and 12 April 2004 by G. Maschio and A. Lima, at Caiçara, ECFPn, Caxiuanã National Forest (1°47'20.9"S, 51°26'11.5"W), Melgaço municipality; MPEG 28839, collected on 14 November 2005 by G. Maschio and Calisto, at Marinaú, Caxiuanã National Forest (1°49'51.4"S, 51°20'26.5"W), Portel municipality; MPEG 19311, 19337, 19350, 19376–77, 19405–07, collected between 24 November and 16 December 2000 by R. Rocha, J. Bernardi, and G. Silva, at Arroz Cru, Belo Monte Hydroelectric Power Station (3°23'27"S, 51°55'30"W), Vitória do Xingu municipality; MPEG 24904–08, 24910–15, 24917–19, 25433–40, 25657, collected between 5 November 2007 and 18 January 2008 by M. Hoogmoed, A. Lima, and R. Rocha, at Bom Jardim, Belo Monte Hydroelectric Power Station (3°24.8'S, 51°45.8'W), Vitória do Xingu municipality; MZUSP 7681, collected between 20 October and 5 December 1959 by A. Hoge, at Marajó Island (0°49'S, 49°08'W), Cachoeira do Arari municipality; MZUSP 53697, collected on 8 February 1979 by M. Rodrigues, at Bujuré, Tapajós River, Amazonia National Park (4°39'02"S, 56°23'24"W), Itaituba municipality; MZUSP 52488, 53630, collected on 31 October 1978 and 29 January 1979 by M. Rodrigues, at Uruá, Tapajós River, Amazonia National Forest (4°30'S, 56°16'W), Itaituba municipality; MZUSP 53683–84, collected 1–5 February 1979 by M. Rodrigues, at Limão Waterfall, Tapajós River (4°41'S, 56°21'W), Trairão municipality; MZUSP 67482–89,

collected between 23 January and 3 March 1987 by L. Vitt, at Juruá, Xingu River (3°24'S, 51°53'W), Vitória do Xingu municipality; USNM 158083, collected on 16 August 1965 by P. Humphrey, at Belém municipality (1°26'S, 48°29'W), field number PHS 32125; USNM 162209, collected on 22 July 1966 by P. Humphrey, at IPEAN (1°27'S, 48°29'W), Belém municipality; USNM 288896–97, collected on 1–2 February 1981 by R. Crombie and G. Busack, at Tapajós River, Amazonia National Park, ca. 66 km SW of Itaituba (1°41'25.9"S, 56°26'35.6"W), Itaituba municipality, field number USNM-FS 046930, USNM-FS 046942. FRENCH GUIANA: MNHN-RA-2002.601, collected on 22 July 2002 by P. Gaucher and J-C. De Massary, at Saint Marcel (2.39, -53.01); MNHN-RA-1950.22, collected by A. de la Rüe, at Bienvenue, Canopi (3.17, -52,34); MNHN-RA-2015.40, collected on 3 March 2015 by N. Vidal, at Crique Alama, borne 1, Mitaraka (2.27, -54.51); MNHN-RA-2020.0024, Toponowoni; MNHN-RA-2020.0025, Awala; MNHN-RA-2020.0026, Mont Galbao; MNHN-RA-2020.0027, MNHN-RA-2020.0028, Mont Lucifer; MNHN-RA-2020.0029, Terrain Comté; MNHN-RA-2020.0030, DZ no 5; MNHN-RA-2020.0031, Gaa Kaba; MNHN-RA-2020.0032, Mana. GUYANA: Upper Demerara-Berbice: AMNH 151893, collected on 11 March 1997 by C. Cole and C. Townsend, at Berbice River Camp at ca. 18 mi (linear) SW Kwakwani, ca. 2 mi downriver from Kurudini River confluence (5°05'06"N, 58°14'14"W); USNM 566400, collected on 11–14 March 1997 by C. Cole and C. Townsend, at Kwakwani, ca. 18 mi (airline) SW of, ca. 2 mi downriver from confluence of Berbice River and Kurudini River, Berbice River camp (5°05'06"N, 58°14'14"W). Upper Takutu-Upper Essequibo: AMNH 61381, collected on April 1938 by R. Snedigar, at Marudi (2°18'N, 59°01'W). SURINAME: Brokopondo: AMNH 119395, collected on 8 July 1980 by C. Cole, C. Townsend and J. Cole, at Brownsberg Nature Park, trail to Irene Falls & Toeval meertje (4°56'49.9"N, 55°09'28.5"W). SURINAME: RMNH 15200, collected on 20 August 1961 by M. Hoogmoed, at Brown's Mountain [Brownsberg] (4°56'N, 55°10'W); RMNH.RENA.4858, collected on 2 December 1910 by K. Hulk, at forest on the Lucie River.

Alopoglossus avilapiresae: BRAZIL: State of Acre: MPEG 20667–84 (667, 668, 671, 680, females; 683, male; others juveniles), Juruá River, 5 km north of Porto Walter (8°15'31.2"S, 72°46'37.1"W), between 14 February and 17 April 1996, Vitt, Ávila-Pires, Caldwell & Oliveira, field number LJV 6167, 6242, 6280, 6288, 6291, 6294, 6322, 6363, 6380, 6395, 6411, 6423, 6437, 6523, 6574, 6607, 6633, 6645, sequentially; MPEG 30374–76, males, Porto Walter, Sobral, on left side of Juruá River (8°22'S, 72°49'W), 11–14 March 1992, Gascon; MZUSP 53504, collected on 15 January 1979 by P. Vanzolini, at Porto Walter municipality (8°16'S, 72°44'W), field number 783684; MZUSP 88649, collected on 20–22

November 2000 by M. Barbosa, at Estirão do Panela, Serra do Divisor National Park (8°52'S, 72°47'W), Marechal Thaumaturgo municipality, field number MBS 16. BRAZIL: State of Amazonas: AMNH 113136–40, collected on 18–28 May 1970 by B. Malkin, at Belém Stream, near Solimões River, ca. 40 km E of Leticia (3°55'S, 69°37'W), Tabatinga municipality; CHUNB 13534–35, collected by R. Brandão, at Codajás municipality (3°12'S, 62°42'W), field numbers UNB 2322, UNB 2320; CHUNB 13632, collected at Amanã municipality (3°30'S, 61°36'W), field number UNB 2323; INPA-H 9515, collected on 5 February 2001 by A. Duarte, at Maraã municipality, Amanã, Baré (2°28'54.95"S, 64°42'36.98"W), field number RCV 01-322; INPA-H 9514, collected on 30 January 2001 by A. Duarte, at Amanã, Baré (2°28'54.9"S, 64°42'37"W), field number RCV 01-274; INPA-H 9394, collected on 1 February 2001 by A. Duarte, at Amanã, Boa Esperança (2°29'17.6"S, 64°45'12.9"W), field number RCV 01-292; INPA-H 9382, collected on 12 January 2001 by A. Duarte, at Amanã, Boa Vista (2°20'32.7"S, 64°51'33.8"W), field number RCV 01-74; INPA-H 11112, 11119, collected on 9 September 2003 and 6 September 2006 by R. Bernhard, at Maraã, Mamirauá Sustainable Development Reserve, Paraná Trail (2°21'42.68"S, 65°15'35.45"W); INPA-H 19847, collected on 2 September 2007 by V. Carvalho and M. Gordo, at km 19 AM-352 road (3°09'29.2"S, 60°42'49.1"W), Novo Airão municipality; MPEG 4652, female, São Gabriel da Cachoeira, Missão Salesiana do Jauareté, Turí River, affluent of the right side of the Uaupés River, Santa Cruz (0°30'30.85"N, 69°25'48.46"W), 12 March 1971, Moreira; MPEG 16003, female, Tabatinga (4°13'57.59"S, 69°56'23.16"W), 22 December 1989, Ávila-Pires, field number TCAP 1863; MZUSP 13060, collected on 8–28 April 1966 by B. Malkin, at Belém Stream, Solimões River (3°55'S, 69°37'W), Tabatinga municipality; MZUSP 38369, collected on 12–18 January 1975 by Expedition MZUSP-USNM, at Beruri municipality (3°54'09"S, 61°20'22"W), field number 741611. COLOMBIA: Amazonas Department: MCZ 141227, collected on 14 November 1973 by M. Corn, at near Amazon River, Leticia municipality (4°12'22"S, 69°56'W). PERU: Department of Cusco: CORBIDI 8321, collected on 28 November 2010 at La Convención Province, KP 50, Nativa Poyentimari Community (12°11'18.73"S, 73°0'3.32"W). PERU: Department of Huánuco: CORBIDI 14749, collected on May 2014 by K. García, at Cacataibo, Codo del Pozuzo (9°29'25.51"S, 75°30'47.34"W), Puerto Inca municipality. PERU: Department of Junín: CORBIDI 15836, collected on 25 July 2014 by E. Almora, at Portillo Alto, Fundo Santa Teresa, Río Negro (11°10'9.72"S, 74°38'54.9"W), Satipo municipality. PERU: Department of Loreto: CORBIDI 15219, collected on 17 October 2014 by P. Venegas, at Campamento Anguila, Tapiche (6°15'54"S, 73°54'36"W), Requena

municipality; CORBIDI 1579, collected on November 2008 by M. Medina, at Campamento San Jacinto, Trompeteros (2°42'15.6"S, 76°18'46.2"W), Loreto municipality; CORBIDI 1711, collected on 7 October 2008 by P. Venegas, at Parque Ecologico Munichis, Yurimaguas (5°53'53"S, 76°13'55"W), Alto Amazonas municipality; CORBIDI 2276, collected on 1 November 2008 by D. Vásquez, at Sierra del Divisor, Soplin (6°55'7.4"S, 76°50'46"W), Requena municipality; CORBIDI 4111, 4126, collected on January 2009 by R. Santa Cruz, at Sierra del Divisor, Zona de Amortiguamiento, Alto Tapiche (6°31'13"S, 74°1'0.1"W), Requena municipality; CORBIDI 4770, collected on March 2008 by V. Duran, at Andoas, Trompeteros (2°40'15.6"S, 76°18'46.2"W), Loreto municipality; CORBIDI 5964, collected on 16 October 2009 by P. Venegas, at Campamento Curupa, Napo (2°53'7.6"S, 73°1'4.7"W), Maynas municipality; CORBIDI 6326, collected on 16 February 2010 by P. Venegas, at Centro de Investigacion Jenaro Herrera, Jenaro Herrera (4°53'43.78"S, 73°39'2.97"W), Requena municipality; CORBIDI 8763, collected on 19 November 2010 by C. Landauro, at Morona, Sector 2 (3°11'13.14"S, 77°26"W), Datem del Marañón municipality. PERU: Department of Madre de Dios: CORBIDI 18297, collected on 17 August 2016 by A. Garcia-Ayachi, at Las Piedras Amazon Center, Tambopata (12°4'14.8"S, 69°29'57.5"W), Tambopata municipality. PERU: Department of Puno: CORBIDI 13176, collected by P. Venegas and L. Lujan, at Parque Nacional Bahuaja Sonene-Campamento Satelite, Ayapata (13°14'23.81"S, 70°8'27.4"W), Carabaya municipality. PERU: Department of San Martín: CORBIDI 16160, collected on 27 February 2014 by G. Chávez, at Concesión Palmito, Caynarachi (6°10'45.14"S, 76°18'37.32"W), Lamas municipality; CORBIDI 3662, collected on April 2002 by P. Venegas, at Río Chambira, Shamboyacu (7°2'15.03"S, 76°5'26.25"W), Picota municipality.

Alopoglossus carinicaudatus: PERU: Department of Loreto: CORBIDI 297, collected on 9 October 2007 by P. Venegas and M. Yanez-Muñoz, at Redondococha, Teniente Manuel Clavero (0°34'16.7"S, 75°13'9.19"W), Putumayo; CORBIDI 12663, collected on 26 October 2012 by P. Venegas, at Medio Campuya, Rosa Panduro (1°31'3.4"S, 73°48'58.2"W), Putumayo. ECUADOR: Department of Orellana: QCAZR 6362, collected on 22 February 2003 by S. Ron, at Parque Nacional Yasuní, Estación Científica Yasuní PUCE, sendero Ceiba (0°40'32.74"S, 76°23'45.82"W), Alejandro Labaka; QCAZR 11600, collected on 22 March 2013 by F. Ayala, at Parque Nacional Yasuní, Tambococha (0°58'42.2"S, 75°25'32.48"W), Nuevo Rocafuerte; QCAZR 5216, collected on 11 June 2012 by M. Read, at Vía Pompeya Sur-Iro, cerca del Km 83, Sitio Auditivo A33 (0°51'0.82"S, 76°17'25.97"W); QCAZR 9144,

collected on 6 September 2009 by S. Ron, at Vía Pompeya Sur–Iro, km 80, puente sobre el Río Beye (0°50'24.43"S, 76°18'8.68"W), Cononaco.

Alopoglossus collii: BRAZIL: State of Mato Grosso: MZUSP 97934–35, collected by Op. Coatá, at UHE Guaporé (15°07'S 58°58'W), Vale de São Domingos; UFMT 4105, PCH Ombreiras Margem direita do rio Jauru (15°19'2.3"S, 58°51'42.8"W). State of Rondônia: CHUNB 18037–40, 18599, collected between 01 July and 24 August 2000 by G. Colli, at Pimenta Bueno (11°51'45.2"S, 60°56'18"W); CHUNB 11472, collected between 20 August and 22 September 1999 by D. Mesquita, at Vilhena (12°07'19.1"S, 60°16'39.1"W); MPEG 21951, collected on 20 July 2001, at Fazenda Jaburi (11°38'02"S, 60°43'51"W), Espigão do Oeste.

Alopoglossus meloi: BRAZIL: State of Amazonas: CZPB-RP 0027, collected on 22 September 2011 by A. Almeida, D. Oliveira, L. Frazão, S. Marques and T. Hrbek, at São José do Jatobá Village, Igarapé do Tabocal, eastern Jatapú River, São Sebastião do Uatumã municipality (1°55'53"S, 58°15'21"W), field number CZPB-2940; MPEG 29381, collected on 05 October 2009 by R. Ávila, at Marajatuba, Urucará municipality (2°22'47"S, 57°38'42"W), field number M3 R74. BRAZIL: State of Pará: MHNCI 13588, adult female, collected on June 2009 by F. Oliveira, at Saracá-Taquera National Forest, Oriximiná municipality (1°44'11"S, 56°24'36"W); MHNCI 13950, Almeidas Plateau, Saracá-Taquera National Forest; MPEG 24372, collected on 29 January 2007 by E. Pereira and team, at Porto Trombetas, Aramã Plateau, Terra Santa municipality (1°52'25"S, 56°24'55"W), field number R138; MPEG 15348 and MPEG 16201, collected on 06 December and 11 December 1988 by M. Hoogmoed, T. Ávila Pires and R. Rocha, at Cruz Alta, 6 km south of Trombetas River, Oriximiná municipality (1°30'56"S, 56°45'51"W), field number TCAP 1153 and TCAP 1213; MPEG 28271, collected on 29 June 2008 by R. Pinto and team, at Porto Trombetas, Saracá-Taquera National Forest, Saracá Plateau, Oriximiná municipality (1°41'20"S, 56°29'35"W), field number R 212; MPEG 19880, collected on 10 October 2001 by U. Galatti and J. Bernardi, at Porto Trombetas, Saracá Mine, in a reforestation area, Oriximiná municipality (1°40'41"S, 56°23'57"W), field number TROMBE 058; MPEG 24373, collected on 05 February 2007 by E. Pereira and team, at Porto Trombetas, Greig Plateau, Terra Santa municipality (1°50'39"S, 56°31'42"W), field number R 201; MZUSP 53791–94, 54357–58, Taboleiro Leonardo, Trombetas River; MZUSP 78122, 78207–08, Vai-Quem-Quer.

Alopoglossus theodorusi: FRENCH GUIANA: MNHN-RA-2020.0019, Saut Maripa, St. Georges (3°48'40.17"N, 51°53'22.72"W), collected on 03 May 2012, by A. Fouquet, field number AF740; MNHN-RA-2020.0020, Armontabo (3°51'50"N, 52°29'18"W), collected on

30 August 2003, by P. Gaucher, field number PG172; MNHN-RA-2020.0021, Mont Galbao (4°29'17"N, 52°02'40"W), collected on 19 October 2018, by E. Courtois & M. Dewynter, field number AF4793; MNHN-RA-1996.4471–73, Camp de Saint-Eugène (4°51'02"N, 53°03'21"W), 7–27 September 1993, I. Ineich; MNHN-RA-2001.358, DZ n°5 (4°03'N, 52°01'W), M. Blanc; MNHN-RA-2020.0022, MNHN-RA-2020.0023, DZ n°5 (4°03'N, 52°01'W), 15 September 2001, M. Blanc, field numbers RG5 and RG6.

Hemipenial morphology. *Alopoglossus angulatus*: INPA-H 26240; *Alopoglossus avilapiresae*: INPA-H 9515 (holotype); *Alopoglossus gansorum*: INPA-H 14005 (paratype); *Alopoglossus indigenorum* INPA-H 25543 (holotype), INPA-H 30243 (paratype).

Figure S1. Bayesian phylogenetic tree (A) and haplotype network (B) inferred from a fragment of the nuclear DNA locus *PRLR*. Tree nodal support values indicate posterior probabilities of the Bayesian inference (above the branches, below 0.7 omitted) and bootstrap values of a Maximum Likelihood inference (below the branches, below 70 omitted). The size of the circles in the haplotype network indicates the relative frequency of the haplotype. Distinct colors in the tree sample names and circles of the haplotype network correspond to distinct species according to the inset legend.

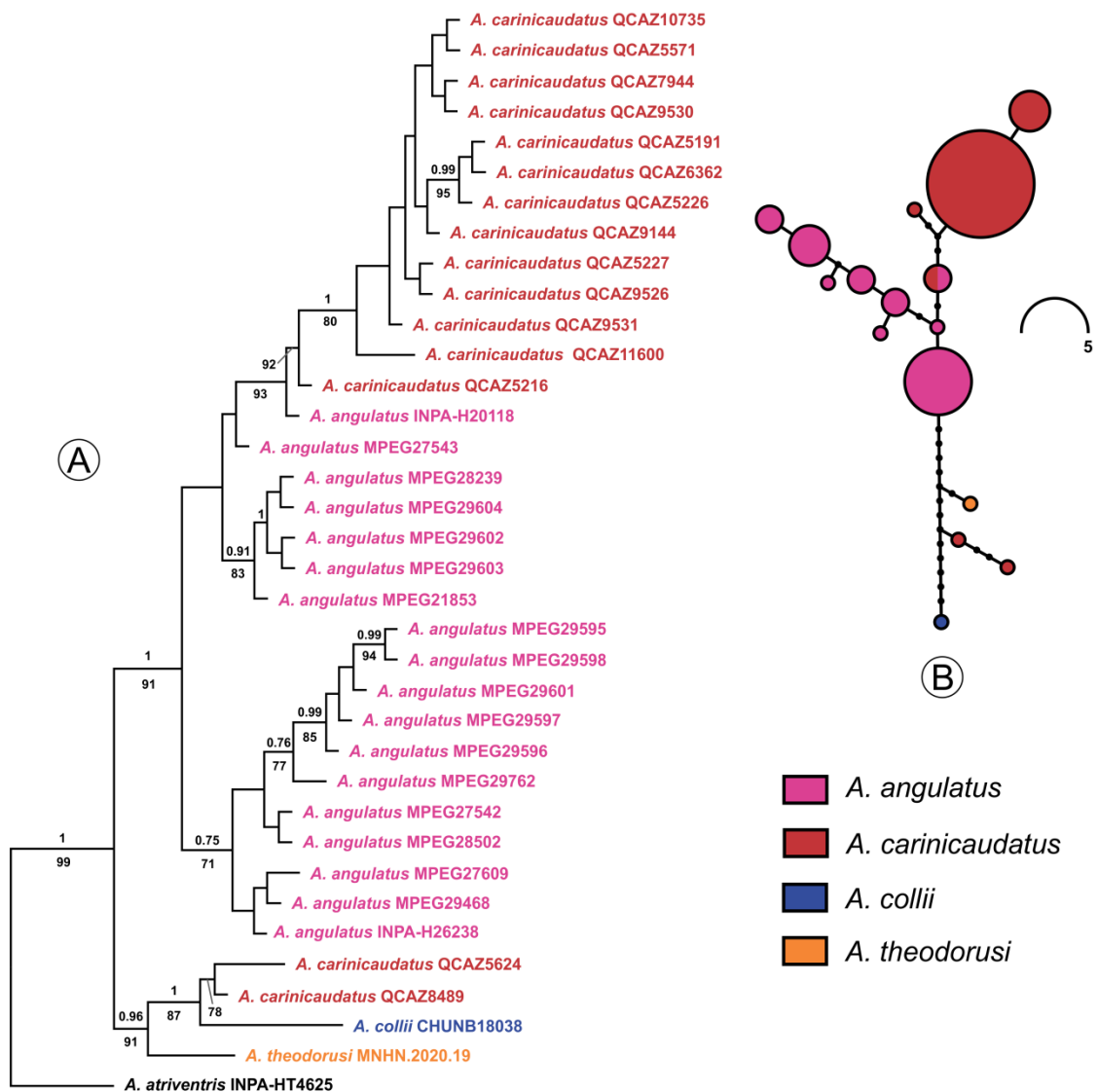


Figure S2. Bayesian phylogenetic tree (A) and haplotype network (B) inferred from a fragment of the nuclear DNA locus *SINCAIP*. Tree nodal support values indicate posterior probabilities of the Bayesian inference (above the branches, below 0.7 omitted) and bootstrap values of a Maximum Likelihood inference (below the branches, below 70 omitted). The size of the circles in the haplotype network indicates the relative frequency of the haplotypes. Distinct colors in the tree sample names and circles of the haplotype network correspond to distinct species according to the inset legend.

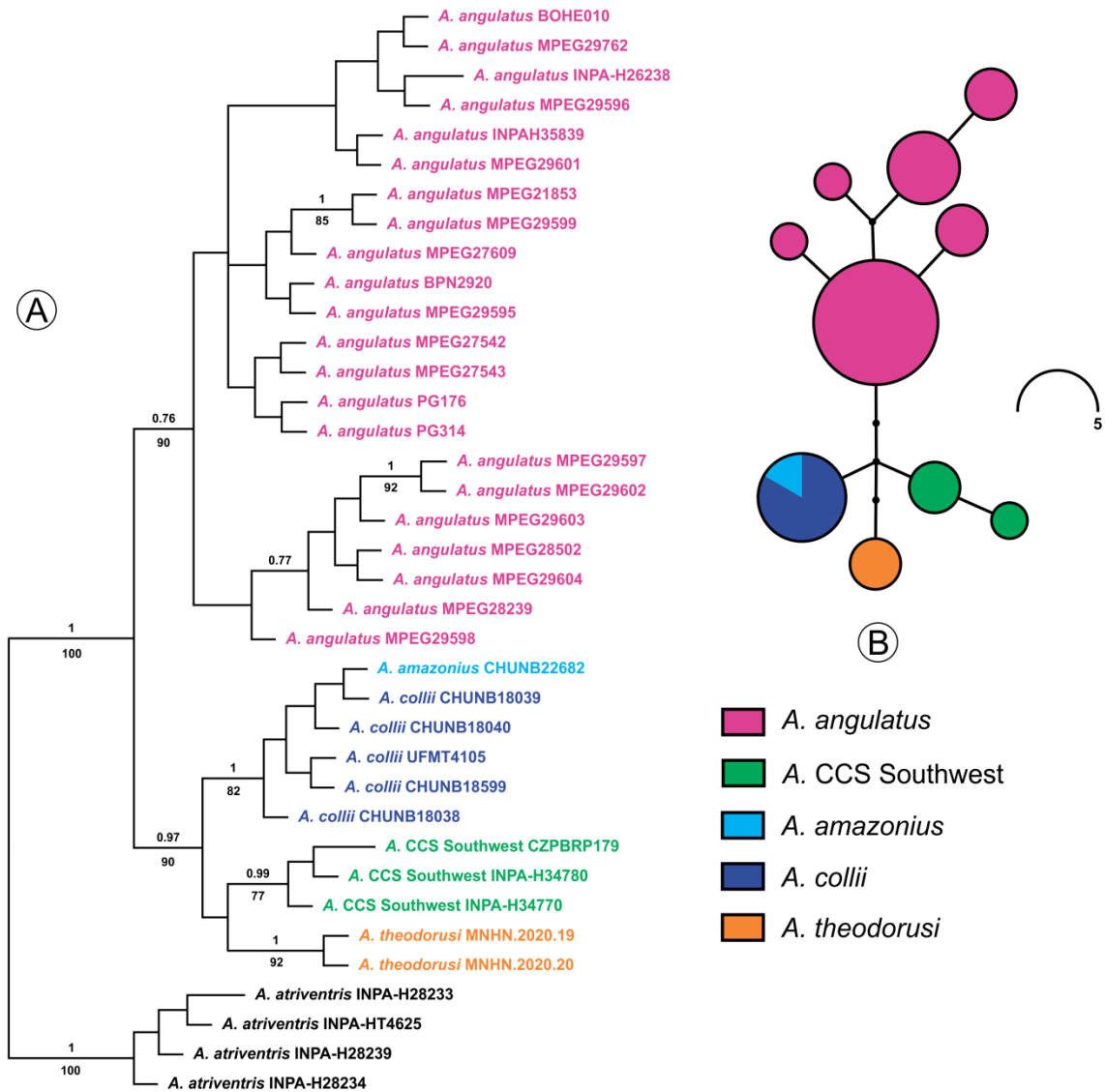


Figure S3. Hemipenis of the paratype of *Alopoglossus indigenorum* sp. nov. (INPA-H 30243). Scale bar: 1 mm.

